SAPIENZA UNIVERSITY of ROME

PhD in CELLULAR AND DEVELOPMENTAL BIOLOGY

-XXIII CYCLE-

DOCTORAL THESIS:

PARKINSONISM AND NEUROINFLAMMATION: CARVING OUT A ROLE FOR MMP-9?

TUTOR:

Prof. Maria Egle De Stefano

Dept.: Biologia e Biotecnologie "Charles Darwin"
Neurobiology research centre "Daniel Bovet"
University of Rome La Sapienza

PhD STUDENT:

Valentina Annese

CO-TUTOR:

Dra. Maria Trinidad Herrero

School of Medicine
Research centre of "Neurología y Neurocirugía Experimental"
Campus Espinardo, University of Murcia

Academic year 2010-1011

Human knowledge is insufficient and the conclusions of science cannot indicate by themselves the path towards integral human development. There is always a need to push further ahead: this is what is required by charity in truth. Going beyond, however, never means prescinding from the conclusions of reason, not contradicting its results. Intelligence and love are not in separate compartments: ***love is rich in intelligence and intelligence is full of love****.*

Benedict XVI

Charity in Truth

Encyclical Letter, 2009

"There are many success stories in the history of Parkinson's disease. Our understanding of the condition has greatly evolved since it was first identified as the shaking palsy 193 years ago. We have made progress in defining the underlying pathology and tracking disease progression, and better treatments improve patient quality of life. Yet, a cure remains elusive. Unlike other neurodegenerative conditions, Parkinson's disease has had a successful symptomatic drug available for more than 40 years. Levodopa is the mainstay of Parkinson's disease treatment, but although its pharmacology and delivery have been altered and improved over the years, it is still far from ideal. And herein lies perhaps the ultimate frustration: despite several decades of searching, levodopa is still the best there is. That is not the only challenge. Can we detect the disease before major, perhaps irreversible degeneration has occurred? What will it take to replicate this disease in animal models to enhance our understanding of it and aid development of novel treatments? And how can new, potentially disease-modifying therapies be appropriately tested in patients?"

Michelle Grayson, Associate Editor, Nature Outlooks, August 2010

INDEX:

INTRODUCTION

Neuroinflammation in neurodegeneration

Inflammatory responses have now been associated with many chronic neurodegenerative conditions (e.g., Multiple sclerosis, Alzheimer disease, Amyotrophic lateral sclerosis and Parkinson's disease). Neuroinflammation is a process not easy to define: traditionally, it involves the succession of complex and integrated cell processes, the integrity of which is mediated by the synthesis/release of pro-inflammatory mediators, such as cytokines and chemokines. Inflammatory responses are usually localized and characterized by an active communication between immune, vascular, and parenchymal cells. Outside of the CNS, cell types recruited in inflammation are monocytes, neutrophils and macrophages. These cells elaborate integrated cascades producing reactive oxygen species at sites of infection or injury. Resident populations of tissue macrophages play key roles as sentinels of infection and injury, but are also increasingly recognized as having an influence on normal tissue homeostasis.

In the brain all neural cells, such microglia, astrocytes, neurons and oligodendrocytes participate to the inflammatory response with different roles and timing. Additionally, dysfunction of the blood-brain barrier (BBB) combined with infiltration of peripheral immune cells could be important players. Similarly to other districts, in the CNS the microglia exhibit a dormant phenotype in healthy condition and may play important roles in maintenance of tissue homeostasis in processes like neuropathic pain, stress, autonomic and immune response through the communication with astrocytes and neurons, analogously to the homeostatic role described for the "alternatively activated" macrophages in other tissues (Milligan, 2009; Streit, 2005; Verkhratsky, 2007). Neuro-inflammation is normally considered a protective

mechanism that circumscribes the damaged areas in the brain, destroys affected cells and modify the extracellular matrix (Streit, 2002; Correale and Villa, 2004; Bauer, 2007; Sofroniew, 2001). Without local and well balanced inflammatory responses, brain tissue would be more vulnerable to acute trauma and microbial, viral and prion infections. The firs and dominant reaction to all types of CNS injuries consists in the activation of resident immune cells, often referred to as gliosis, at the sites of damage (Kreutzberg, 1996; O'Callaghan, 2005; Glass, 2010). Morphologically, gliosis consists in macroscopic changes in glial cells phenotypes, mainly consistent in the activation and transformation of microglial cells into phagocitic cells, and, to lesser extent, in reactive astrocytosis (Narassimahan, 2005; Kattenmann, 2006; Kattenmann, 2007; Napoli and Neumann, 2009; Sofroniew, 2010). Mediators of this gliosis already identified are cytokines, chemokines and reactive oxidant species. Microglia and astroglia *per se* are also a source of inflammatory mediators and reactive oxidant generators, which can perpetuate the inflammatory reaction in an autocrine manner, given rise to the so called "dark-side" of glia (Miller, 2005).

All glial cells normally switch to what can be considered an "activated" phenotype in response to a pathogen invasion or tissue damage, thereby promoting an inflammatory response which serves to further engage the immune system and initiate tissue repair. In most cases, this response is self-limiting, resolving once infection has been eradicated, or the tissue damage has been repaired. However, sustained inflammation, which results in tissue pathology, implies the persistence of an inflammatory stimulus or a failure of the normal resolution mechanisms. A persistent stimulus could be determined by environmental or endogenous factors (e.g. protein aggregates) that may be perceived by the resident glia like a "danger signal". In these cases, the normal restoring mechanism is bypassed, leaving the place to a chronic

inflammatory process. Chronic neuro-inflammation differs from the acute inflammation mainly because it is below the threshold of pain perception. This condition makes possible that the inflammatory state may continue for years, causing a persistent insult to the brain and producing neurotoxic factors that impair the pathological state, ultimately showing clinical manifestations. The molecular mechanisms and the internal and external factors that modulate the dynamic aspects of the acute and chronic neuro-inflammations remain unclear. Furthermore, it is poorly understood to what extent neuroinflammation is beneficial for the injured or infected brain, and how may contributes to secondary brain injuries and progressive neuronal loss.

Mechanisms of neuroinflammation

Inflammatory responses to infectious agents are typically initiated by pattern recognition receptors, which bind to so-called pathogen-associated molecular patterns (stranger signals). One class of pattern recognition receptor is exemplified by the Toll-like receptors (TLRs), which recognize a diverse set of pathogen-associated molecules that are not present in the host. For example, TLR4 recognizes the lipopolysaccharide (LPS) associated with gram-negative bacteria, whereas TLR3 recognizes viral double-stranded RNA. These receptors are expressed on many cell types, but are highly expressed on cells that play central roles in innate immune responses, including macrophages and microglia. Pattern recognition receptors have more recently been found to also be capable of responding to endogenously derived molecules, such as components released from necrotic cells (danger signals) and by molecules that may be formed as a consequence of pathogenic mechanisms. Roles of TLR2 and TLR4 have recently been established in the pathogenesis of several chronic inflammatory diseases by using animal models, and specific TLR4 polymorphisms have been demonstrated to be associated with several human age-related diseases, including atherosclerosis, type 2

diabetes, and rheumatoid arthritis, raising the question of whether these receptors also contribute to inflammatory programs associated with neurodegenerative disease (Balistreri, 2009). In addition to pattern recognition receptors, purinergic receptors are expressed on microglia and astrocytes and respond to ATP released from cells following death, traumatic injury, or ischemia (Di Virgilio, 2009). Microglia and astrocytes express a number of so-called "scavenger receptors" that have been demonstrated to be involved in the uptake of a number of substrates, including oxidized proteins, lipids and apoptotic cells, and that may also contribute to cell signaling (Husemann, 2002).

Normally, to bring about an effective immune response, the initial detection of a microbial pathogen must be amplified to recruit additional cells to sites of infection, induce antimicrobial activities and initiate the development of an adaptive immunity. Therefore important subsets of highly induced genes include: cytokines which amplify the program of inflammation, and chemokines (e.g., Monocyte chemotactic protein-1, MCP-1), which recruit additional immune cells. Generally, the onset of inflammation is often characterized by the release of pro-inflammatory cytokines, such as (Tumor necrosis factor, TNF), interleukin (IL)-1 and adhesion molecules. Many of these secreted factors influence the system in both autocrine and paracrine fashions. In addition to the activation of local glia and the recruitment of blood-borne leukocytes, local synthesis of inflammatory-related cytokines elicits a wide range of effects including: cell adhesion, migration, survival, differentiation, replication, secretory function and death. In the same cell, a cytokine can exert opposite effects, inducing death, survival, or proliferation depending upon the functional context in which it acts. For IL-1 and TNFα, these effects are mediated primarily by IL-1 type I receptor (IL-1R1) and TNFR1 (p55) or 2 (p75), respectively. While a pathophysiological role for IL-

1 as part of inflammatory processes in the brain has been established, is still unclear how exactly the signaling process contributes to neuronal death and/or protection. However, experimental data support its role as a key mediator of inflammation and neuronal death in acute brain injuries, such as stroke and trauma (Allan, 2005).

The multiple functions of microglia related to an innate immune response are associated with TNFα signaling and its regulation of both inflammation and apoptosis. TNFα is a multipotent, inflammatory cytokine that can induce apoptosis via activation of receptors containing a homologous cytoplasmic sequence, which identify an intracellular death domain. These include TNFR1 and CD95 (APO-1/Fas) and their corresponding death ligands, TNFα and the structurally related type II transmembrane protein, FasL. The release of TNFα and FasL shedding by microglia are implicated in neurotoxicity (Badie, 2000; Taylor, 2005).

Membrane receptors implicated in apoptotic neuronal death, involve downstream intracellular death-signaling complexes, such as AP-1, NF-κB, and caspases. TNFR1 activation, for example may provide a molecular mechanism for the rapid apoptosis of injured or sick neurons through a caspase 3-mediated pathway (Yang, 2002).

The tissue distribution of these receptors and the differentiation state of the target cells influence the cellular response to cytokines. Neither TNFα nor IL-1β have been demonstrated to cause neuronal death in healthy brain tissue or normal neurons, (Gendelman, 1999), and a normal cellular architecture is maintained in mice deficient in pro-inflammatory cytokines or in their receptors. However the cascades in which these cytokines take part support the hypothesis that localized pro-inflammatory cytokine activation could initiate neuronal death in altered tissue. In fact, increases in TNFα and IL-1β levels and activation have been observed prior to neuronal death (Matusevicius,

1996; Lefebvre d'Hellencourt, 2005; Harry, 2008; Kaushal, 2008; Harry, 2008). In addition, in the neuro-inflammatory cascades, genes that encode proteins with antimicrobial activities (e.g., Inducible nitric oxide synthases, iNOS) and/or that influence substrate metabolism, protein synthesis, cell motility, phagocytosis, apoptosis, and antigen presentation are induced. The generation of reactive oxygen species (ROS), e.g., through the nicotinamide adenine dinucleotide phosphate (NADPH)-oxidase system, is an important antimicrobial mechanism, but also exemplifies a system that can result in collateral damages to the tissue, e.g., to the parenchymal cells in the brain.

ROS are multi-potent, diffusible molecules capable of carrying out signal transduction processes in response to extracellular stimuli and their role in enhancing gliosis has been proposed by studies showing its inhibition following antioxidant treatment. Recently, NADPH oxidase was identified as the ROS-producing molecule in astrocytes: here cytokine stimulation leads to a rapid NADPH oxidase activation followed by the expression of pro-inflammatory products, such as iNOS (Pawate, 2004). The generation of ROS and the induction of iNOS enhance NO production from both glial and endothelial cells. NO is both a vasorelaxant, and neurotransmitter that at high concentrations, forms peroxynitrite. Moreover by nitrosylation of cell signaling messengers NO may act as an immune regulator (Guix, 2005). ROS signaling has been considered as a unifying factor underlying multiple forms of neuro-inflammation and microglia responses. However, many of these studies have been conducted *in vitro* and raise the question of how to transpose these mechanisms to an *in vivo* situation.

CNS is an immunologically privileged site and circulating immune cells normally do not have access to it in the absence of inflammation or injury. As dendritic cells, with specialized antigen-presenting capabilities, in the peripheral immune system, microglia appear to be the major initial sensors of danger or stranger signals recognized

by TLR4, and they secrete inflammatory mediators such as TNF-α and IL-1β that can act on astrocytes to induce secondary inflammatory responses (Saijo, 2009). However, not only CNS resident cells are involved in neuro-inflammation. A somehow indirect mechanism of communication between the systemic and central immune systems exists. Cytokines circulating within the bloodstream can signal via binding to receptors on neurovascular endothelial cells. Pro-inflammatory cytokines released upon immune challenge can also activate vagal afferent signaling and subsequent direct, or indirect, activation of vagal efferents. This has been proposed as a demonstration that the sensory vagal afferents, together with the regulatory vagal efferents, form an inflammatory reflex that continually monitors and modulates the inflammatory status in the periphery (Tracey, 2002).

Peripheral lymphocytes (T and B cells) that infiltrate the brain have been shown to participate in the local response to acute and chronic CNS injury, in addition to resident microglia and infiltrating macrophages. T-cells participate in different ways. The exacerbated immune response may be deleterious for the CNS as occurs in multiple sclerosois (MS). T-cells are primed to react to specific myelin antigens in MS, but could also promote neuronal survival in animal models of nerve crush and other physical injuries (Schwartz, 1999) and have been shown to protect hippocampal neurons against chemical exposure to the organometal trimethyltin (Kurkowska-Jastrzebska, 2007). There are also new evidences that cytokines produced during infection/inflammation activate the adaptive central nervous system responses, including acute stress responses mediated by the hypothalamo-pituytary-adrenal axis (Serrats, 2010). Overall, these studies demonstrate that CNS responses previously considered to be the result of CNS tissue specific cells may involve contributions from multiple cell types, the actions of which are significantly influenced by the systemic state of the organism.

Finally, the variety of factors secreted during neuroinflammation could also affect another group of cells resident of the CNS, modifying their functions: the oligodendrocytes (OLs). OLs are mature glial cells that myelinate axons in the brain and spinal cord. As such, they are crucial for the appropriate function and efficient neuronal signaling. OLs and their precursors are very vulnerable to conditions common to CNS injury and diseases, such as inflammation, oxidative stress and elevated glutamate levels which leads to excitotoxicity. Thus, these cells become dysfunctional or die in several pathologies including Alzheimer's disease (AD), spinal cord injury and ischemia. In the adult brain, the consequence of their death, or of any other defect in the differentiation of the precursors cells (OPCs) into myelin sheath producing mature OLs, is an inadequate re-myelination in case of injuries. The failure of remyelination has profound consequences for the function and preservation of axons, the progressive and irreversible loss of which accounts for the progressive nature of the above mentioned neurodegenerative diseases. In MS, for example, neuro-inflammation seems to be crucial in determining the severity of the progression of the disease. Although many studies in the past few years have concentrated on putative inhibitory signals, in their attempt to account for the failure of OPCs to undergo complete differentiation in demyelinated MS plaques, an alternative explanation is that these lesions fail to remyelinate because of a deficiency in the signals that induce differentiation. This hypothesis, based on the absence of promoting factors, is difficult to prove, but it is consistent with a model of remyelination, in which the acute inflammatory events have a key role in activating precursors and in creating an environment that is conducive to remyelination. MS lesions are rarely devoid of any inflammatory activity; however, chronic lesions are relatively non-inflammatory compared with acute lesions and constitute a less active environment in which OPCs differentiation might become

quiescent. The difference between inflammatory and non-inflammatory environments, which models chronic lesions in a promoting regenerative behavior, has been demonstrated in two recent studies based on the myelinating potential of transplanted OPCs (Setzu, 2006; Foote & Blakemore, 2005). Chronic lesions usually contain scarring astrocytes, which are hypertrophied and nonreactive, in contrast to the reactive astrocytes associated with acute lesions and that support remyelination through the production of growth factors (Redwine & Armstrong, 1998; Albrecht, 2003; Williams, 2007). Although these non reactive astrocytes are likely to be the consequence and not the cause of remyelination failure, their presence might not be helpful when attempting to promote remyelination in chronic lesions.

In this introductory section, only a few of the inducers, sensors, transducers and effectors of neuro-inflammation that could contribute to neuronal dysfunction or death have been mentioned. Although the inducers of inflammation may be generated in a disease-specific manner, there is a clear evidence for a remarkable convergence of the mechanisms responsible for signaling, transducting and amplifying inflammatory processes, which result in the production of neurotoxic mediators. Over more, a major unresolved question is whether inhibition of these responses will be a safe and effective strategy for reversing or slowing the progression of neurodegenerative diseases. To effectively respond to this question, it would be necessary to learn more about how neuro-inflammation is induced in the CNS and why it may contribute to different brain pathologies.

Neuroinflammation in Parkinson's disease and experimental parkinsonism

Increasing evidence suggests that some neurodegenerative diseases, as Parkinson's disease (PD), are influenced by marked inflammatory phenomena (Appel, 2009; Hirsch and Hunot, 2009; McAllister and van de Water, 2009). PD is the second most common

neurodegenerative disease after Alzheimer's disease (AD) and represents the most common movement disorder. Currently, about 2% of the population over the age of 60 is affected. Prominent clinical features are motor symptoms (bradykinesia, tremor, rigidity, and postural instability) and non-motor-related symptoms (anosmia, autonomic dysfunction, depression, cognitive deficits and sleep disorders). Major neuropathological hallmarks of the disease are the loss of dopaminergic neurons in the substantia nigra *pars compacta* (SN*pc*) in the midbrain, as well as in other brain regions (Fig. 1A, B), and the formation of intracellular proteinaceous inclusions, mainly containing aggregates of α-synuclein, preferentially localized within affected neurons perikaryon and processes, called Lewy bodies and Lewy neurites, respectively (Braak, 2003). In fact, as AD, PD can be defined as a "proteinopathy", characterized by the accumulation and aggregation of misfolded proteins.

A

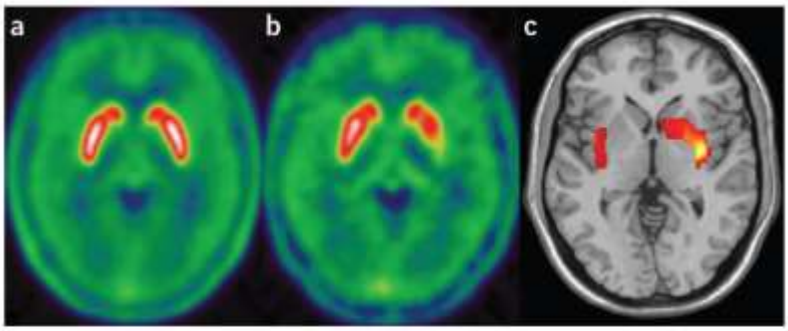

B

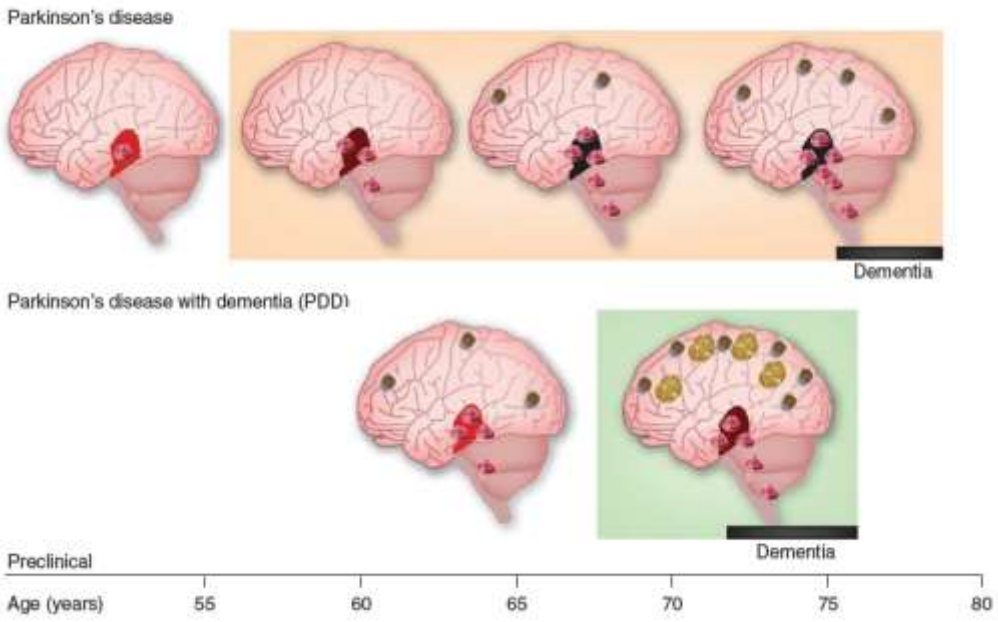

Fig.1 (A) Striatal dopamine innervation assessed by 18F-dopa positron emission tomography. (a) Mean control values for eight control subjects shows high uptake (highest value in white) in the striatum. (b) Subject with Parkinson's disease (right) featuring slowness and rigidity on the right limbs but minimal signs on the left limbs. Uptake is markedly reduced (70% below normal) in the left posterior putamen and reduced to a minor extent in the anterior putamen and caudate of the left hemisphere. (c) SPM2-based analysis (yellow represents the largest statistical difference and red the smallest one), showing the difference in uptake between a and b to highlight the caudorostral pattern of denervation. The statistical map is rendered over the MRI for anatomical localization.
(B) Distribution of Lewy bodies in Parkinson's disease. Diagrammatic representation of pathological data from longitudinally studied cases showing the severity of midbrain dopamine cell loss and Lewy body infiltration over time in an average individual who develops symptoms around 55 years of age versus one who develops symptoms after the age of 70. The severity of dopamine cell loss is related to the duration of symptoms, with those with longer durations having greater cell loss (represented as progressively darker color). The infiltration of Lewy bodies appears more marked in late-onset disease, and in many instances, individuals with late-onset disease have additional age relate pathologies (represented as cortical plaques). Dementia, as indicated in the lower bar, occurs earlier in the disease in older onset individuals, consistent with the greater pathology observed. *(Obeso JA et al., 2010)*

The etiology of the most common forms of PD remains poorly understood. Originally thought to be a disease characterized by loss of one neuronal type, PD is now recognized to have a prominent inflammatory component (Block and Hong, 2007; McGeer and McGeer, 2008; Nagatsu and Sawada, 2005). Post-mortem analysis of the most evident degenerating region of PD patients brains, the SN*pc*, revealed an increased number of activated microglial cells expressing human leukocyte antigen (HLA)-DR and CD11b (McGeer, 1988; Gerhard, 2006) and reactive astrocytes (Forno, 1992; Damier, 1993; Braak, 2007), indicating events of active nerve degeneration. By positron

emission tomography of PD patients it has been shown also a marked increase in the expression by glial cells of peripheral benzodiazepine receptor, reflecting the evident gliosis. In addition, increased levels of cytokines in brain and blood have been reported (Nagatsu and Sawada, 2005). The biochemical and histological hallmarks of the inflammatory activation, such as increased levels of cytokines and glial activation may be intimately related with new processes of neuronal degeneration (Bjorkqvist, 2009; Hirsch and Hunot, 2009). For example, increased levels of pro-inflammatory cytokines, such as TNF-α (Mogi, 1994b; Reale, 2009; Scalzo, 2009) and interferon γ (IFN-γ) (Mount, 2007; Reale, 2009) have been shown in the blood serum of PD patients and post-mortem analysis of PD-affected human brains show a similar increase of these cytokines in the nigrostriatal system (Mogi, 1994a; Mogi, 1994b). The cause of this cytokine-mediated inflammatory reaction observed in the brain, as well as outside the central nervous system (CNS), is poorly understood. It may be potentially mediated by the activation of glial cells that are thought to produce and release these cytokines in the CNS during dopaminergic degeneration (Hirsch, 1998; Nagatsu and Sawada, 2007). Although these inflammatory components are not specific for PD, they might provide useful biomarkers for monitoring the progression of the disease.

As is the case for AD, rare mutations in a number of genes cause familial forms of PD and provide insights into general pathogenic mechanisms (Gasser, 2009). Among these, are mutations in α-synuclein, parkin 1 and 4 (PARK1 and PARK4) and DJ-1 (PARK7). Alpha-synuclein is a 140 amino acid protein that is physiologically present in the presynaptic terminals of neurons. It plays a major role in PD neuropathology: α-synuclein aggregates in PD and becomes the major fibrillar protein included in Lewy bodies in both sporadic and inherited forms of PD. Moreover, point mutations (A53T, A30P, E46K) and gene multiplications of human wild-type α-synuclein are related to

rare familial autosomal-dominant forms of early-onset PD. In PD, the aggregation of α-synuclein from monomers, *via* oligomeric intermediates, into fibrilary aggregates is considered the disease-causing toxic mechanism. Recent reports indicate that the accumulation of α-synuclein can result in the formation of intermediate state oligomers, which lead to neuronal cell death (Danzer, 2007). One line of research proposes that neuronal death itself, with the consequent release of protein aggregates, induces activation of microglia. Additional activation of microglia may be due to the release of aggregated proteins from neurons into the extracellular space (Roodveldt, 2008). This finding is interesting, as the α-synuclein-related neuropathological alterations in sporadic PD and in most of the forms of familial PD were initially thought to be intracellular. Recent data challenge this model and indicate the importance of extracellular α-synuclein aggregates in PD (Lee, 2008). Extracellular α-synuclein is probably phagocytosed by microglia (Zhang, 2005), and aggregated, nitrated, and oxidized forms of α-synuclein have been found to induce microglial activation (Reynolds, 2008; Zhang, 2005). Sensing mechanisms for α-synuclein aggregates are similar to those for viruses and toxins, as extracellular α-synuclein is suggested to be sensed and internalized by cell surface gangliosides in BV-2 cells (a microglia cell line) *in vitro*. The internalization of α-synuclein by microglia is followed by activation of the NADPH oxidase, production of ROS and release of proinflammatory cytokines (Zhan, 2005). However, it has recently been reported that microglial immunity stimulated by nitrated α-synuclein is regulated by CD4+ T regulatory (Treg) cells. Treg cells may alter the proteome of microglia in response to nitrated α-synuclein, thereby protecting dopaminergic neurons (Benner, 2008; Reynolds, 2008). A characteristic of dopaminergic neurons of the SN is an increase of the intracellular oxidative processes related to the synthesis of dopamine (Thomas, 2008), making them particularly

vulnerable to oxidative stress. In addition, high rates of catecholamine metabolism drive the production of neuromelanin, and high amounts of neuromelanin are suspected to increase the vulnerability of dopaminergic midbrain neurons to oxidative stress (Kastner; Herrero, 1993a-b). In fact, a direct effect of neuromelanin on the activation of microglia through the activation of the NF-κB pathway has been shown in cultures of rodent microglial cells (Wilms, 2003).

As the vast majority of PD cases are sporadic, environmental factors that interact with common, but less penetrant, susceptibility genes are likely to influence the onset of most cases of sporadic PD (Tansey, 2007). PD-causing toxins, like insecticide or drug derivate, are known to induce neuronal degeneration associated with reactive microgliosis, which exacerbates neurotoxicity.

The role of bacterial or viral infection as an initiating factor in human PD is unclear, but intracranial infusion of the bacterial lipopolisaccaride (LPS) in rodents is used as an alternative model for microglia-induced loss dopaminergic neurons, evaluated by tyrosine hydroxylase (TH) immunolabeling (Castaño, 2002; Herrera, 2000). LPS-induced inflammation can also synergize with mutations in *α-synuclein* and *Parkin* genes, which are associated to familial PD, to potentiate the loss of TH-positive neurons in animal models (Gao, 2008). Whether other neuronal populations are affected remains to be established.

PD is unique among the neurodegenerative disorders, in that we understand a great deal about its circuitry and physiology, which are to a large extent caused by the loss of the dopaminergic neurons of the SN*pc* (Fig. 3). This knowledge has led to effective symptomatic treatment of the motor manifestations of the illness, initially with levodopa (l-DOPA) and then later with dopamine receptor agonists and deep brain stimulation (Obeso, 2010).

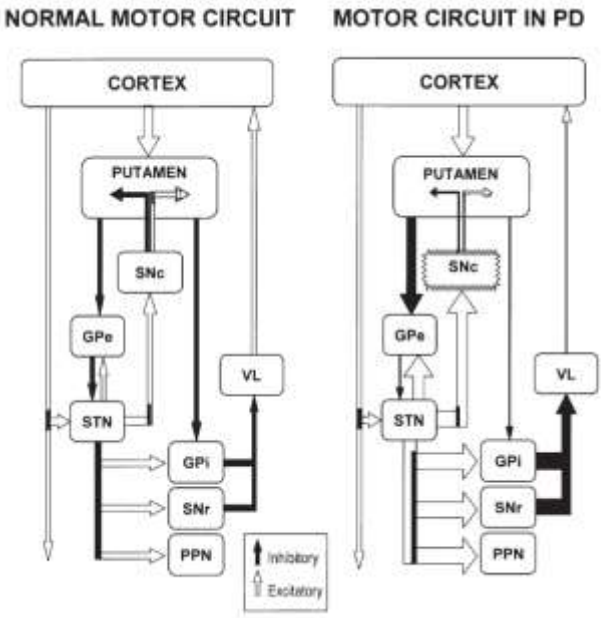

Fig. 2. Summary of the main connections of the "motor circuit" of the basal ganglia. In the normal state, the putamen receives afferents from the motor and somatosensory cortical areas and communicates with the GPi/SNr through a direct inhibitory pathway and though a multisynaptic (GPe, STN) indirect pathway. Dopamine is believed to modulate striatal activity, mainly by inhibiting the indirect and facilitating the direct pathways. In Parkinson's disease (PD), dopamine deficiency leads to increased inhibitory activity from the putamen onto the GPe and disinhibition of the STN. In turns, STN hyperactivity by virtue of its glutamatergic action produces excessive excitation of the GPi/SNr neurons, which overinhibit the thalamocortical and brain stem motor centers. (*Obeso JA et al., 2002)*

Yet, the efficacy of symptomatic therapies wanes after five to ten years, and patients develop increasing motor impairment, gait and postural difficulties, and cognitive dysfunction. The major goal of medicine is to develop disease-modifying treatments, therefore a better understanding of the disease pathophysiology, embodied in better animal models, is necessary.

In order to be both a good model of human PD and a good test subject for new therapies, the ideal animal model should have a number of characteristic features: First, there should be a normal complement of dopaminergic neurons at birth, more than 50% of which are then selectively, gradually and measurably lost in adulthood; Second, the model should have motor deficits, including the cardinal symptoms of PD; Third, it should show the characteristic Lewy body neuropathology; Fourth, if the model is genetic, it should be based on a single mutation to allow robust propagation and facilitate crossing with enhancer, or suppressor, strains; Fifth, it should have a relatively a short disease time-course of a few months, allowing rapid and less costly screening of therapeutic agents.

Traditional animal models of PD are based on the use of toxins, which selectively accumulate in the SN*pc* neurons, causing cellular dysfunction and death. 6-hydroxydopamine (6-OHDA) is one of such compounds that produce SN degeneration in mice, rats, cats and primates. The standard approach is to use 6-OHDA to create a unilateral lesion in the brain, which is followed by administration of amphetamine. This causes the animal to start rotating 'away from' the lesion. This rotary behavior can be reversed, for example by treatment with dopaminergic stem cells that restore normal circuitry (Marin, 2006; Jenner, 2008).

The insecticide rotenone can also be used to create an animal model, as its administration specifically inhibits the complex I of the mitochondrial electron-transport chain. Betarbet and colleagues (Betarbet, 2007) produced a model of PD by infusing rats intravenously with rotenone. The rats developed progressive degeneration of nigrostriatal neurons, as well as cytoplasmic inclusions reminiscent of Lewy bodies. They also exhibited bradykinesia, postural instability and an unsteady gait, all of which improved after treatment with the dopamine agonist apomorphine. Other compounds that have been shown to produce selective degeneration of dopaminergic neurons include paraquat and trichloroethylene, both of which have been implicated in the causation of human Parkinson's disease. However, there is substantial variability in all of these models, which limits their usefulness for therapeutic development.

The best characterized toxin-based model of PD uses the MPTP (1-methyl-4-phenyl-1,2,3,6-tetrahydropyridine). Although MPTP-treated monkeys remain the gold standard for pre-clinical testing of new therapies, most of the studies geared toward unraveling the mechanisms underlying the dopaminergic neuronal death have been performed in mice using several different well validated regimens. MPTP has become the most commonly used, for at least three reasons. First, MPTP is the only known

dopaminergic neurotoxin capable of causing a clinical picture in both humans and monkeys indistinguishable from PD (Langston, 1983). Second, although handling MPTP requires a series of precautions, its use is not otherwise technically challenging: it does not require any particular equipment such as stereotaxic frame, nor it requires surgery on live animals as for 6-hydroxidopamine or rotenone. Third, MPTP produces a reliable and reproducible lesion of nigro-striatal dopaminergic pathway after its systemic administration, which is often not the case for other documented toxins (Bove, 2006). The importance of this compound was discovered accidentally in 1982, when a group of young drug takers in California developed subacute onset of severe parkinsonism, caused by contamination of a synthetic opiate with MPTP. The post-mortem study of human subjects accidentally intoxicated showed not only the characteristic dopaminergic degeneration already observed in sporadic PD, but also the same maintained glial reaction in the SN*pc* evidenced by activated microglia and reactive astrocytes, many years after the neurotoxin insult (Langston, 1999).

The administration of MPTP was subsequently shown to model Parkinson's disease in both mice and primates, by inhibiting part of the electron-transport chain in dopaminergic neurons of the SN. The metabolism of MPTP is a complex, multistep process (Tipton and Singer, 1993; Dauer and Przedborski, 2003) (Fig. 3). After systemic administration, the highly lipophilic MPTP rapidly crosses the blood-brain-barrier. Once in brain, the pro-toxin MPTP is assumed by glial cells, possibly astrocytes, metabolized in 1-methyl-4-phenyl-2,3-dihydropyridinium by the monoamine oxidase B (MAO-B) and then (hypothetically by spontaneous oxidation) transform into 1-methyl-4-phenylpyridinium (MPP^+), which is the active toxic compound. Thereafter, MPP^+ is released into the extracellular space. Since MPP^+, unlike its precursor MPTP, is a polar molecule, it cannot freely enter cells, but depends on plasma membrane carriers

to gain access to neurons. In particular, MPP^+ has a high affinity for the dopamine transporter localized on the plasma membrane of dopaminergic neurons, as well as for serotonin transporters (Javitch, 2000). Once inside dopaminergic neurons, MMP^+ can be sequestered into synaptosomal vesicles (Liu Y, 1992), or concentrate within mitochondria (Ramsay, 1986), where MPP^+ inhibits part of the electron-transport chain by specifically inhibiting the complex I. This results in the reduction in ATP synthesis and, more importantly, in the increased production of free radicals, which causes oxidative stress and activation of programmed cell death molecular pathways.

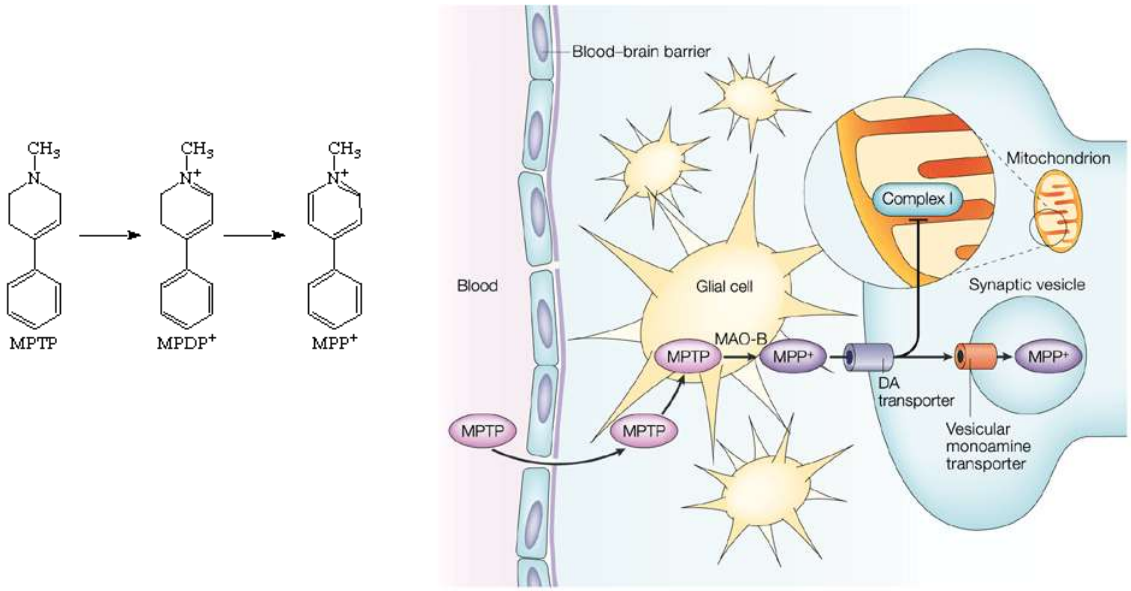

Fig. 3. MPTP metabolism. MPTP is a pro-toxin that, due to its lipophilic nature, rapidly crosses the blood–brain barrier and is metabolized to 1-methyl-4-phenyl-2,3-dihydropyridinium (MPDP+) by the enzyme monoamine oxidase B (MAO-B) present in glial cells. Here, probably by spontaneous oxidation, it is converted in 1-methyl-4-phenylpyridinium (MPP+), the active toxic compound. MPP+ is released in the extracellular space and taken up by the DA transporter present on the plasma membrane of the synaptic endings of DA neurons. Once inside DA neurons, MPP+ is concentrated by an active process within the mitochondria, where it impairs mitochondrial respiration by inhibiting complex I of the electron transport chain *(Vila and Przedborski, 2003)*

MPTP toxicity in primates replicates all of the cardinal clinical signs of Parkinson's disease. It has, therefore, proved to be useful for studying the striatal circuitry involved in Parkinson's disease pathophysiology. MPTP causes loss of neurons located in the SN*pc* and in the *locus coeruleus*, which are particularly

vulnerable to the pathologic process in Parkinson's disease, whereas other neurons, such as those of the dorsal motor nucleus of the vagus and of the *nucleus basalis* of Meynert, are spared. Acute administration of MPTP does not induce Lewy body formation, although chronic administration triggers the production of α-synuclein inclusions.

One of the most interesting aspects concerning the pathophysiology of MPTP-induced parkinsonism in monkey is a prominent glial response, which lasts years after MPTP injections and establishment of a stable parkinsonism. This inflammatory reaction is confined to the SN*pc* and striatum (McGeer, 2003; Barcia, 2004) and is simultaneous to a persistent increase in TNF-α levels in the blood (Barcia, 2005). This evidence indicates that the glial cell reaction and inflammatory response persist over a period of at least 2 years in parkinsonian primates, even though new neurotoxic insults are apparently absent. This combines with observations on autopic human brain of drug addicted and PD patients (Langston, 1999; McGeer, 2004). The current hypothesis is that in PD as well as in MPTP-induced parkinsonism, the initial neuronal damage triggers glial activation and a neuroinflammatory response, which are able to perpetuate themselves, possibly contributing to progressive neuronal loss. To date, the mechanisms involved in the perpetuation of this glial cell activation in brain remain unclear. Pro-inflammatory cytokines like TNF-α and IFN-γ are good candidates (Tedeschi, 1986; Dickson, 1993; Benveniste, 1994; Hanisch, 2002), although, it has not been clearly demonstrated whether microglia, or astroglia, produce and release these cytokines *in vivo*, or how this process may take place in parkinsonism. On the contrary, it is well known that TNF-α and IFN-γ are important cytokines involved in dopaminergic degeneration. In fact, blocking TNF-α activity protects against dopaminergic neuronal loss, and mice lacking the TNF-α receptor are protected against MPTP-induced degeneration (Sriram, 2002; Ferger, 2004; McCoy, 2006; Sriram, 2006). Similarly, IFN-

γ knock-out mice are less susceptible to MPTP-induced neuronal loss and it has been reported that dopaminergic neuronal loss may be mediated by IFN-γ (Mount, 2007). However, very little is known about the mechanisms involving pro-inflammatory cytokines in microglia and astroglia activation during dopaminergic degeneration. It has been recently suggested that astrocytes may amplify the neuro-toxic effects initiated by microglia in dopaminergic degeneration *in vitro*, but it is unclear how this intercellular crosstalk may actually occur *in vivo* (Saijo, 2009).

Astrogliosis and microgiosis have been reported in the SN and striatum of mice exposed to MPTP, but subjected to a different time course (Czlonkowska, 2001; Breidert, 2002): a notable microglial activation is observed 2 days after MPTP treatment, while the astrocytic reaction peaks 5 days after MPTP injection and is less transient than the microglial one (Breidert, 2002) (Fig. 4). These two cell types also differ in term of the cell proliferation activities, as newborn microglial cells can be identified by bromodeoxyuridine (BrdU) labelling in both MPTP-treated mice and monkeys, while no BrdU staining is observed in astrocytes (Tandé, 2006; Brochard, 2009). Therefore, microgliosis involves both increase in the number of microglial cells and prominent morphological changes, while astrocytosis is only the result of phenotypical change (increased expression of GFAP and morphological changes). So far, the role of astrocytes in parkinsonian syndromes is poorly understood, but it can be hypothesized that a direct participation of astrocytes to neuronal death initiation is unlikely because it takes place too late in the degenerative process. Only a selective blockade of the astroglial reaction may help in clarifying the contribution of astrocytes in Parkinson's disease.

Cells of the peripheral immune system may also play a part in neurodegeneration, as observed in different animal models. Kurkowska-Jastrzebska and

colleagues (Kurkowska-Jastrzebska, 1999) reported infiltration of T lymphocytes in the brains of mice exposed to MPTP and, more recently, a high number of infiltrating CD8+ T-cytotoxic and CD4+ T-helper cells in the nigro-striatal pathway after MPTP injection in mice has been described (Brochard, 2009). Since no B lymphocytes were detected after MPTP exposure, this cell infiltration must be selective for T cells. Furthermore, this infiltration selectively targeted the nigro-striatal pathway, as no T cells were observed in brain regions not affected by neuron degeneration. T-cell transmigration was already evident 2 days after MPTP injection, increasing progressively for at least 7 days, to cease after 21 days (Brochard, 2009). Therefore, brain infiltration by T cells happens after microglial activation, but precedes astrogliosis (Fig. 4). In addition, no intracerebral clonal expansion of T cells was detected, which suggested their continuous extravasation and long-term survival in the brain parenchyma. By transfer strategies, it has been shown that CD4+ T-helper cells, but not CD8+ T-cytotoxic cells, were deleterious for dopaminergic neuron survival, suggesting that the adaptive immune system might contribute to neuronal degeneration in the MPTP mouse model (Brochard, 2009). The mechanisms involved in such cell-specific and region-specific T-cell recruitment are still unknown, but they might involve early microglial cell activation and innate neuroinflammatory processes that could modify the local microenvironment. The contribution of T cells to dopaminergic neuron degeneration supports findings of a recent study, showing that nitrated α-synuclein immunity accelerates the degeneration of dopaminergic neurons in the SN (Benner, 2008).

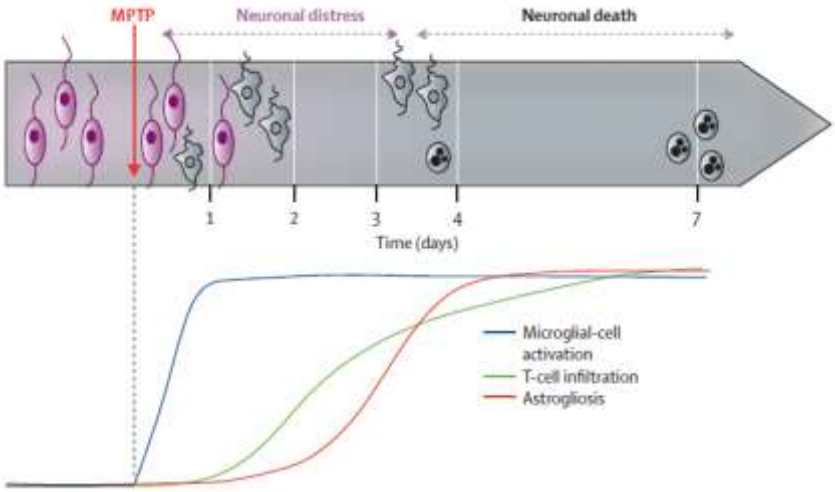

Fig. 4. Sequence of the cellular events occurring in the substantia nigra after MPTP injection in mice. After exposure to MPTP, some dopaminergic neurons are affected by the neurotoxin, leading to neuronal distress. This distress phase might last a few days (3–4 days) and is followed by destruction and elimination of the affected neuron cell body. 7 days after exposure, dopaminergic cell death usually does not progress further. During this time frame, microglial cells are rapidly activated (12–24 h after exposure to MPTP), well before the physical destruction and elimination of dopaminergic nerve cells. Therefore, microglial cells are probably highly sensitive to mild neuropathological changes. The astroglial cell reaction happens later, usually 3–4 days after exposure to MPTP, concomitantly with dopaminergic cell death. Infiltration of T lymphocytes into the brain is seen as early as 2 days after exposure to MPTP and increases continuously for up to 7 days. The inflammatory reaction of activated microglial cells within the substantia nigra might contribute to the site-specific recruitment of these adaptive immune cells. MPTP=1-methyl-4-phenyl-1,2,3,6-tetra-hydro-pyridine *(Hirsch and Hunot, 2009)*.

These data from animal models indicate that the mechanism of cell death in the nigrostriatal pathway involves non-neuronal cells. An analysis of the molecular factors involved in these cellular interactions in MPTP animal models might enable the identification of targets able to reduce microglial cell activation and lymphocytic infiltration and, hence, neuronal degeneration. Overall, although a large number of therapeutic approaches have been tried in the MPTP model, their predictive efficacy in humans has been inconsistent (Beal, 2001). Even though the extent to which MPTP-based models mimic the entirety of the human condition is controversial, they are considered a convenient mean to quickly replicate much of the cellular dysfunction seen in Parkinson's disease.

Remodeling of brain extracellular matrix in neurodegeneration: what we know about metalloproteinases in PD and parkinsonism?

Compared to systemic extracellular matrix (ECM), the adult brain ECM is unusual in at least two respects. First, unlike other organs, the brain exhibits a limited, ultrastructurally well-defined, stromal space. Despite the elegant descriptions by Camillo Golgi and Santiago Ramon y Cajal at the turn of the previous century, prior to the 1970s, it has been generally accepted that brain tissue consists predominantly of closely apposed neurons and glia, leaving little room for significant amounts of ECM. The advent of several new technologies gradually revised this theory, demonstrating a variety of ECM molecules filling significant amounts of ECM space (Yamaguchi, 2000). Second, common ECM components of systemic organs (eg, fibronectin and collagen) are virtually absent from the adult brain ECM, while different types of proteoglycans are abundantly expressed and localized within intercellular spaces between neurons and glia (Bandtlow, 2000; Yamaguchi, 2000; Dityatev and Schachner, 2003). In retrospect, what was previously described as a "perineuronal net" (PNN) by Golgi and Ramon y Cajal in 1890 is consistent with the "new discoveries" of brain ECM. PNNs are reticular networks, constituted by ECM proteins, which embrace the surface of neuronal cell bodies and proximal dendrites and fill the space between neurons and astrocytic processes. Histologically bland in their appearance, PNNs vary in type and distribution, each with a potentially unique molecular structure surrounding a wide variety of neurons (Dityatev and Schachner, 2003). This structure includes lecticans, hyaluronic acid (HA), tenascin-C and tenascin-R. It is thought that the HA–lecticans–tenascin complexes deposited on the neuronal surface may form a repulsive barrier against approaching axons and dendrites. The absence of synaptic contacts along those neuronal surfaces covered by PNNs supports this hypothesis. Although the

physiological role of PNNs has not been fully elucidated, their postnatal appearance suggests a role in limiting the development of new synaptic contacts (Yamaguchi, 2000). PNNs also contain a variety of proteoglycans, the diversity of which dependent on the differential expression of genes encoding core proteins, on alternative splicing and on transcription–termination, as well as on variations in the length and types of glycosaminoglycan (GAG) side chains. Chondroitin sulfate (CS) or heparan sulfate (HS) side chains constitute most of the CNS proteoglycans; some of them belong to the ECM, while others are ether bound to the cell surface by a transmembrane domain or anchored with short tails made of glycosyl phosphatidylinositol (GPI). The ECM capacity of binding growth factors via HS and CS modulates their interaction with the cell surface. In fact, the localization and biological activity of factors such as the fibroblast growth factor (FGF) strongly depend on the presence and composition of the ECM, where the differential binding characteristics of specific HS structures can potentiate, or inhibit, its biological activity (Bandtlow and Zimmermann, 2000). Other growth factor families, i.e. the vascular endothelial growth factor (VEGF) and the platelet-derived growth factor (PDGF), are known to bind to heparin/HS, which can modulate their biological activities (Raine and Ros, 1992; Neufeld, 1999).

Brain ECM provides not just physical support to the various cell types herein present, but also a local homeostatic control crucial for the survival of differentiated neurons, which are believed incapable of regeneration (Dityatev, 2008; Faissner, 2010). In addition to the control of a plethora of cell signaling molecules, the ECM can also physically buffer ions and neurotransmitters associated with synaptic activity.

Several studies have shown changes in the ECM associated with neuropathological states, but a few studies have really demonstrated a mechanistic connection between these changes and neuronal death. Neurodegenerative states can be

divided into two groups, based on the major changes in ECM (Fig. 4). The first group comprehends age-related progressive neurodegenerative diseases, such as AD, characterized by changes in the expression of proteoglycans and by formation of protein aggregates and amyloidosis. It is not known whether protein aggregation, or deposition, is the primary event, which successively leads to changes in proteoglycan expression, or whether the two processes are interconnected. An alternative could be that changes in proteoglycans are the primary events that trigger protein aggregation. All these changes are, however, accompanied by secondary microglial activation.

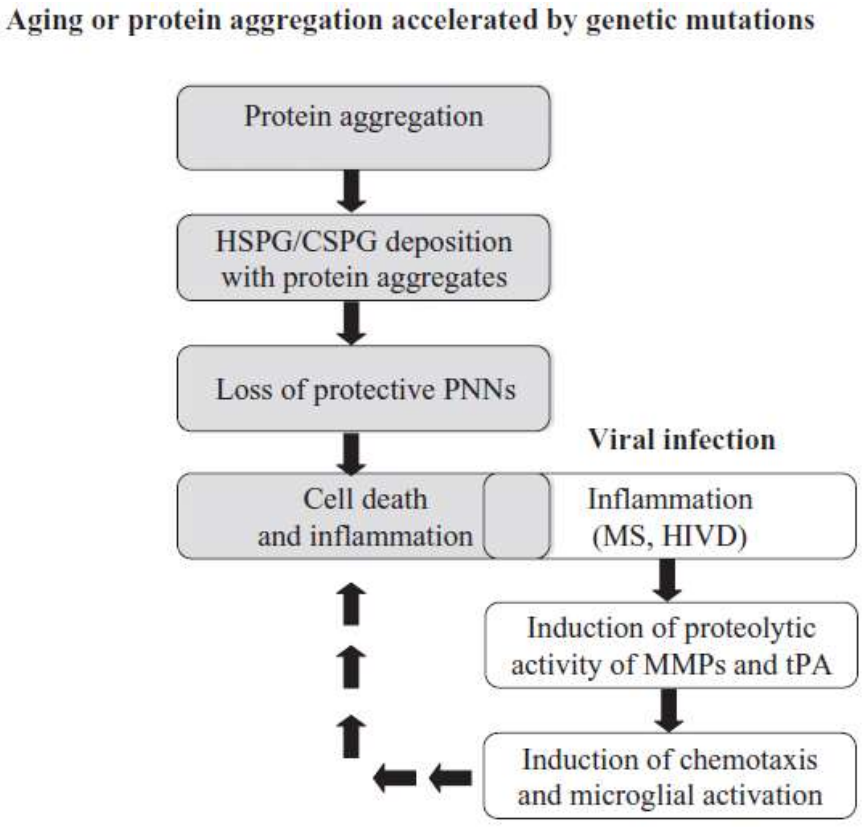

Fig. 4. Possible mechanisms of extracellular matrix (ECM)-related neurodegeneration. Aging or protein aggregation accelerated by genetic mutation can be associated with ECM alterations that would result in the co-deposition of ECM components [eg, heparan sulfate proteoglycans (HSPGs) and chondroitin sulfate proteoglycans (CSPGs)]. Those ECM alterations can result in the loss of protective perineuronal nets (PNNs) and increased susceptibility to cell death. Dying neurons can induce inflammation, degradation of ECM and induction of a more robust inflammatory response. Alternatively, inflammatory-induced neurodegeneration can induce ECM degradation through proteolytic activity [eg, matrix metalloproteinase (MMPs) and tissue plasminogen activator (tPA)], induction of chemotaxis and microglial activation. The resulting trafficking of inflammatory cells and secretion of cytokines can induce neuronal death that would feed the vicious cycle. Abbreviations: MS = multiple sclerosis; HIVD = human immunodeficiency virus dementia *(Bonneh-Barkay and Wiley, 2009).*

Up to date, no clear correlation between ECM breakdown and neuronal death is known. From the work of Brückener and colleagues (Brückener, 1999; Morawski, 2010) it seems that neurons surrounded by PNNs are spared from neurodegenerative changes in AD. Breakdown of the PNNs, mostly around parvalbumin-positive neurons, but without determining the loss, suggests changes in the neuronal environment that could affect their function or susceptibility to further insults.

The two major systems that regulate brain ECM composition in health and diseases are the matrix metalloproteinases (MMPs) and plasminogen activator (PAs)-plasmine system (Teesalu, 2002; Yong, 2005; Adibhatla, 2008; Bonneh-Barkay, 2009; Candelario-Jalil, 2009). MMPs are a large family of more than 20 members, among which two collagenases, the metalloproteinase-2 (MMP-2) and metalloproteinase-9 (MMP-9) are the most abundantly expressed in brain. Synthesized as pro-enzymes, all MMPs need the removal of a pro-peptide, which masks the zinc-containing catalytic site of the protein, for their enzymatic activation (Page-McCaw, 2007) (Fig. 5). MMPs are synchronously expressed with their tissue inhibitors of metalloproteinases (TIMPs), a family formed by 4 members, the role of which is highly complex, ranging from MMP activation and/or silencing, in strict relation to the their amount and timing of production. Activation of MMPs can also be determined by the serine protease plasmin, generated by the cleavage of plasminogen by the tissue or urokinase-like plasminogen activators (tPA and uPA, respectively) (Michaluk and Kaczmarek, 2007; Adibhatla, 2008) functionally linking the two proteolytic systems.

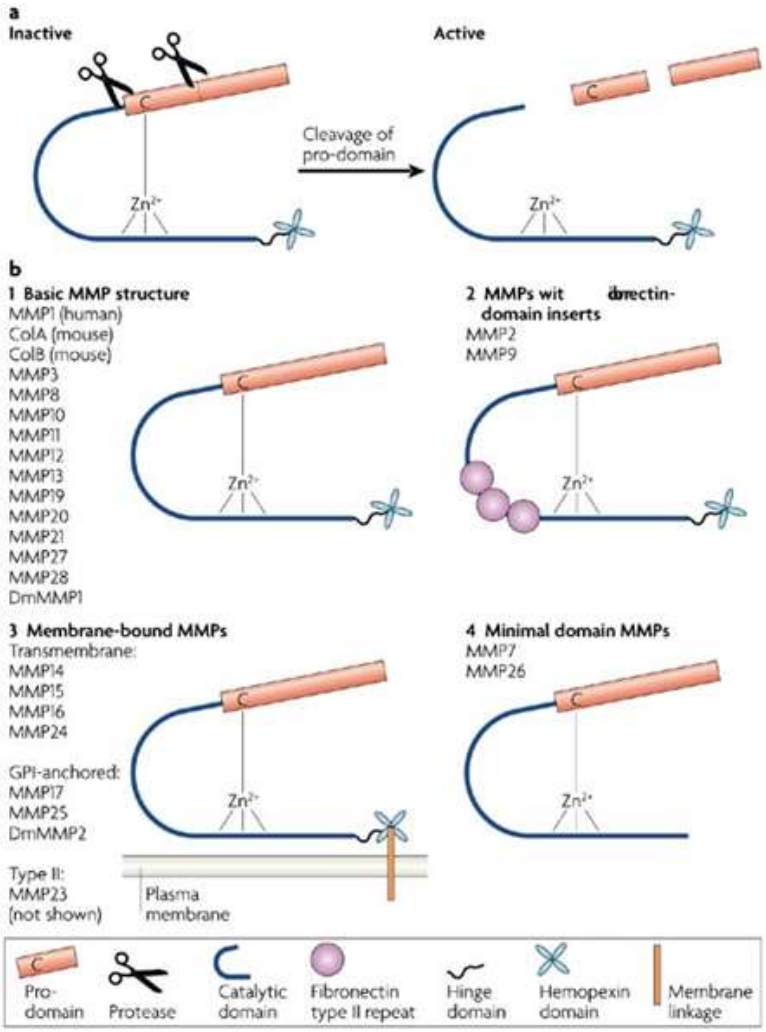

Fig. 5. Matrix metalloproteinase family. (a) MMPs are expressed as pro-proteins. A conserved Cys residue in the pro-domain coordinates the zinc ion, which would otherwise be used for catalysis. The pro-domain is removed by a combination of a cleavage in the domain and a cleavage between the pro-domain and the catalytic domain. (b) Most MMPs share a conserved domain structure of pro-domain, catalytic domain, hinge region and hemopexin domain (1). All MMPs are synthesized with a signal peptide, which is cleaved during transport through the secretory pathway. MMP2 and MMP9 have three fibronectin type II repeats in their catalytic domains (2). Membrane type MMPs (MT-MMPs) are linked to the plasma membrane either by a transmembrane domain or by a glycosylphosphatidylinositol (GPI) linkage, attached to the hemopexin domain (3). Minimal MMPs lack the hinge and hemopexin domains (4). MMP21 has a truncated hinge domain. Drosophila melanogaster DmMMP2 has an insertion of 214 amino acids into its hinge domain. MMP23 (not shown) has a non-conserved N-terminal domain that consists of an immunoglobulin IgC2 domain and a ShKT domain; it is unclear if MMP23 contains a Cys residue switch. *(Page-McCaw A, 2007)*

PAs are secreted in a precursor form as single-chain polypeptides and *in vitro* are converted by plasmin to active double-chain forms. Regulation of PAs activities in the nervous system can occur at multiple levels: transcription, translation, secretion and inhibition by anti-proteases (Benarroch, 2007; Zori, 2008; Mitsui, 2008). Despite high

levels of tPA mRNA in the hippocampus CA1 region, for example, protein and enzymatic assays do not show evidence for tPA presence, suggesting a stringent translational control (Salles, 2002). Synaptic signaling can ease this control and lead to tPA secretion and activation in the extracellular space. Inhibition of tPA activity is under tight control of a variety of anti-proteases of the serpin family (eg, protease-nexin 1, neuroserpin and plasminogen activator inhibitor 1 (Gualandris, 1996). Some of the tPA activities are not linked to plasminogen activation, as tPA can directly cleave the NR1 subunit of the NMDA receptor, enhance NMDA-mediated intracellular calcium levels and, not ultimately, promote MMP-9 activity up-regulation and ECM degradation in response to specific functional inputs, thus ultimately determining synaptic plasticity or neuronal degeneration (Madani, 2003). tPA is expressed by both neurons and microglial cells, especially in brain regions involved in learning and memory. As the activity of tPA in neural tissue is related to neurite outgrowth, regeneration and migration, this has suggested that it might be involved in physiological processes requiring elevated neuronal plasticity (Melchor and Strickland, 2005). Moreover, the tPA/plasmin system can contribute to neuroinflammation. Studies in vitro have demonstrated that, under glutamate stimulation, both wild type neurons and microglia release tPA, which in turn elicits microglia activation in an autocrine/paracrine manner by binding thr annexin II receptor (Siao & Tsirka, 2002). Recently, experiments conducted on co-cultures of monocytes and brain endothelial cells showed that monocytes induce tPA release by endothelial cells. This subsequently activates the extracellular signal-related kinase (ERK1/2) signaling, which is involved in monocyte diapedesis (Reijerkerk, 2008).

MMPs are constitutively secreted; however, they can be trapped at the cell surface by either binding to cell adhesion molecules and cell surface proteoglycans or

through transmembrane domains (the membrane-type of MMPs, MT-MMP). Another subgroup of MMPs comprehend the A disintegrin and metalloproteinases (ADAMs) and ADAMs with thrombospondin motifs (ADAMTS) (Page-McCaw, 2007). ADAMs are membrane-anchored enzymes that possess both proteolytic and adhesive activities. They are involved in the shedding of cytokines, receptors and growth factors from the cell surface, as well as in the adhesion to integrins. The TNFα-converting enzyme, or ADAM17, is the most characterized protease releasing TNFα from the cell surface (Bridges and Bowditch, 2005). ADAMTSs are secreted enzymes involved in the cleavage of ECM proteoglycans and in the processing of collagen (Porter, 2005).

Several secreted MMPs have been shown to contribute to the migratory ability of monocytes and in the motility of astrocytes (Vos, 2000; Matias-Roman, 2005; Ogier, 2006; Sithu, 2007). In brain, they are secreted by neurons, oligodendrocytes, microglia and endothelial cells (Lo EH, 2002). Similarly, in the CNS TIMPs are expressed in neurons and astrocytes (Crocker, 2004). The abundant expression of some metalloproteinase members following nervous system injuries leads to several undesirable outcomes, including the breakdown of the blood–brain barrier, the development of demyelination (Yong, 2001), as the deposition of purified MMPs in the brain parenchyma results in the loss of myelin (Anthony, 1998) and axonal injury (Newman, 2001). However, it is not clear whether these outcomes are primary or secondary to other processes that develop as the result of the large amounts of MMPs released into the brain parenchyma.

The modulation of neuroinflammation is another significant outcome of the changes in metalloproteinase expression, release and activation following nervous system injury. Several MMPs can generate encephalogenic fragments from CNS proteins, examples of which include the cleavage of myelin basic protein into fragments

producing neuroinflammation in animals (Proost, 1993). Many inflammatory molecules, such as TNFα, are synthesized as precursors, which require processing by metalloproteinase to transform into their active form. On the other hand, MMPs can also degrade inflammatory molecules, such as the IL-1β, terminating their activity (Ito, 1996). By their interaction with chemokines, MMPs also modulate leukocyte trafficking into tissues (McQuibban, 2000; Van Den Steen, 2003; Li, 2002; Nagase, 2006). The interaction of MMPs and chemokines, besides producing pro- and/ or anti-inflammatory signals, can also generate toxic molecules. For example, MMP-2, by removing four amino acids from the N-terminus of the chemokine CXCL12, produces a neurotoxic species of this chemokine (Zhang, 2003).

Interaction among proteases can significantly alter the predicted outcome of a single proteolytic activity. For example, thrombin and MMP-9 conjunct activities mediate the killing of neurons in the mouse brain *in vivo* (Xue, 2006). Perhaps the most significant consequence of the overexpression of MMPs in the CNS is the regulation of cell survival and death. Various mechanisms have been proposed to contribute to metalloproteinase-mediated cell death (Fig.6) (Yong, 2005).

The adherence of cells to the ECM provides survival signals through mechanisms that include activation of integrin receptors engaged in the linkage with particular ECM proteins. When such anchored cells are detached from the substratum, the loss of integrin signaling can result in apoptosis, a phenomenon that has been referred to as anoikis ('homelessness'). An advantage of anoikis is that cells that are detached from their usual locations do not become the seed of a tumor elsewhere. Therefore, in the CNS, the degradation of ECM proteins and the loss of integrin signaling by abnormally expressed MMPs affect cell survival (Gu, 2002; Zalewska, 2002).

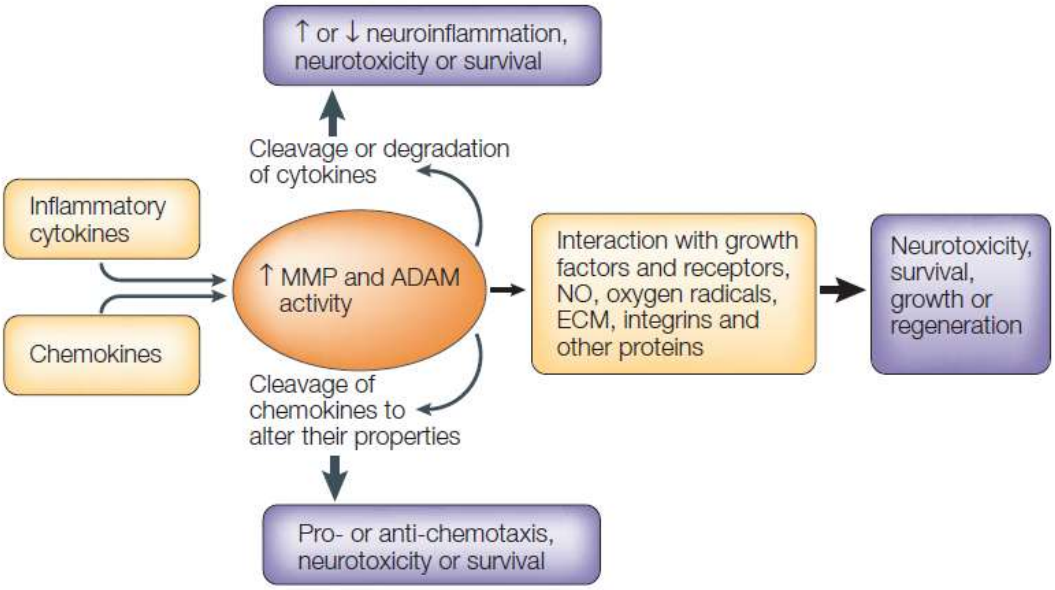

Fig. 6. Interactions between metalloproteinases, cytokines, chemokines and other molecules present at a site of injury and their consequences. The expression and activity of metalloproteinases can be up-regulated by inflammatory cytokines and chemokines; the elevated protease activity can, in turn, process cytokines and chemokines to alter their properties. In addition, metalloproteinase activity can result in the processing of growth factors and receptors, free radicals, extracellular matrix (ECM), integrins and other proteins. The net result of these interactions includes the alteration of the extent of neuroinflammation, neurotoxicity or survival, and growth and regeneration. Therefore, it is not only important to determine whether there is a change in metalloproteinase activity, but also whether this affects the interactions of MMPs with other molecules in their microenvironment. ADAM, A disintegrin and metalloproteinase; MMP, matrix metalloproteinase; NO, nitric oxide *(Yong, 2005)*.

Notably, the disintegrin domain of ADAMs can also interact with integrins (Bridges & Bowditch, 2005) and MMPs can directly engage integrin-mediated signaling (Dumin, 2001). The direct disruption of survival-promoting components of the ECM, such as laminin, can also determine death of ECM-anchored neurons (Chintala, 2002; Gu, 2005). Besides their direct action, MMPs also interact with other functional molecules in their vicinity and alter their properties. An example is the interaction between MMP-9 and nitric oxide to form a stable S-nitrosylated MMP-9, which is toxic for neurons. S-nitrosylated MMP-9 has been detected both *in vitro* and *in vivo*, in an animal model of stroke injury (Gu, 2002).

Reactive oxygen species produced after CNS injuries might contribute to induction and/or activation of MMPs, thereby exacerbating injury, although inactivation

of MMPs by oxidants through the modification of amino acids crucial for the enzymatic activity can also occur (Parks, 2004).

Evidences are emerging of long-term effects of MMPs in neurodegenerative diseases, including damage to the white matter in patients with vascular cognitive impairment, degradation of amyloid peptides in Alzheimer's disease and apoptosis of dopaminergic neurons in Parkinson's disease. Lorenzl and colleagues (Lorenzl, 2002) investigated levels and tissue localization of MMP-2 and MMP-9 in *post-mortem* brain tissue from parkinsonian patients and age-matched control. Results obtained by gel zymography on brain areas homogenates, suggested a reduction in MMP-2 levels in the SN of PD compared to control cases, while those in the cortex and hippocampus remained unaltered (Lorenzl, 2002). MMP-9 levels were always unaffected in all brain regions investigated. Furthermore, by immunohistochemistry, it appeared that MMP-2 was localized primarily in astrocytes and microglia cells, whereas MMP-9 was predominantly neuronal. Levels of TIMP-1, one of the endogenous tissue inhibitors of MMPs, were also significantly elevated in the SN of PD patient brains *versus* controls, while those of TIMP-2 were unchanged (Lorenzl, 2002). The same authors also analyzed MMPs levels in the cerebrospinal fluid of PD patients and in mice acutely injected with MPTP, although quality of results is quite discussible (Lorenzl, 2003; Lorenzl, 2004).

Recent studies *in vitro* have implicated MMPs in the death of dopaminergic neurons. Apoptotic dopaminergic neurons release MMP-3, a MMP associated to inflammatory processes throughout tissues, which acts as a microglia-activating molecule (Mun-Bryce, 2002; Woo, 2008). This suggests that, besides its role in degrading extracellular macromolecules, MMP3 is also a signaling molecule, mediating the interaction between apoptotic neurons and microglia (Kim, 2005). It has

demonstrated that primary mouse mesencephalic cells in culture die when treated with BH4 (tetrahydrobiopterin), a selective dopaminergic neuronal toxin; however, treatment with the MMP-3 inhibitor NNGH (N-isobutyl-N-[4-methoxyphenylsulfonyl]-glycylhydroxamic acid) prolongs cell survival by decreasing the release of TNFα from activated microglia. These data strongly suggest that microglia, activated by MMP-3, causes neuronal degeneration by releasing the pro-inflammatory cytokine TNFα. Furthermore, MMP-3 induces dopaminergic neuron apoptosis not only by this TNFα-mediated extracellular mechanism, but also *via* intracellular signalling, by activating the pro-apoptotic enzyme caspase 3. The mechanisms ruling this intracellular action of MMP3 are still unclear (Choi, 2008).

It has been recently demonstrated that monomeric α-synuclein increases, in a dose-dependent manner, both mRNA level and activity of MMP-9, but not MMP-2, in cultured rat primary astrocytes and microglia (So, 2010). The maximal stimulation is observed in the presence of 50 nM alpha-synuclein. In contrast, tPA activity is decreased, with only marginal changes in the level of mRNA encoding tPA, if any. Overexpression of α-synuclein in rat primary astrocytes also increases MMP-9 activity in the same cell type (So, 2010). MMPs secreted from the α-synuclein–stimulated microglia activate the microglia itself by stimulating the protease-activated receptor-1 (PAR-1) in both autocrine and paracrine manner (Lee, 2010). Other findings obtained *in vitro* in a well-characterized model of pathological α-synuclein aggregation indicate that MMP-1 and MMP-3 may also influence the pathogenesis of PD *in vivo* by the generation of specific aggregation-enhancing α-synuclein fragments, which result from limited proteolysis (Levin, 2009). Altogether, these data are consistent with the possibility that alterations in MMPs/TIMPs levels may contribute to PD pathogenesis.

MMPs in neurodegeneration: therapeutic implications

If MMPs had diverse and widespread functions, what are the prospects for MMP inhibitors in the treatment of neurological diseases? This is a complex issue that requires careful consideration. MMP inhibitors could be useful in treating acute neurological insults, in which the expression of several MMPs is elevated and their overall activity detrimental. Such pathological conditions would include stroke and spinal cord injury, in which a brief period of treatment with MMP inhibitors could be sufficient to reduce the subsequent loss of neurological functions. It is instructive that the use of the MMP inhibitor GM6001 for only the first 3 days after spinal cord injury in rodents was sufficient to improve neurological functions (Noble, 2002). Similarly, in mice, treatment with GM6001 for the first 2 days after hemorrhagic stroke was adequate to reduce neutrophil infiltration, oxidative stress, brain edema and neurotoxicity (Hwang, 2005). Chronic usage of selective MMP inhibitors in diseases such as multiple sclerosis, AD or PD will be more problematic as the long-term application of these inhibitors might affect reparative processes, as an eventual re-myelination. Since different MMPs may carry out either beneficial or detrimental activities in chronic diseases and certain MMPs may exert a different functions depending the phase of the disease in which are released, the outcome of targeting MMPs using a non-specific inhibitor might be complex. To achieve selectivity of function, the first step should be a thorough understanding of the role that MMPs play in the patho-physiology of a given disorder, so that the use of inhibitors selective for a single MMPs and administered in a time-dependent fashion can be considered.

Another approach to consider for the block of MMP activity as a therapeutic approach in neurodegenerative diseases, is the understanding of the stimulus/i that increase the activity of a given MMP, so that its removal or targeting might offer a

mean of indirect control of MMP activity (Fig. 7) (Yong, 2005). The inhibition of MMPs by using inhibitors, which are selective for individual MMPs, offers another level of intervention. The first generations of MMP inhibitors lacked selectivity or ability to discriminate between MMPs and ADAMs, however newly generated inhibitors are now being chosen for their improved selectivity. Finally, the identification of the substrates that mediate the activity of a given MMP in a particular disease could be the most crucial endeavor, as these substrates are probably unique for a given disease, as reported above. The modulation of the availability of substrates for MMPs, as well as the specific targeting of the coupling effectors-substrates, could conceivably lend selectivity even if one inhibitor could not target the upstream MMP because of its various functions. The methods with which to identify MMP substrates are becoming more sophisticated and manageable (Overall, 2004), making it possible to derive means of affecting the substrate of interest, so as to block a specific action of a MMP rather than targeting the enzyme and all of its associated activities.

In summary, MMPs are implicated in diseases of the nervous system and it is important to target their activity. Although the long-term impact of MMP inhibitors in neurological conditions is not clear because of the complexity of MMP function, the evidence suggests that the short-term use of inhibitors after acute insults, such as stroke and spinal cord injury, will have beneficial outcomes. Genetically modified animals, that under-express or over-express MMP, ADAM, and TIMP genes, are being developed or are already available. These animal models, coupled with the use of selective inhibitors, should aid in unraveling the critical roles they play in the brain, and ultimately provide information that will be useful in designing novel agents to reduce injury or promote healing.

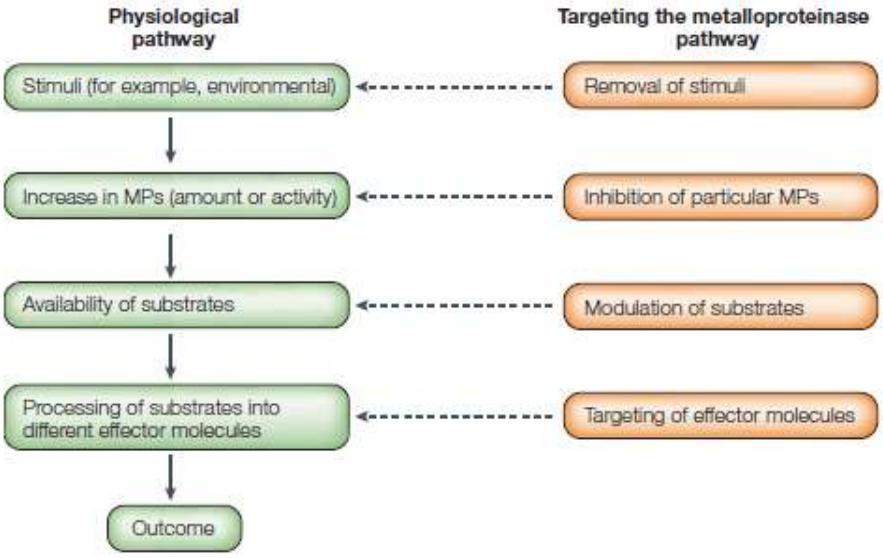

Fig. 7. Multiple ways of targeting metalloproteinases. If the stimuli, including environmental cues, for up-regulating the expression of MMPs can be identified, these could be removed to normalize the expression of MMPs. Various pharmacological inhibitors are available that could be used to target the increase in the content or activity of MMPs. At present, many inhibitors are relatively non-specific and fail to discriminate between MMPs and ADAMs. However, it is anticipated that pharmacological inhibitors will become more selective, as this is a drug discovery goal in the pharmaceutical industry. A perhaps more selective approach to targeting the MMPs is to identify the substrates that modulate the action of a particular metalloproteinase in a given context, and to either modulate the availability of these substrates or to target the effector pathway that results from them. The ability to inhibit the detrimental aspects of MMPs in the CNS while maintaining or even enhancing the beneficial ones will required improved selectivity for targeting particular MMPs and their substrates *(Yong, 2005)*.

AIM of the PROJECT

PD is characterized by the progressive depletion of the nigro-striatal system, in which loss of the SN*pc* dopaminergic neurons and degeneration of their fibers projecting to the striatum induces motor disturbances. Nigro-striatal fiber degeneration in parkinsonism is irreversible and the possibility of axon regeneration of the survived neurons is one of the main challenges in neuroscience. Studies on the regeneration of spinal cord neuron axons have suggested that reorganization of the extra-cellular matrix (ECM) is a crucial event for successful fiber growth in the CNS (Larsen, 2003; Yong, 2005). However, in PD, the associated inflammatory reaction also requires ECM re-arrangement, therefore disfavoring neuronal rescue. Both brain neurons and glial cells (i.e. astrocytes, microglia and oligodendrocytes) participate to ECM remodeling by releasing extracellular proteinases, as the MMPs, and activation of different classes of extracellular proteinases has been described in several neurodegenerative diseases, such as multiple sclerosis and Alzheimer disease. The possible role of extracellular proteases, and particularly of MMPs, in the etiology of PD is, however, far from being uncovered. Data on post-mortem PD human brains and on PD patient serum are not conclusive (Lorenzl, 2002) and somehow differ from the results reported in parkinsonian mice obtained by MPTP, or 6-HODA, administration (Lorenzl, 2004; Hebert, 2003; Kim, 2005; Choi, 2008; So, 2010; Lee, 2010). It is, therefore, important to understand whether and in which direction MMPs can modulate the progression of parkinsonism and of the associated inflammatory reaction. In this thesis work, we used parkinsonian mice, obtained by acute administration of the mitochondrial neurotoxin MPTP, to thoroughly investigate: a) whether some of the most important extracellular protease

systems was involved in the onset and progression of the parkinsonian syndrome and of the associated neuroinflammatory reaction; b) the specific role of MMP-9, which resulted as the main protease whose activation was significantly modulated in the response of the nigro-striatal pathway to MPTP intoxication and the evolution of the accompanying neuroinflammatory response. Data obtained in mice were then compared with those obtained from the elective animal model of parkinsonism: monkeys chronically (1-2 years) intoxicated with MPTP until achievement of stable parkinsonism.

MATERIALS AND METHODS

Animals

All animals were housed and handled in accordance with the guidelines laid down by the European Convention for the protection of Vertebrate Animals used for Experimental and other Scientific Purposes (ets no. 123, June 15th, 2006), by the International Primatological Society and by the National Institutes of Health Guide for the Care and Use of Laboratory Animals (NIH Guide, revised 1996).

MPTP treatment in mice

Two-three month-old male mice were used. C57BL/6 mice and B6.FVB(Cg)-*Mmp9*^{tm1Tvu}/J mice and their matching wild-type were purchased from The Jackson Laboratory. Mice were housed in a special room, separated from the others, with adequate temperature (21° C), 12 hours day-night cycle and with food and water *ad libidum*. MPTP treatment was performed according to the established protocol for acute toxin treatment (Hunot et al., 20004). Briefly, mice were injected intra-peritoneum (i.p) with 80 mg/kg MPTP·HCl (Sigma-Aldrich, St. Louis, MO, USA) in 0.9% NaCl, subdivided in four injections of 20 mg/Kg MPTP-HCl, separated by a 2-h interval from one another. Control animals received equivalent injections of saline. Mice were killed at established time points (see specific paragraphs) and brains removed and processed for different analysis.

MPTP treatment in Monkeys

For this study, brain sections from a colony of chronic parkinsonian macaques (*Macaca fascicularis*) were used. Monkeys were chronically treated with MPTP and housed until establishment of stable parkinsonism (2-5 years) in the Primate Unit of the University of

Murcia. We analyzed brain sections obtained from 6 young adult animals ~~from~~ of both sexes. Four animals were treated with weekly low intravenous doses of MPTP (0.3 mg/Kg), according to Herrero et al., (1993) and Barcia et al., (2003). Each animal received different MPTP doses according to the level of parkinsonism reached and their susceptibility to the toxin (Table I). Monkeys were observed by different researchers after administration of each dose and followed through the progression of the parkinsonian syndrome. Motor symptoms were assessed using a previously described rating scale ranging from 0 to 25 (Herrero et al., 1993). The degree of disability increased normally with every new injection and remained stable for 2 years. MPTP-treated monkeys showed parkinsonian symptoms with a typical parkinsonian posture different degrees of bradykinesia and akinesia and sporadic freezing phenomena; some of them showed action tremor, paradoxical kinesia and, occasionally, vertical and horizontal saccadic ocular movements. Intoxicated animals showing clear impairment ~~of~~ in motor score were classified as parkinsonian. With this classification we obtained a population of subjects similar to the scenario occurring in PD patients. Animals were sacrificed 2 years after the last MPTP administration. Monkeys not treated with MPTP were used as controls.

Table 1

Monkey	Sex	Motor Score	MPTP Accumulative dose mg/kg	Years after MPTP
C1	Male	0.0	0	-
C2	Male	0.0	0	-
C3	Female	0.0	0	-
P1	Male	3.5	1.8	2
P2	Female	4.2	0.9	2
P3	Male	5.0	1.8	2
P4	Female	9.2	0.9	2
A1	Male	0	1,8	2

Table 1. Values of the motor score reached by the animals, accumulative dose of MPTP (mg/kg) of each animal and the time of sacrifice after the last MPTP dose. C; Control animals, A; Asymptomatic animals, P; Parkinsonian animals.

Real Time Reverse transcriptase-Polymerase Chain Reaction

mRNA levels of extracellular proteases were assessed in control and MPTP-treated mouse brains by Real Time Reverse transcriptase-Polymerase Chain Reaction (*real time* RT-PCR). Animals were deeply anesthetized with isoflurane (Merial, Harlow, UK) and killed by decapitation at different times after the last MPTP injections: 1 hour (h), 24 h, 48 h, 72 h, 1 week (wk) and 2wks. Brains were rapidly removed, frozen in liquid nitrogen-cooled isopentane and stored at -80 °C until use. Frozen brains were revived in a cold saline solution (NaCL 0.9%), placed in a matrix for brain slicing (AgnTho's, Lidingö, Sweden) and cut in 1 mm-thick coronal sections. The dorsal striatum and the SN*pc* were removed, according to the mouse brain stereotaxic coordinates ("The Mouse

Brain in Stereotaxic Coordinates" Paxinos and Franklin, 2001) (Fig. 1), by excision with a thin needle and a punching devise of 0.75 mm of internal diameter (AgnTho's, Lidingö, Sweden), respectively. Samples were immediately homogenized for mRNA extraction.

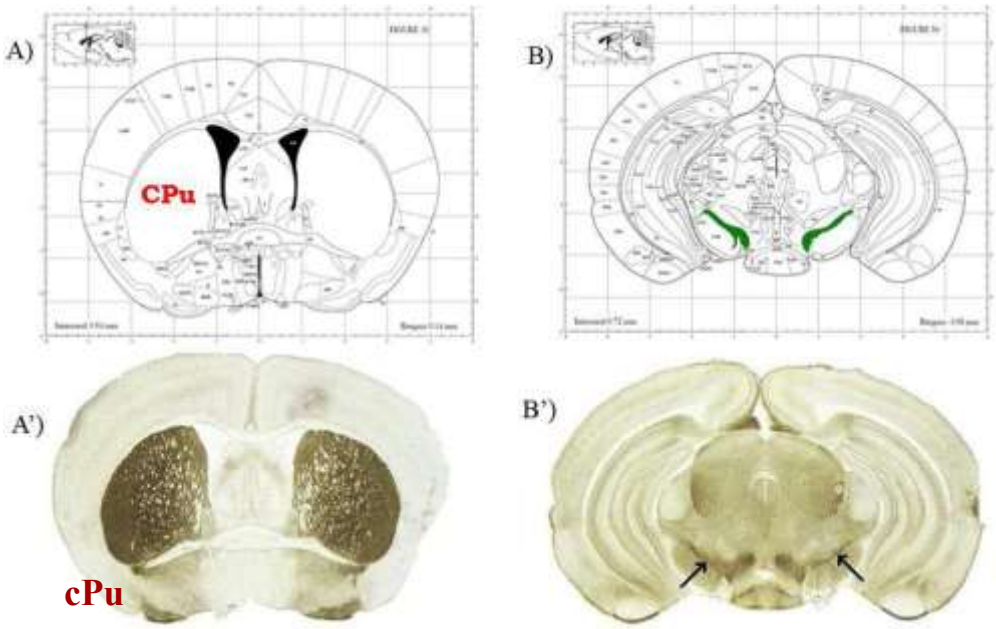

Fig. 1. Diagrams of stereotaxic coordinates (**A, B**) and corresponding Choline Acethyl Transferase immunoreacted sections (**A', B'**) at the level of which the striatum (caudate-putamen, Cpu in **A**) and the SN*pc* (green labeling in **B** and indicated by arrows in **B'**) are dissected (Paxinos and Franklin, 2000).

RNA extraction, quantification and reverse transcription

Total RNA from the SN*pc* and striatum of 6-8 control mice and for each time point of MPTP-treated mice was isolated using the RNeasy Micro kit (Qiagen, Milan, Italy). Tissues were homogenized in ice-cold reducing lyses buffer, containing 1% β-mercaptoethanol, by using a ground-glass micro-homogenizer. After centrifugation (14000 rpm, at 4 °C for 5'), the supernatants were collected and loaded onto a RNeasy silica membrane capable and concentrated RNA was eluted in water. RNA was additionally purified by the genomic DNA using the DNA-free kit (Ambion, Austin, TX, USA), according to the manufacturer's instructions. Yield and integrity of the purified RNA were

assessed by spectrophotometric analysis at 260 nm. RNA was reverse-transcribed as previously described (Del Signore et al., 2006) by using the c-DNA synthesis kit (Bioline. London, UK). Briefly, 2 µL of Random Primers and 2 µl of deoxynucleotide triphosphates (dNTP), included in the reverse-transcription kit, were added to the RNA eluted from the Rneasy membrane. The total volume was brought up to 20 µl with bi-distilled water and the all mix was first incubated at 65°C for 10 min and then chilled on ice for 2 min. After transferring the mix in a tube containing 2 µl of RNase inhibitor, 8 µl of 5 X retro-transcription (RT) buffer and 0,5 µl of Moloney Murine Leukemia Virus (M-MLV) reverse transcriptase, bi-distilled water was added up to a final volume of 40 µl. This second reaction mix was incubated at 37°C for 1 h to allow the retro-transcription reaction, at the end of which the reverse transcriptase was inactivated by heating at 70°C for 15 min and then chilling on ice. c-DNA samples were diluted in bi-distilled water to a final volume of 100 µl and stored at -20°C until use.

Real time RT-PCR

2,5 µl of the obtained cDNA were amplified by *real-time* RT-PCR in 25 µl of the reaction mixture containing 12,5 µl of 2X SYBR Green JumpStart Taq ReadyMix (Sigma-Aldrich), 0,25 µl of Internal Reference Dye and 3 µl each specific primer (5 µM final concentration Forward + Reverse) (Sigma-Aldrich) using an iCycler iQ Real-Time Detection System (Bio-Rad, Milan, Italy). Specific primers (Table 2) were designed by using the Beacon Designer software (Premier Biosoft International, Palo Alto, CA, USA) and syntesized by Genosys (Sigma-Aldrich). Each sample was amplified in duplicate. Amplification was carried out for 30-35 cycles (30 s at 95 °C, 30 s at 62 °C and 45 s at 72 °C). Amplicons were detected after each elongation step and were analyzed using the iCycler iQ software (Bio-Rad). A melting curve was obtained after completion of the cycles to verify the presence of a single amplified product. Hypoxantinephospho-ribosyl-

transferase (HPRT) was used as internal standard (Steel & Buckley, 1993); amplification efficiencies of HPRT and of all genes of interest were set to be approximately equal. Data were calculated based on the threshold cycle (Ct) and are expressed as fold increases in mRNA expression. Comparative expression levels were calculated by the $2^{-\Delta\Delta Ct}$ method (Livak & Schmittgen, 2001), which means that the relative gene expression corresponds to $2^{-\Delta\Delta Ct}$, where ΔΔCt is: (Ct gene in MPTP-treated samples - Ct HPRT in MPTP-treated samples) - (Ct gene in Control samples - Ct HPRT in control samples). Data were analyzed using the two-tail Student's *t*-test or one-way ANOVA test following a post-hoc analysis (followed by Dunnet multiple comparisons tests). The null hypothesis was rejected for α risk equal to 5%.

Gene (and length of amplicon)	***Primer sequence (5'- 3')***
tPA (132 bp)	
Forward:	TGGTGCCATGTGATGAAGG
Reverse:	GGTGATGTCTGTGTAGAGTCC
Plasminogen (109 bp)	
Forward:	ATCGTCCACTACCATCACAGG
Reverse**:**	GTTCATCTCCAAGCCAGCATC
MMP-2 (144 bp	
Forward:	AAGAGTTGGCAGTGCAATACC
Reverse**:**	CGATGGTGTTCTGGTCAAGG
MMP-3 (149 bp)	
Forward:	GCATTCACACCCTGGGTCTCC
Reverse:	CCTGGGAAATCCTGGCTCCAT G
MMP-9 (137)	
Forward:	GGCGTGTCTGGAGATTCG
Reverse:	ATGGCAGAAATAGGCTTTGTC
HPRT (160 bp)	
Forward:	AGTCCCAGCGTCGTCATTAG
Reverse:	CCATCTCCTTCATGACATCTCG

Table 2. Primers (5'-3') used for Real-Time RT-PCR. This table shows forward and reverse primer sequences with the length of amplified fragments (bp) used in Real time RT-PCR experiments.

Western Immunoblot

Primary antibodies

Rabbit polyclonal antibodies against MMP-9 (diluted 1:2000) and tyrosin hydroxylase (TH) (diluted 1:1000) were from Chemicon (Temecula, CA, USA). Rabbit polyclonal antibodies against tPA (diluted 1:500) and plasminogen (diluted 1:2000) were from Innovative Research (Asbach, Germany). Mouse monoclonal antibody against Glyceraldehyde-3-Posphate Dehydrogenase (GAPDH) (diluted 1:5000) was from Abcam (Cambridge, MA, USA).

Preparation of tissue extracts

The SN and striatum from the frozen brains of control and treated mice were dissected as described for the real time RT-PCR. Tissues were immediately homogenized with a ground-glass micro-homogenizer in ice-cold RIPA buffer, containing 50 mM Tris/HCl pH 7.6, 150 mM NaCl, 1 mM EDTA, 1% SDS, 1% Triton X-100, 1 X of a cocktail of inhibitors (Sigma-Aldrich, St Louis, MO, USA), 1 mM PMSF, 0.2 mM Na_3VO_4 and 1 mM NaF. After centrifugation (15000 X g for 15 min at 4°C), a measured volume of the supernatant was analyzed to determine the total protein concentration using the Micro BCA kit (Pierce, Rockford, IL, USA). Other aliquots of the supernatant were mixed with 4 X reducing loading buffer (200 mM Tris/HCl pH 6.8, 4% SDS, 30% glycerol, 4% β-mercaptoethanol, 4% blue bromophenol), boiled for 3 min and stored at -20 °C until use.

Electrophoresis and immunoblotting

For each sample, 80 µg of proteins were separated on 8% SDS-polyacrylamide gels. Molecular mass standard (ColorBurst©, Sigma-Aldrich, St. Louis, MO, USA) containing the precisely sized recombinant proteins of 210, 90, 65, 40, 30, 20, 13, 8 KDa, along with human recombinant gelatinases MMP-9 and MMP-2, tPA or plasminogen, used as positive controls, were loaded on separate lanes in the same gel with the SN and striatum homogenates. Samples run at constant voltage (200 mV), at RT for 1 h. After electrophoresis, proteins were transferred onto a nitrocellulose membrane using a transfer buffer composed by 50 mM Tris/HCl, 380 mM glycine, 0,1% SDS and 20% methanol. Pounceau S staining (Biorad) of the nitrocellulose membrane was used to verify the correct electrophoretic migration and the uniform protein loading among lanes. Non-specific biding sites were blocked by an incubation in 5% dry milk (Carnation instant no-fat milk, Nestlé, USA) (DM), diluted in TTBS 1X (20 mM Tris/HCl pH 7.5, 500 mM NaCl, 0,05% Tween-20) for 2 h at RT. Membranes were incubated overnight, at 4 °C, in either one of the primary antibodies diluted in 3% BSA, 0.05% NaN_3, in 1 X TTBS. After rinsing twice in 1 X TTBS and three times in 2.5% DM in 1X TTBS, membranes were incubated, for 1 h at RT, in the appropriate horseradish peroxidase (HRP)-conjugated secondary antibody (Promega, Madison, WI, USA): either goat anti-rabbit IgG or goat anti-mouse IgG,, diluted 1:10000 and 1:15000 in 2.5% dry milk in 1 X TTBS, respectively. Antibody binding sites were revealed by using an enhanced chemiluminescence (ECL) kit (Pierce, Rockford, IL, USA) and exposing the membranes to the Hyperfilm ECL, from GE Healthcare (Waukescha, WI, USA). The intensity of the immunopositve bands was evaluated by densitometric analysis by using the ImageQuant 5.2 software (GE Healthcare). The optical density (O.D., arbitrary gray units) of each band of interest was normalized against the O.D of

the band immunopositive for the GAPDH in the same lane, used as the internal reference protein. Within each experiment, densitometric values were expresses as the ratio of O.D. MPTP treated mice/ O.D. control mice.

In situ zymography

In order to localize the gelatinolytic activity of MMP-2 and MMP-9 in both SN*pc* and striatum of control and parkinsonian mice, we performed the *in situ* zymography technique on fresh brain cryosections. Animals were anesthetized with isoflurane and killed by decapitation. Brain were rapidly removed, frozen on dry-ice and stored at -80°C until use. After embedding in Tissue-Tek® O.C.T. ^{TM} compound, unfixed brains were cut encompassing the entire midbrain and striatum in coronal, 10 µm-thick serial sections by using a cryostat. Frozen sections were directly mounted on Super Frost Ultra Plus® glass slides (Menzel- Gläser, Braunschweig, Germany) and incubated overnight at 37 °C in a gelatinase activation buffer made of 50 mM Tris/HCl, pH 7,6, 150 mM NaCl, 5 mM $CaCl_2$, 0.2 mM NaN3 e 50 µg/ml of DQ™ Gelatin from Pig Skin Fluorescein-Conjugated (Molecular Probes, Eugene, OR, USA). Negative controls were obtained by adding 20 mM EDTA to the activation buffer. After rinsing in phosphate buffer saline (PBS), sections were post-fixed, for 30 min at RT, with 4% formaline in PBS. Nuclei were counterstained by incubating the section for 30 min with the blue fluorescent probe diamidino-2-phenylindole (DAPI) (1:1000, Invitrogen). Sections were rinsed, mounted on glass slides and coverslipped with the ProLong antifade (Invitrogen). Sites of proteolytic activities, visible as a fluorescent emission consequent to the specific enzymatic cleavage of gelatine by MMPs, were viewed at a Leica DMIRE2 confocal microscope (Leica Microsystems, Exton, PA) (see below the "Confocal analysis" section).

Immunohistochemistry and immunofluorescence

Mice

Four to five mice for each experimental condition and time point were used. Mice were deeply anesthetized by an intraperitoneal injection of Ketamine (50 mg/kg body weight) and Xylazine (50 mg/kg body weight) and perfused transcardially with an oxygenated Ringer solution, pH 7.3, followed by 4% freshly depoymerized paraformaldehyde (PFA) in 0,1 M phosphate buffer (PB), pH 7,4. Brains were removed and cryo-protected in 30% sucrose, at 4 °C, until they sank. Free-floating coronal sections (25 µm-thick), encompassing the entire midbrain and striatum, were cut at a cryostat and stored in a cryo-protectant (1:1 ethylene glycol and 0,2 M PB, pH 7.4, with addition of 0.5 M sucrose) at -20 °C. Free-floating sections were immunoreacted with the following primary antibodies: sheep anti-TH (1:1000, Chemicon), in order to visualize and quantify levels of the catecholamine biosynthetic enzyme after MPTP treatment; rabbit anti- Iba-1 (1:500; Wako, Chuo-Ku, Osaka, Japan), in order identify activated microglia, rabbit anti-MMP-9 (1:1000, Chemicon) in combination with either mouse anti-NeuN (1:500, Chemicon), used as a neuronal marker, or mouse anti-glial fibrillary acid protein (GFAP) (1:500, Chemicon), used as astrocyte marker, or mouse anti-myelin related protein (MRP) (1:30000, Chemicon), used as oligodendrocyte marker. Moreover, in order to localize MMP-9 in microglial cells, a rhodamine-conjugated tomato lectin (Griffonia Simplicifolia Lectin I, 1:100, Vector, Burlingame, CA, USA) (Pott Godoy, 2008) was used in combination with the anti- MMP-9 immunolabeling.

Monkeys

Monkeys were sacrificed with a lethal injection of pentobarbital after a pre-anaesthesia with ketamine (8mg/Kg body weight) after one, two or five years from the last MPTP

injection. Brains were rapidly removed, one hemisphere rapidly frozen on dry ice and stored at -80 °C for successive Western immunoblot analysis. The other half was fixed for 3 days in 4% freshly depoymerized PFA dissolved in 0.1 M PB, pH 7.4. Fixed mesencephalons were sectioned into 40 μm-thick serial sections (Vibratome, Leica Microsystem, Wetzlar, Germany). Sections of the striatum were immunolabeled with the same antibodies used for mice, with the exception of the oligodendrocytes marker anti-MRP, which was substituted by a mouse anti-myelin basic protein (MBP) (1:100, Chemicon). We were technically unable to co-localize MMP-9 with any of the primate-specific microglial markers.

Immunohistochemistry

Endogenous peroxidases were inhibited by incubating tissue sections in 0.3% H_20_2 and 10% methanol in PBS, pH 7.4, for 15 min at RT. Antigen retrieval was performed by pre-treating sections with citrate buffer, pH 6.0, for 30 min at 65 °C, After a permeabilization with 1% Triton X-100 for 5 min, non-specific antibody binding sites were blocked with an incubation in 10% normal horse serum (NHS) in 0.1 M PBS, pH 7.4, for 60 min at RT. Slices were successively incubated for 48 h, at 4 °C and under constant shaking, with either one of the following primary antibodies, TH, MRP and MBP, diluted in PBS containing 1% NHS, 0.5% Triton X-100, and 0.1% NaN_3 followed by an incubation with either a biotinylated donkey anti-sheep IgG (for TH) or donkey anti-mouse IgG (for MRP and MBP) antibodies (Jackson Immuno Research), all diluted 1:500 in the same diluent used for the primary antibodies. After 2 hrs at room temperature, sections were incubated in the avidin-biotin-peroxidase complex, diluted 1:100 (ABC kit; Vectastain Elite, Vector Labs, Burlingame, CA, USA) for 30 min at RT. Antibody binding sites were revealed by incubating the sections in 0.25 mg/ml 3,3'-diaminobenzidine (DAB) and 0.03% H_2O_2 in PBS, pH 7.4, for 10 min at RT.

Negative controls were obtained by omitting the primary antibodies. Sections were mounted on gelatin-coated slides and dehydrated in a series of ethyl alcohols and xylene before being coverslipped.

Immunofluorescence

Revelation of MMP-9 by IF was enhanced by using the Renaissance® Tyramide Signal Amplification (TSA)-biotin system kit (PerkinElmer). After a pretreatment with citrate buffer, pH 6.0 for 30 min at 65°C, and quenching of the endogenous peroxidase activity, sections were incubated in a TNB blocking buffer (0.1 M Tris/HCl pH 7.5, 0.15 M NaCl, 0.5% blocking reagent by the manufacturer), for 1 h at RT. Sections were then incubated for 48 hours (at 4°C, under constant shaking) with the rabbit anti-MMP-9 primary antibody, in combination with either one of the other primary antibodies (see above), diluted in TNB blocking buffer, and rinsed 3 x 10 min in TNT buffer (0.1 M Tris/HCl pH 7.5, 0.15 M NaCl, 0.05% Tween20) at RT, under agitation. Amplification of the signal was obtained by incubating the sections, for 30 min at RT, first with a with biotinylated goat anti-rabbit IgG secondary antibody (1:100, Vector Labs, Burlingame, CA, USA), diluted in TNB blocking buffer, and then in 1:100 streptavidin–HRP conjugate (SA-HRP) (TSA-biotin System kit, PerkinElmer), for 30 min at RT. After a 3 x 10 min rinse in TNT buffer, the amplification reaction was carry out by incubating sections, for 10 min at RT, with a biotinyl tyramide working solution, according to the manufactures instruction: 1:50 Biotinyl Tiramide Stock Solution diluted in 1 X Amplification Diluent (TSA-biotin System kit, PerkinElmer). The reaction of amplification was blocked by rinsing section, 3 x 10 min, in TNT buffer. Finally, the fluorescent signal was obtained by 30 min incubation in the SA-Fluorescein conjugate, diluted 1:500 in TNB (TSA-biotin System kit, PerkinElmer).

After a thorough rinse in PBS, binding sites between the other primary antibodies and their antigens were revealed by incubating sections with the appropriate secondary antibodies conjugated with either Alexa Fluor 633 or Alexa Fluor 594 (1:1000) (Molecular Probes, Carlsbad, CA, USA). After a 3 x 10 min rinse in PBS, sections were incubated in DAPI for 30 minutes for nuclear staining. Sections were rinsed, mounted on glass slides and coverslipped with the Prolong® Gold antifade reagent.

Confocal analysis

Fluorescent brain sections were examined using a Leica DMIRE2 confocal microscope (Leica Microsystems, Exton, PA) with a 63 X immersion-oil objective and analyzed with Leica Confocal Software (Leica Microsystems, Heidelberg 19 GmbH). Optical sections were 0.5 µm-thick and a series range for each section was set by determining an upper and lower threshold by using the Z/Y Position for Spatial Image Series setting. Images could be viewed both as single 0.5 µm-thick planes and layered stacks of planes. Confocal microscope settings were established and maintained by Leica and local technicians for optimal resolution. (For further details see Barcia, 2006, 2008),

Quantification and sterological analysis

SN*pc* and striatum were identified according to the Monkey Brain Atlas (Paxinos, 1999) and The Mouse Brain Atlas in Stereotaxic Coordinates (Paxinos and Franklin, 2001). Quantification of HRP-DAB immunolabeled cells in the SN*pc* was performed on coronal sections (two from each monkey and three from each mouse). The number of cells was estimated using a system of a computer assisted image analysis, with a Zeiss Axioplan 2 microscope connected to a digital camera. The region of interest was located at a 1.25 X objective and then One-two images were taken from each brain hemisphere using a 20 X objective. Labeled cells were counted in each photographic field and the

obtained numbers were expressed as number of cells/mm^2. The OD of the TH immunolabeling in the striatum was determined by the ImageJ software (Burger and Burge, Springer Verlag) and was considered as an index of the dopaminergic density of innervation. Both concentrations of the anti-TH antibody and of the DAB solution, as well as the time of DAB-H_2O_2 reaction, were optimized to fall within the linear range of the plot of the immunostaining intensities and the scanned OD. Image analysis was performed on coronal sections (two from each monkey and three from each mouse) using the 1.25 X objective.

The quantification of MMP-9 co-localization with the different cell markers, as well as OL activation, was obtained by confocal microscope analysis. Three representative sections of either SN or striatum from every control and MPTP intoxicated mouse were chosen and from each one of these, three random images were captured. Cells positive for both MMP-9 and another cell marker were counted only when the area of co-localization was detected in the majority of the 0.5 µm-thick optical layers throughout the entire stack. The density of the different type of cells, which expressed MMP-9, was quantified on a single 0.5 µm -thick optical section. The obtained results were expressed as the number of double immunopositive cells/mm^2. All quantifications were done blindly.

These same parameters were used for quantifying activated OLs in both the SNpc and striatum of mice (MRP immunopositive cells) and monkeys (MBP immunopositive cells).

Quantification of activated OLs phenotype in mice

Sections containing MRP- (mice) were scanned in confocal planes of 0.5 µm along the thickness of the section configuring a xyz stack as described above. The rendered transparency of the 5 µm stacks was converted by the image software Image-J in black

and white images. The area occupied by the total number of OLs present in each photographic field (three stacks of images for each animal), taken throughout mice SN*pc* and striatum was measured on these processed images. The area occupied by OLs was not measured in monkeys because their processes were completely intermingled and the software was unable to distinguish and define each individual cell unit. All quantifications were done blindly.

Electron microscopy

Mice were deeply anesthetized and perfused transcardially with a fixative composed of 2% freshly depolymerized paraformaldehyde + 2% glutaraldehyde in 0.1 M PB, pH 7.4. Brains were removed and the area containing striatal fibres was dissected into 1mm3 cubes, postfixed with 1% OsO4 and dehydrated in ascending concentration of ethanol (50%, 70% and 90%) followed by 90% acetone, before being embedded in Epon 812. Ultra-thin sections were cut in an ultramicrotome (Reichert-Imy E Ultracut), collected on copper grids and stained with 2% uranyl acetate and 2.5% lead citrate. Sections were examined using a transmission electron microscope (Philips TECNAI 12).

Statistical Analysis

All statistical analyses were performed using either the one-way ANOVA test following a post-hoc analysis (followed by Dunnet multiple comparisons tests), or by the Student's *t*-test, or both. Differences were considered statistically significant for $p \leq 0.05$. All data were always expressed as the mean $\pm$ standard error of the mean (SEM).

RESULTS

Evaluation of MPTP neurotoxicity by TH immunolabeling of the dopaminergic pathway

To test whether MPTP administration was effective in inducing death of the SN*pc* dopaminergic neuron, we studied protein levels and/or localization of TH in the nigro-striatal pathway of control and MPTP-injected animals by Western immunoblot and immunohistochemistry, respectively.

TH protein levels and immunolabeling in the SN and striatum of control and parkinsonian mice

TH protein levels in the SN and striatum of control and MPTP-treated mice, sacrificed 1, 24, 48, 72 hrs, 1 and 2 wks after the last injection, were detected by Western immunoblot (Fig. 1A, SN; Fig. 2A, striatum) and densitometric analysis of the immunopositve bands (Fig. 1A', SN; Fig. 2A', striatum) . In the SN, the intensity of the TH immunopositive bands, which migrated at the expected molecular mass of 54 KDa (Fig. 1A), decreased significantly, respect to control, by 48 hrs after the last MPTP injection, remaining lower until 1 wk (Fig. 1A'). This value recovered to control levels by 2 wks after intoxication (Fig. 1A, A'). As expected, in the striatum, the decrease in protein levels was anticipated with respect to the SN (Fig. 2A), being abruptly and significantly decreased by 24 hrs after MPTP injection (Fig. 2A'). Protein levels tended to increase by approximately 72 hrs after injection, although they never reached levels comparable to control in the considered post-treatment time frame (fig. 2A, A'). These results were confirmed by immunohistohemistry, flanked by stereological or densitometric evaluation of the immunopositive elements. In the SN*pc* of control mice,

TH immunoreactivity strongly labeled numerous neuronal cell bodies and fibers (Fig. 1B), which appeared drastically reduced early after MPTP injection (Fig. 1B, 72 hrs) and that partially recovered 2 wks later. A stereological study conducted on photographic fields including the whole SN*pc* taken from different brain sections (Fig. 1B'), further demonstrated that after MPTP administration the number of TH-immunopositive (TH^+) neurons was significantly reduced by half (40-50%) as early as 24 hrs, reaching the 70-80% after 72 hrs (Fig.1B'). This number recovered slightly after 2 wks from treatment, remaining however significantly lower than control (Fig. 1B'). Loss of TH^+ neuron in the SN*pc* largely reflected that of TH^+ fibers, which these neurons project to the striatum (Fig. 2B). Densitometric analysis of random areas of the striatum of different brain sections confirmed a significant and dramatic decrease in the striatal dopaminergic projections 24, 48 and 72 hrs after the MPTP injection (Fig. 2B'). However, 2 wks after MPTP treatment, the increase in TH^+ fibers in the striatum, was comparable to control, despite the reduced number of neurons, suggesting terminal axon sprouting of survived neurons and partial rescue of the dopaminergic pathway.

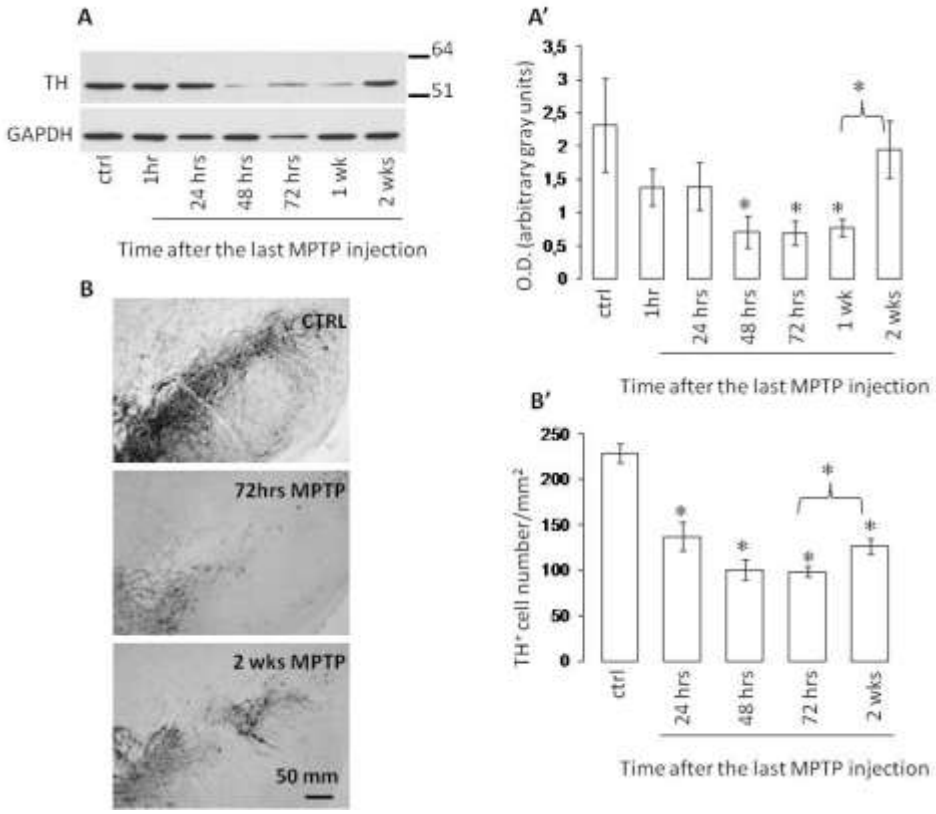

Fig. 1. TH expression in the SN of control and MPTP-treated mice. A-A') TH Western immunoblot (A) and relative densitometric analysis (A') on protein extracts from the SN of control (ctrl) and MPTP-treated mice scarified at different time after the last toxin injection. In the representative Western immunoblot shown in A, the TH antibody recognizes a protein band of about 54 kDa. GAPDH, shown below, is used as the internal reference protein. Molecular mass standards, expressed in kDa, are indicated on the right hand side. A') Densitometric analysis reveals that the intensity of the immunopositive bands decreases significantly, respect to control, by 48hrs up to 1 wk after MPTP injection. After two weeks, levels of TH increase significantly respect the previous dates, returning to control levels. O.D: optical density. Data are the mean ± s.e.m. of 6-7 animals/experimental group. *p≤0.05, calculated by the one way ANOVA Duncan's test. **B-B')** TH-DAB immunolabeling (B) in the SN*pc* of three representative brain sections from control and MPTP-injected mice and relative quantitative analysis (B'). **B**) Compared to control mice, 72 hrs after MPTP injection, a drastic decrease in the intensity of the immunolabeling and in the number of immunopositive elements (neurons and fibers) is observed. This reduction persists at later dates, although 2 weeks after MPTP injection a partial recovery of the immunostaining can be appreciated. **B')** Quantitative analysis of the TH immunopositive (TH+) cells/mm^2 shows a significant decrease, respect to control, by 24h. A partial, but significant, recovery is observed 2wks after treatment. n = 4-5 animals/experimental group; bars represent the mean ± s.e.m.; *p≤0.05, calculated by the one way ANOVA (Duncan's test).

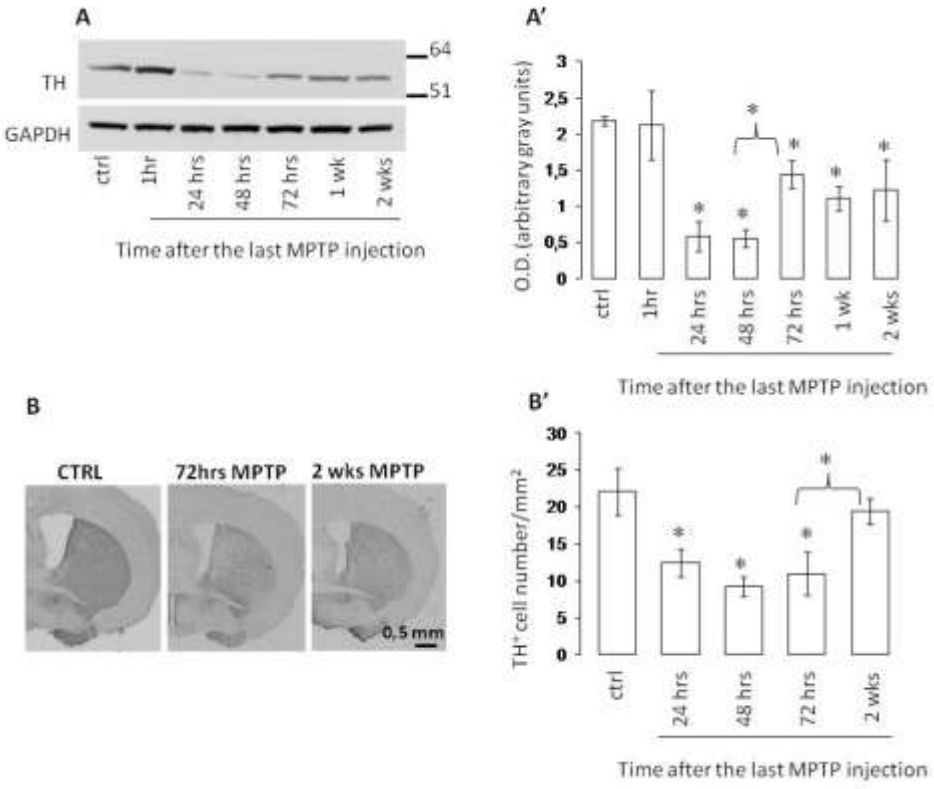

Fig. 2. TH expression in the striatum of control and MPTP-treated mice. A-A') TH Western immunoblot (A) and relative densitometric analysis (A') on protein extracts from the striatum of control (ctrl) and MPTP-treated mice scarified at different time after the last toxin injection. **A)** Representative TH western immunoblot, performed on striatal protein extracts. A') Densitometric analysis of the immunopositive bands reveals a significant decrease, compared to control, in TH protein levels by 24hrs after MPTP injection. O.D.: optical density. n = 6-8 animals/time point; bars represent the mean ± s.e.m. of the optical densities; *p ≤ 0.05 calculated by the one way ANOVA Duncan test. **B-B')** TH-DAB immunolocalization in striatum of both control and MPTP-injected mice and relative densitometric analysis of the immunolabeled areas. **B)** In the dorsal striatum of control animals, the TH immunostaining due to the dopaminergic fibers projecting from the SN is intense. After MPTP injection, a dramatic reduction in the density of TH immunopositive fibers is observed (72hrs in B), followed by a partial recovery at later dates (2wks in B). **B')** The values of the O.D. associated with the TH immunopositive areas statistically confirm these observations. n = 4-5 animals/experimental group; bars represent the mean ± s.e.m.; *p≤0.05, calculated by the one way ANOVA (Duncan's test).

TH immunolabeling in the SN and striatum of control and parkinsonian monkeys

Sample sections from the monkey striatum, taken from the different series used in the following experiments, were tested in parallel to the mice striatum to evaluate the appropriate reduction in TH immunolabeling, as the confirmation of an established parkinsonian phenotype. Both SN*pc* and striatum (caudate and putamen) of control animals were characterized by an intense TH immunostaining (Fig. 3B,C, control). Comparing the two groups of monkeys (control and MPTP-treated), we observed a dramatic decrease in the intensity of immunolabeling in both SN*pc* and striatum of

intoxicated monkeys (Fig. 3B,C, MPTP). Stereological quantification of dopaminergic neurons (TH^+ cells) in the SN*pc* confirmed this decrease as significant compared to control (Fig. 3B'). A significant decrease in TH-immunoreactivity was also found in both caudate nucleus and putamen of parkinsonian animals compared with the corresponding areas in control monkeys (Fig. 3C').

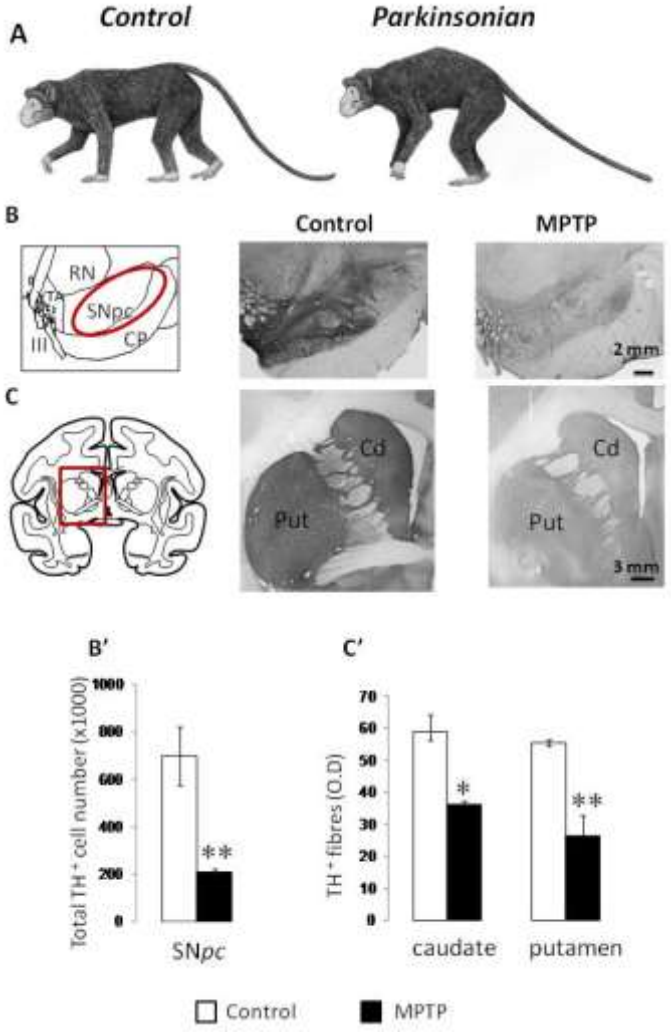

Fig. 3. Persistent TH depletion induced by MPTP chronic treatment in monkeys. A) Artistic drawing of the typical gait posture of a normal monkey (control) compared with the characteristic parkinsonian posture (Parkinsonian). Parkinsonian monkeys present an alteration of their gait posture characterized by curvature of the trunk and rigidity of the limbs, together with rigidity of the tail (drawings by C. Barcia). **B,C)** Analyzed areas are encircled/boxed in red on the section drawings. TH-DAB immunolabeling in SN*pc* (B) and striatum (C) of control and parkinsonian monkeys shows an evident decrease in the number and density of TH^+ cells and fibers, respectively, in parkinsonian monkeys 2 years after the last MPTP injection, compared to control. **B'-C')** These data are confirmed by both stereological quantification of the number of TH^+ cells in the SN*pc* and densitometric analysis of areas occupied by TH^+ fibers in the striatum. Control group: n = 3 monkeys; Parkinsonian group: n = 5 monkeys. Histograms represent the mean ± s.e.m.; *p≤0.05, **p≤0.01, calculated by the student's *t* test.

Evaluation of mRNA levels of components of the PA-plasmin and MMP systems in the dopaminergic pathway of parkinsonian mice

In the first part of the project we looked for possible changes, in both SN and striatum of parkinsonian mice compared to control, in mRNA levels of several components of the two most important extracellular protease systems, the PAs-plasmin system and the MMPs family, known to play important roles in various physiological and pathological brain processes. Through this initial step, we aimed at understanding whether one or both systems could be involved in the genesis and/or progression of the selective loss of the dopaminergic nigrostriatal pathway induced by MPTP intoxication and of the prominent inflammatory reaction to which it associates.

Study of mRNA levels of tPA, uPA and plasminogen after acute MPTP administration in mice

Real time RT-PCR experiments demonstrated that MPTP acute treatment of mice induced a general down-regulation, or no regulation, of the mRNA levels of the major components of the PA-plasmin system examined. In the SN, transcript levels of tPA, were mainly significantly decreased, respect to control, 48 and 72 hrs after the last MPTP injection, as well after 2 wks. However, a significant (about two-fold), but transient increase was observed 1 hr after intoxication (Fig. 4A); a second significant increase, but much more modest than the first one, was seen at 1 wk. In the striatum of parkinsonian mice, tPA mRNA levels were either comparable (1 hr, 24 hr, 1 wk) or significantly decreased (48 hr, 72 hr, 2 wks) respect to control mice.

uPA is the functional analog of tPA, in that it is involved in the cleavage of plasminogen into the active serine-protease plasmin, although their levels and distribution within various brain regions, as well as their contribution, can vary in different processes. A comparative study of uPA and plasminogen (see below) mRNA expression between control and MPTP mice was only possible for the SN, as their

levels in the striatum of parkinsonian mice were below the sensitivity of the technique. uPA mRNA levels remained unchanged, respect to control, after MPTP treatment (Fig. 4B), while those of plasminogen, more in accord with what observed for tPA, were significantly lower at 48-72 hrs and 1 wk (Fig. 4C).

Fig. 4. mRNA levels of components of the PAs-plasmin system in the SN and striatum of control and MPTP-injected mice. A) After an initial increase 1 hr after MPTP injection, tPA mRNA levels in the SN decrease significantly respect to control by 48 hrs up to 2 wks, although a slight, but significant, increase is observed at 1 wks. A') In the striatum, tPA mRNA levels decrease significantly respect to control 24-48hrs after MPTP injections, being still significantly lower after 2 wks. B) uPA mRNA levels in the SN of control and parkinsonian mice are not different. C) mRNA levels of plasminogen decrease significantly, compared to control, between 48-72 hrs and 1 wk after MPTP injections, returning to control levels 2 wks later. n=6-8 animals/experimental group; bars represent the mean ± s.e.m. of the mRNA levels in MPTP-treated mice/mRNA levels in control animals. *p ≤ 0.05 calculated by the one way ANOVA (Duncan's test).

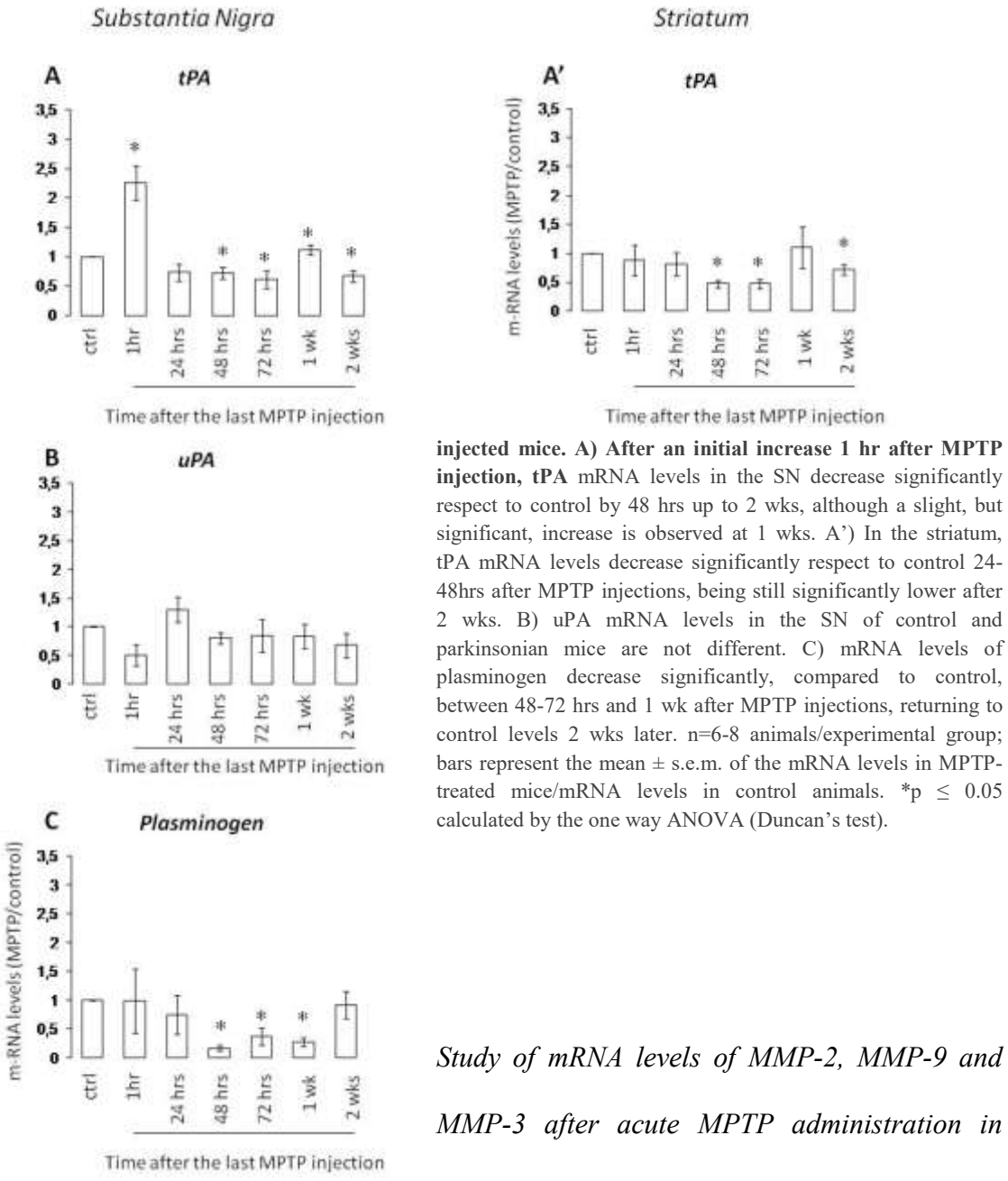

Study of mRNA levels of MMP-2, MMP-9 and MMP-3 after acute MPTP administration in

mice

Based on their large expression in brain in both physiological and pathological conditions, MMP-2, MMP-9 and MMP-3 were identified as the three proteases, the changes of which could be associated to the development of parkinsonism. Analysis of the respective mRNA levels (Fig. 5 A-C, SN; Fig. 5 A'-C', striatum), showed that only the expression MMP-9 is consistently and significantly modulated in both SN and striatum of parkinsonian mice. In fact, mRNA levels for MMP-2 and MMP-3 apparently tended to increase transiently in the SN by 24/48 hrs (Fig. 5A, B) and to oscillate in an apparent random fashion in the striatum (Fig. 5A', B'); these difference, however, were never significant due to quite large standard errors. This may indicate a contribution to the total level of these mRNA by cells incoming (non-resident) into the affected areas, or by local cells activated by the noxious stimulus, which express these MMPs at various degrees, thus confounding the overall picture. Moreover, MMP-2 and MMP-3 mRNAs came out after a higher number of the real time RT-PCR cycles than those imposed for MMP-9, which strongly suggests that their levels in these regions is quite low and, thus, subjected to a high variability in the final analysis. Differently from these, MMP-9 mRNA levels in the SN were about 1.8 and 2.5-fold higher than control 24 hrs and 48 hrs after MPTP treatment, respectively. In the following experimental dates, mRNA levels decreased to values that were no significantly different from control, although still higher than this (Fig. 5C). In the striatum, MMP-9 mRNA levels were significantly increased respect to control 24 hrs and 1 wk after MPTP injection, but significantly decreased at the 48 hrs time point (slightly decreased) and after 2 wks (decreased about half of the control) (Fig. 5C').

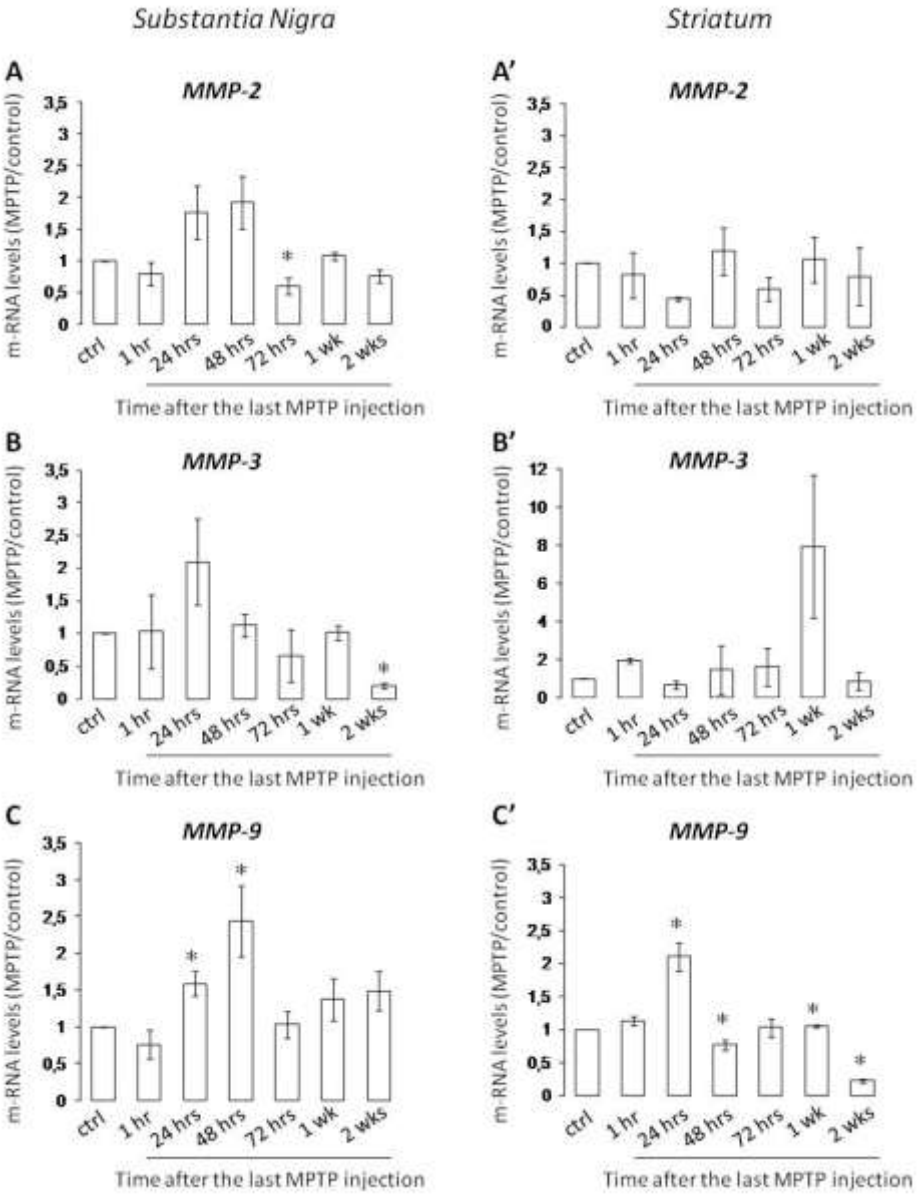

Fig. 5. Study of MMP-2, MMP-3 and MMP-9 m-RNA levels in the dopaminergic pathways of control and parkinsonian mice. A,A') In the SN (A), mRNA levels of MMP-2 decrease significantly respect the control only 72hrs after the toxin administration, although they tend to be higher, but not significantly, at 24 and 48 hrs. In the striatum (A'), MMP-2 mRNA levels follow little oscillations respect to control, but never statistically significant. B,B') In the SN (B), MMP-3 mRNA levels do not significantly differ from control throughout the post-injection time considered, except for the 2wks time point, where they decrease significantly. In the striatum (B') levels oscillate up and down control level, but never significantly. In general, however, standard errors are too large to draw a correct progress of these, as well as of MMP-2, mRNA levels. C,C') MMP-9 mRNA levels increase significantly, compared to control, within the first 24h after the last MPTP injection in both SN (C) and striatum (C'). After 48h, while mRNA levels in the SN further increase and then return to control levels in the following dates, those in the striatum decrease significantly, remaining lower than control. n=6-8 animals/experimental group; bars represent the mean ± s.e.m. of the mRNA levels in MPTP-treated mice/mRNA levels in control animals. *$p \leq 0.05$ calculated by the one way ANOVA (Duncan's test).

Evaluation of tPA, plasminogen and MMP-9 protein levels in the SN and striatum of control and parkinsonian mice

The levels of those proteins, the mRNA of which were seen changing significantly after MPTP injection, were successively investigated by Western immunoblot on protein extracts from SN and striatum of control and parkinsonian mice. This part of the study aimed to uncover possible post-transcriptional regulatory mechanisms in the extracellular protease production.

tPA. The anti-tPA polyclonal antibody used revealed three immunopositive bands of approximately 65 kDa, 40 kDa and 30 kDa, which corresponded, respectively, to the assembled molecule, formed by a heavy and a light chain, to the sole heavy chain and to the sole light chain (Fig. 6A, SN; Fig. 7A, striatum). Identity of the bands was confirmed, as they co-migrated with the corresponding protein standard run on a separate lane in the same gels. Densitometric analysis of the immunopositive bands relative to the whole form of the enzyme, carried out on 6 to 8 different Western blots, did not show any significant changes in tPA protein levels, in both SN and striatum (Fig. 6 A', SN; Fig. 7 A', striatum).

Plasminogen was recognizable as a single immunopositive band, which co-migrated with the corresponding protein standard at a molecular mass of approximately 90 kDa (Fig 6B and 7B). In the SN, densitometric analysis of the immunopositive bands revealed that protein levels of plasminogen changed in accord to what observed for its mRNA, being significantly decreased by 1 hr after MPTP and throughout the post-injection time, compared with control. At a difference, in the striatum (Fig. 7B'), where we were not able to detect reasonable mRNA levels in parkinsonian mice, protein levels remained not significantly different from control until 2 wks, when they decreased

significantly. However, looking at the bar graphs, the behaviour of the protein levels after MPTP injection suggests a post-trasncriptional modulation, characterized by an initial decrease (1 hr), followed by a progressive increase at about control levels (48 hrs) and by another progressive decrease until 2 wks. Except for this last time point, all the other differences were not significant compared to control, due to a high variability within each experimental group, as shown by the large standard error bars.

MMP-9 protein levels changed robustly and significantly in both SN and striatum of all MPTP treated groups respect to control. The polyclonal antibody used to reveal MMP-9 recognized two bands at about 100 kDa and 92 kDa, corresponding to the enzyme pro- and active forms, respectively (Fig. 6C, SN; Fig. 7C, striatum). The human recombinant MMP-9, used as positive control and loaded on a separate lane in the same gels, gave rise to a single immunopositive band corresponding to the active form and migrating slightly below the one of the mouse brain extracts. Densitometric analysis of the immunopositive bands of both pro- and active MMP-9 revealed a significant increase in the protein levels in both SN and striatum, early after the MPTP intoxication (by 24 hrs in the SN and 1 hr in the striatum), compared to control (Fig. 6C', SN; Fig. 7C', striatum). Protein levels of both enzymatic forms remained significantly higher than control throughout the post-treatment time considered.

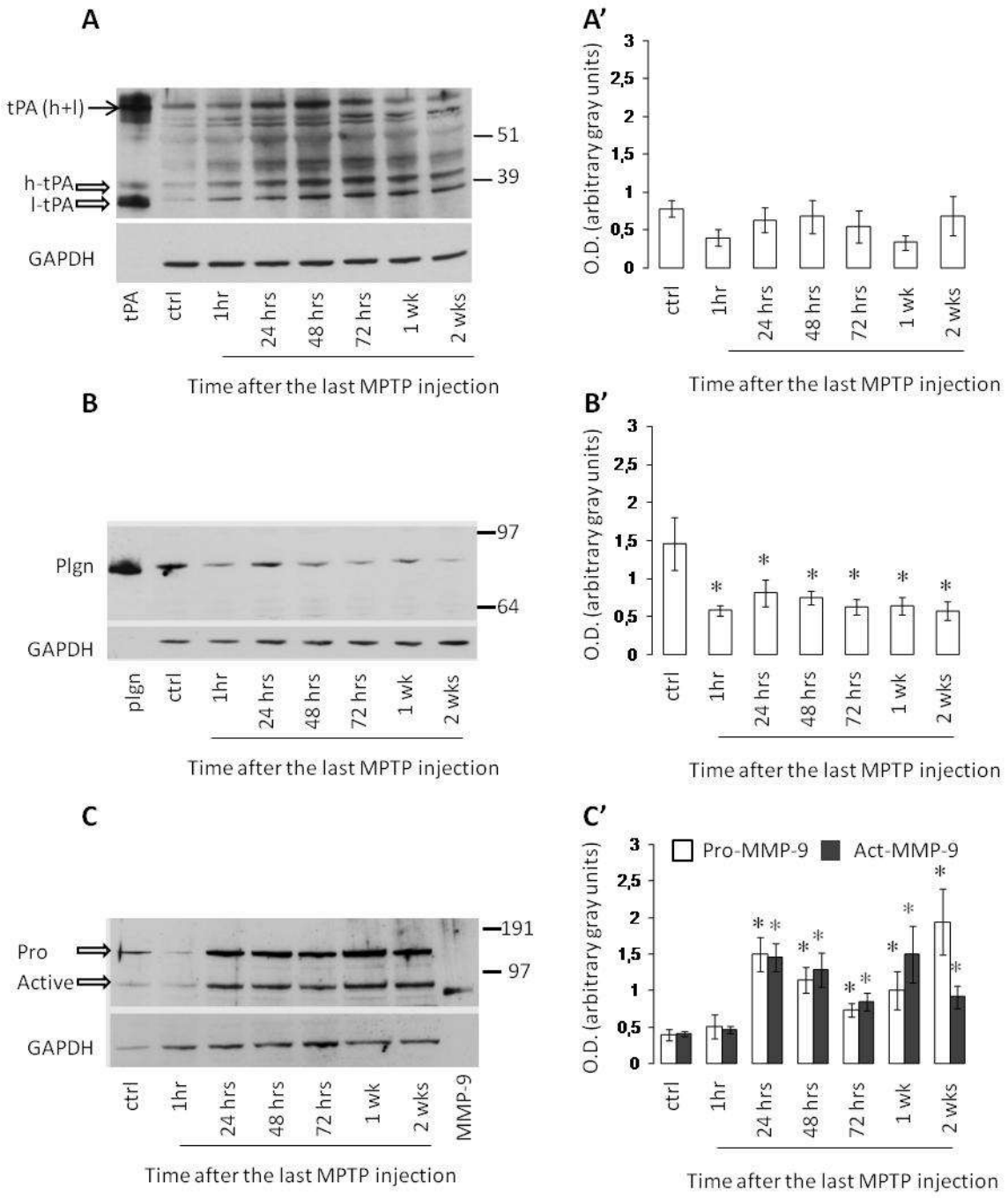

Fig. 6. Western immunoblots of tPA (A), plasminogen (plgn) (B) and MMP-9 (C) in the SN of both control and parkinsonian mice and relative densitometric analysis (A'-C'). A,A') The anti tPA antibody reveals three bands one of approximately 65 kDa, corresponding to the whole molecule, a second of approximately 40 KDa corresponding to the tPA heavy chain (h-tPA) and a third of approximately 30 kDa corresponding to the tPA light chain (l-tPA). Recombinant human tPA (first lane on the left) was used as standard. Densitometric analysis of the tPA immunopositive bands shows no differences between control and MPTP-treated mice. B, B'). The anti-plasminogen antibody recognizes a single band of about 90 KDa, the intensity of which diminishes after MPTP treatment. Human recombinant plasminogen was used as standard and loaded in the first lane on the left. Densitometric analysis confirms a significant and long lasting decrease in the intensity of the immunopositive bands after MPTP injection respect to control. C,C') Typical MMP-9 western immunoblot. The antibody labels two bands at the predicted molecular mass of the pro- (100 kDa) and active (92 kDa) MMP-9. On the right hand side, a recombinant human MMP-9 was used as standard, which migrates at a slightly lower molecular mass respect to the active form o the mouse MMP-9. Densitometric analysis of the immunopositive bands reveals an early and

significant increase, compared to control, in the protein levels of both pro- and active MMP-9, as early as 24hrs after MPTP injection. Protein levels remain significantly higher than control throughout the post-injection time considered. Molecular mass standard, expressed in kDa, are indicated on the right hand side. GAPDH was used as internal reference protein. O.D.: optical density. n = 6-8 animals/experimental group. In the histograms, bars represent the mean ± s.e.m. of the optical densities; *p ≤ 0.05 calculated by the one way ANOVA (Duncan's test).

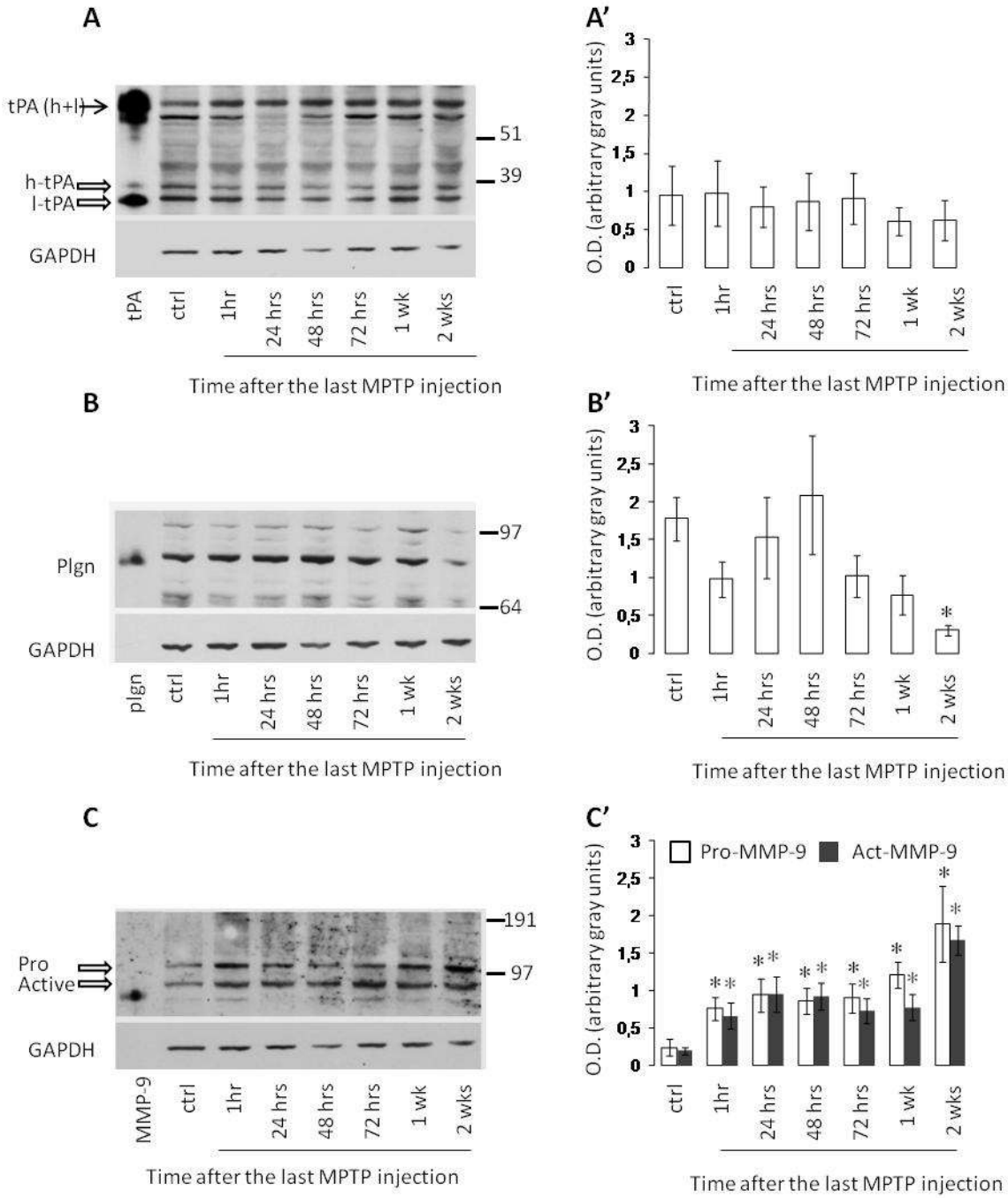

Fig. 7. Western Immunoblot of tPA (A), plasminogen (plgn) (B) and MMP-9 (C) in the striatum of control and parkinsonian mice and relative densitometric analysis (A'-C'). (A, B, C) Typical Western immunoblots for tPA, plasminogen and MMP-9, respectively. A',B') Densitometric analisys of tPA and plasminogen immunopositive bands, respectively. The analysis shows no statistical differences between control and MPTP-treated groups. C') Densitometric analysis of the MMP-9 immunopositive bands reveals that, compared to control, protein levels of both pro- and active MMP-9 increase significantly as early as 1hr after MPTP injection and remain significantly higher than control during the entire considered post-injection time. Molecular mass standard, expressed in kDa, are indicated on the right hand side. GAPDH was used as internal reference protein. O.D.: optical density. n = 6-8 animals/experimental group; bars represent the mean ± s.e.m. of the optical densities; *$p \leq 0.05$ calculated by the one way ANOVA (Duncan's test).

Gelatinase enzymatic activity in control and MPTP-treated mice evaluated by in situ zymography

Increase in gelatinase (MMP-9 and MMP-2) activity after MPTP treatment was confirmed by *in situ* zymography. This technique allows to localize the activity of specific proteases directly on unfixed cryo-sections, by incubating tissue slices in the presence of the specific enzymatic substrate (in this case gelatin for both MMP-2 and MMP-9), conjugated to a quenched fluorochrome (i.e. fluorescein), diluted in an activation medium. Sites of protease activity are revealed by a fluorescent emission consequent to enzymatic cleavage of the specific substrate.

In both SN (Fig. 8A) and striatum (Fig. 8B) of control mice, we observed a number of cells positive for the gelatinolytic activity. Seventy two hours after MPTP treatment (chosen as a representative date of the early post-treatment time), and in accord with the data obtained by Western immunoblot, we observed an increase in the overall intensity of cellular and extracellular gelatinolytic activity, in both brain areas. In addition, the striatum of injected mice was characterized by a prominent increase in the extracellular enzymatic activity, suggesting that in this area ECM remodelling by gelatinases may constitute a rapid response to the toxic insult. Two weeks after treatment, gelatinase activity was still apparently higher than control (not shown).

Control slices, treated by adding EDTA to the incubation medium, were negative (not shown), confirming the gelatinolytic nature of the staining.

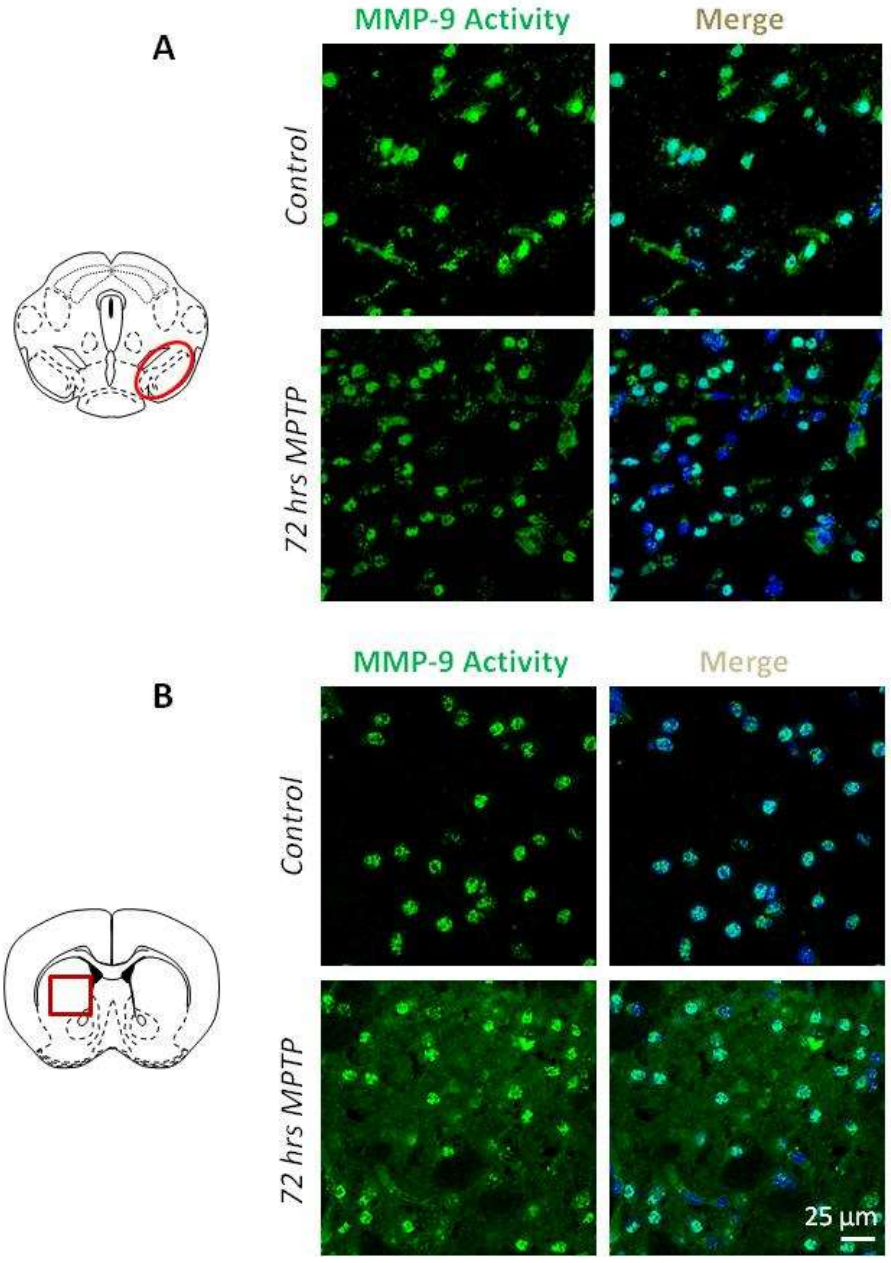

Fig. 8. *In situ* zymography in the SN*pc* (A) and striatum (B) of control and MPTP-treated mice. In both areas, cellular and extracellular gelatinolytic activity increased 72 hrs after MPTP treatment. The extracellular increase is particularly evident in the striatum (B). Nuclei are stained in blue with DAPI.

MMP-9 immunolocalization and stereological analysis in control and parkinsonian mice, alone and in combination with cell specific markers

After corroborating, by a biochemical approach, that in mice MMP-9 synthesis and activation was up-regulated during the period of 2 wks following MPTP acute administration, we analyzed which cell type/s contributed to MMP-9 synthesis and activation in brain of both control and parkinsonian animals. At this purpose we performed a detailed analysis of confocal immuno-microscopy, in combination with a stereological quantification of the positive cells, on serial brain sections of control and MPTP-injected mice, immunolabelled for MMP-9 alone or in combination with NeuN (neuronal marker), GFAP (astrocyte marker), tomato lectin (labelling microglia) or MRP (oligodendrocyte marker). Important piece of our investigation was also to quantify the inflammatory reaction triggered by MPTP treatment, in which astrocytes and microglia are mainly involved, paying attention to a poorly unravelled aspect: the oligodendrocyte reaction associated to the partial depletion of the dopaminergic system.

MMP-9/NeuN/TH triple immunofluorescence in SNpc of both control and MPTP injected mice

In order to demonstrate whether MMP-9 was synthesized by dopaminergic neurons of the SN and whether there were differences in the enzymatic expression between these and non-dopaminergic neurons, we performed a triple immunofluorence for MMP-9 in combination with both NeuN and TH, on both control and MPTP-treated mice.. As shown in Fig. 9A, MMP-9 largely co-localized with NeuN and TH, in both experimental conditions, labelling numerous cell bodies and axons. Stereological quantification of the immunopositive cells showed that almost all neurons $NeuN^+$ and TH^+ were also $MMP\text{-}9^+$ (Fig. 9 B',B'') and that the majority of the $NeuN^+$ neurons were

dopaminergic (Fig. 9B'"), in both control and parkinsonian mice. Extracellular immunopositive spots were also visualized in all confocal pictures taken from both control and treated mice, possibly identifying with both axons cut through their transversal plane and free, secreted MMP-9. As also previously described, MPTP-treatment led to a significant loss of TH^+ neurons (Fig. 8B'', gray bar), with the consequent reduction in the number of $NeuN^+$ cells (Fig. 8B', gray bar). As expected this reduction partially recovered 2 wks after MPTP administration, along with a corresponding increase in $NeuN^+$ cell number (Fig. 8B',B''). The number of MMP-9^+/$NeuN^+$ and MMP-9^+/TH^+ double-labeled neurons, as well as that of MMP-9^+ cells (Fig. 8B) followed the same time course, being lower than control between 24-72 hrs after the last MPTP injection and partially, but significantly recovering after 2 wks. Concomitantly, an increase in the extracellular MMP-9 immunopositivity was observed (Fig. 8A). From this stereological study also emerged an interesting data: while the number of MMP-9^+/TH^+ neurons significantly diminished after MPTP treatment, with a trend similar to the one observed for MMP-9^+/$NeuN^+$ cells (Fig. 8B',B''), the number of the sole non-dopaminergic neurons remained stable and those expressing MMP-9 ($NeuN^+$/TH^-/MMP-9^+) increased significantly 72 hrs after the MPTP injection (Fig. 8B'''). These results suggest that factors possibly released by dying dopaminergic neurons may trigger MMP-9 synthesis in the surrounding non-dopaminergic neurons, in response to the neurotoxic insult.

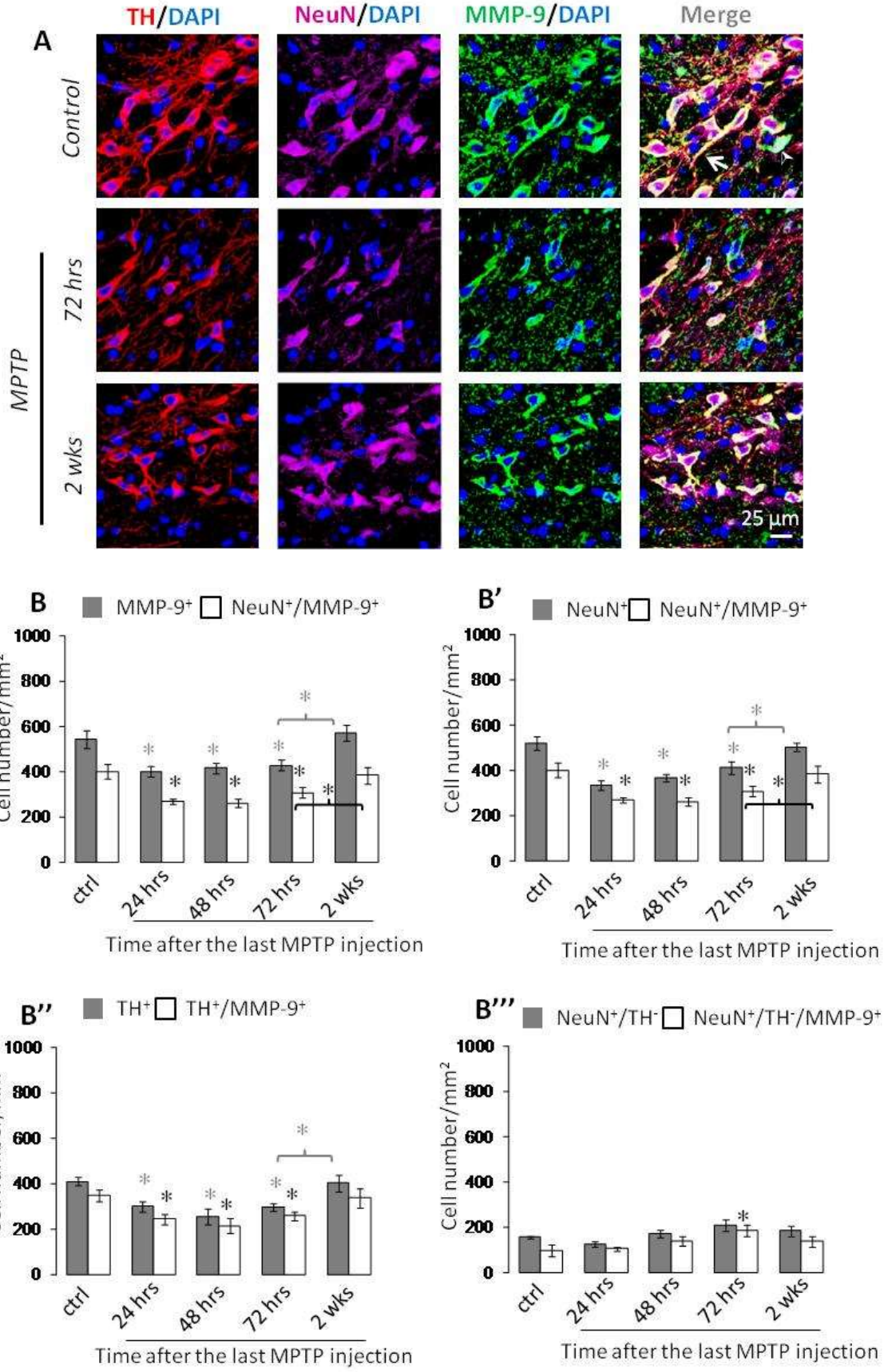
A
TH/DAPI
NeuN/DAPI
MMP-9/DAPI
Merge
Control
MPTP
72 hrs
2 wks
25 µm
B
MMP-9+
NeuN+/MMP-9+
Cell number/mm2
ctrl
24 hrs
48 hrs
72 hrs
2 wks
Time after the last MPTP injection
B'
NeuN+
NeuN+/MMP-9+
B''
TH+
TH+/MMP-9+
B'''
NeuN+/TH-
NeuN+/TH-/MMP-9+

Fig. 9. Co-immunolocalization of MMP-9 (green), NeuN (purple) and TH (red) on SN*pc* sections of control and MPTP injected mice and relative stereological analysis. A) MMP-9 largely co-localizes with both dopaminergic and non-dopaminergic neurons (arrowhead in the merge panel). MMP-9 immunolabeling is observed in both neuronal cell bodies and axons (arrow in the merge panel of control group). Nuclei are stained in blue with DAPI. (B) Stereological quantification of MMP-9^+ cells (gray bar) and MMP-9^+/$NeuN^+$ double labeled cells (white bar). (B') Stereological quantification of $NeuN^+$ cells (gray bar) and MMP-9^+/$NeuN^+$ double labeled cells (white bar). (B'') Stereological quantification of TH^+ cells (gray bar) and MMP-9^+/TH^+ double labeled neurons (white bar). (B''') Stereological quantification of $NeuN^+$/TH^- neurons (gray bar) and MMP-9^+/TH^- neurons (white bar). n = 3 animals/experimental group; bars represent the mean ± s.e.m. of the cell number/mm^2; *$p \leq 0.05$ calculated by the one way ANOVA (Duncan's test).

MMP-9/NeuN co-localization in the striatum of control and MPTP-injected mice

As observed in the SN*pc*, in the striatum of both control and MPTP treated animals, MMP-9 immunnolabeling largely, but not completely, co-localized with the neuronal marker NeuN (Fig. 10A). In fact, as shown in the enlargement of the boxed detail of Fig. 10A (right-hand four panels), not all neurons were immunopositive for MMP-9 and not all MMP-9^+ cells were neurons. Seventy-two hours after the last MPTP injection, a clear increase in both MMP-9 cellular and extra-cellular staining was observed, according to both Western immunoblots and *in situ* zymography data (Fig. 7C and Fig. 8B, respectively). Stereological analysis conducted on random striatal photographic field (Fig. 10B) confirmed that the number of MMP-9^+ cells increased significantly respect to control by 48 hrs after MPTP injection and throughout the following dates. However, the number of MMP-9^+ neurons did not change after treatment, as well as the number of $NeuN^+$/MMP-9^+ neurons, suggesting that in the striatum the increase in MMP-9 may derive from the contribution of other cell types rather than neurons.

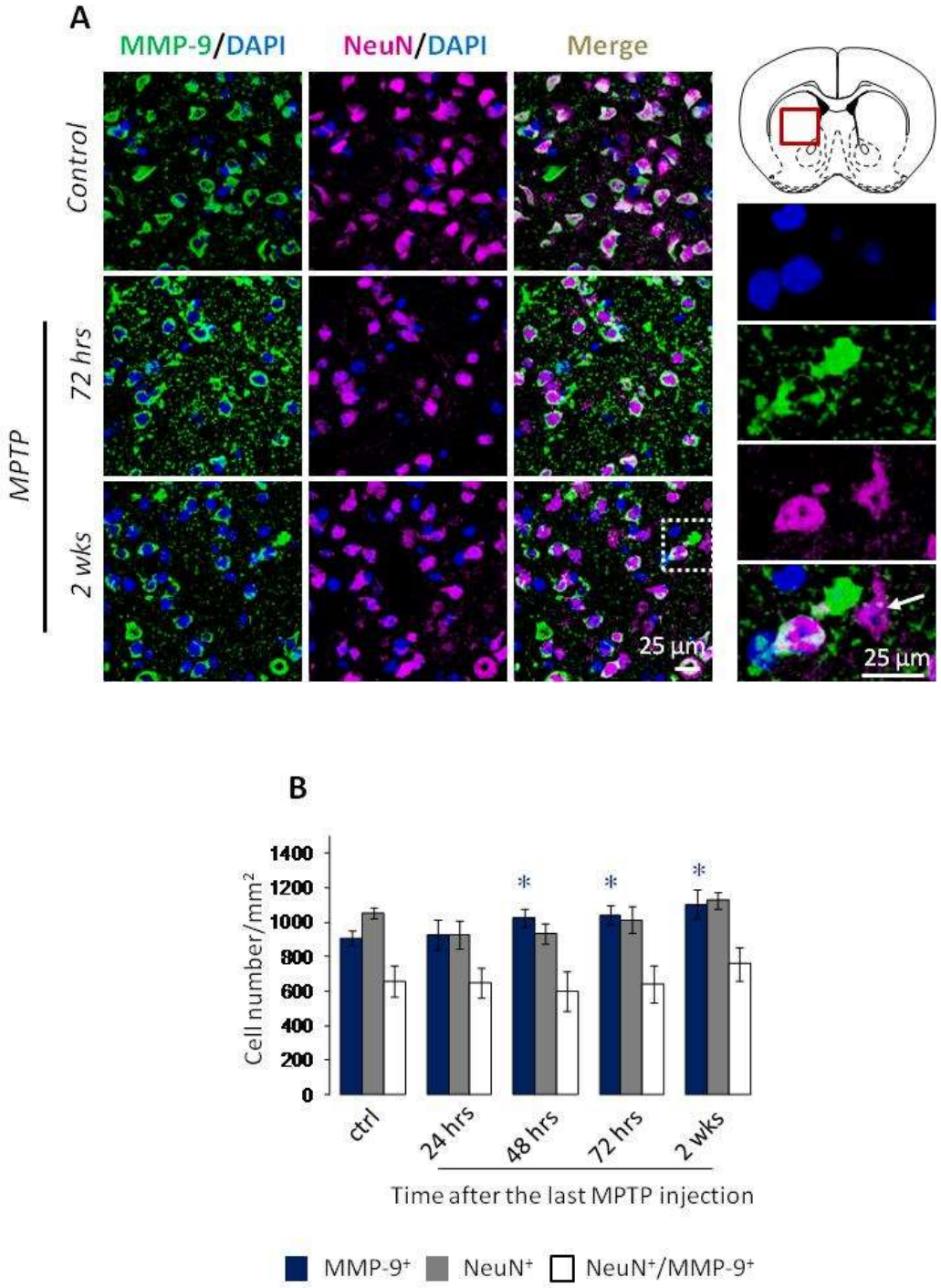

Fig. 10. MMP-9/NeuN immunofluorescence in the striatum of control and MPTP-injected mice and relative quantitative stereological study. (A) Confocal images reveal a large co-localization of the two proteins in both control and treated mice, although not all neurons are MMP-9$^+$ (arrow in the enlargement of the boxed area in A, at the right hand side). Both cellular and extracellular labeling for MMP-9 are increased respect to control after MPTP administration. Green channel: MMP-9, Purple channel: NeuN, Blue DAPI staining: nuclei. (B) Stereological quantification show a significant increase in the number of total MMP-9$^+$ cells (blue bars), by 48 hrs after toxin injection up to the last experimental date of 2 wks, but not determined by neurons.. Actually, the number of MMP-9$^+$/NeuN$^+$ cells (white bar) remains stable in all experimental groups. n = 3 animals/experimental group; bars represent the mean ± s.e.m. of the cell number/mm^2; *p ≤ 0.05 calculated by the one way ANOVA (Duncan's test).

MMP-9/GFAP co-localization in the SNpc and striatum of control and MPTP-injected mice

Double immunolabeling for MMP-9 and the astrocyte marker GFAP was performed on sections of the SN*pc* (Fig. 11A) and striatum (Fig. 12A) of both control and MPTP-treated mice. As first observation, both areas showed a massive astrogliosis after MPTP injection: astrocyte activation was characterized by an increase of their number, size and cell processes $GFAP^+$ (Fig. 11A, SN*pc*; Fig 12A, striatum; red channel). More in detail, stereological quantification of $MMP\text{-}9^+$, $GFAP^+$ and $GFAP^+/MMP\text{-}9^+$ cells in both SN*pc* and striatum, demonstrated a significant increase in the $GFAP^+$ cell number by 24 hrs post-injection and throughout the post-injection time considered (2 wks) (Fig. 11B, SN*pc*; Fig.12B striatum). The number of double labelled $GFAP^+/MMP\text{-}9^+$ cells represented only a small percentage of the entire $MMP\text{-}9^+$ cell population. Actually, $GFAP^+$ cell bodies were rarely fully stained for MMP-9 (see enlargement of the boxed areas in Figs. 11A and 12A, at the left-hand side), but MMP-9 labelling occurred as puncta sparsely associated with the cell processes of activated astrocytes (Fig. 11A, SN*pc*: Fig. 12A, striatum; enlargement of the boxed areas, at the left-hand side). Stereological analysis revealed a significant increase, in both SN*pc* and striatum, in the number of the $GFAP^+/MMP\text{-}9^+$ cells throughout the period of 2 wks following MPTP intoxication compared to control, starting from 24 hrs and 48 hrs, respectively.

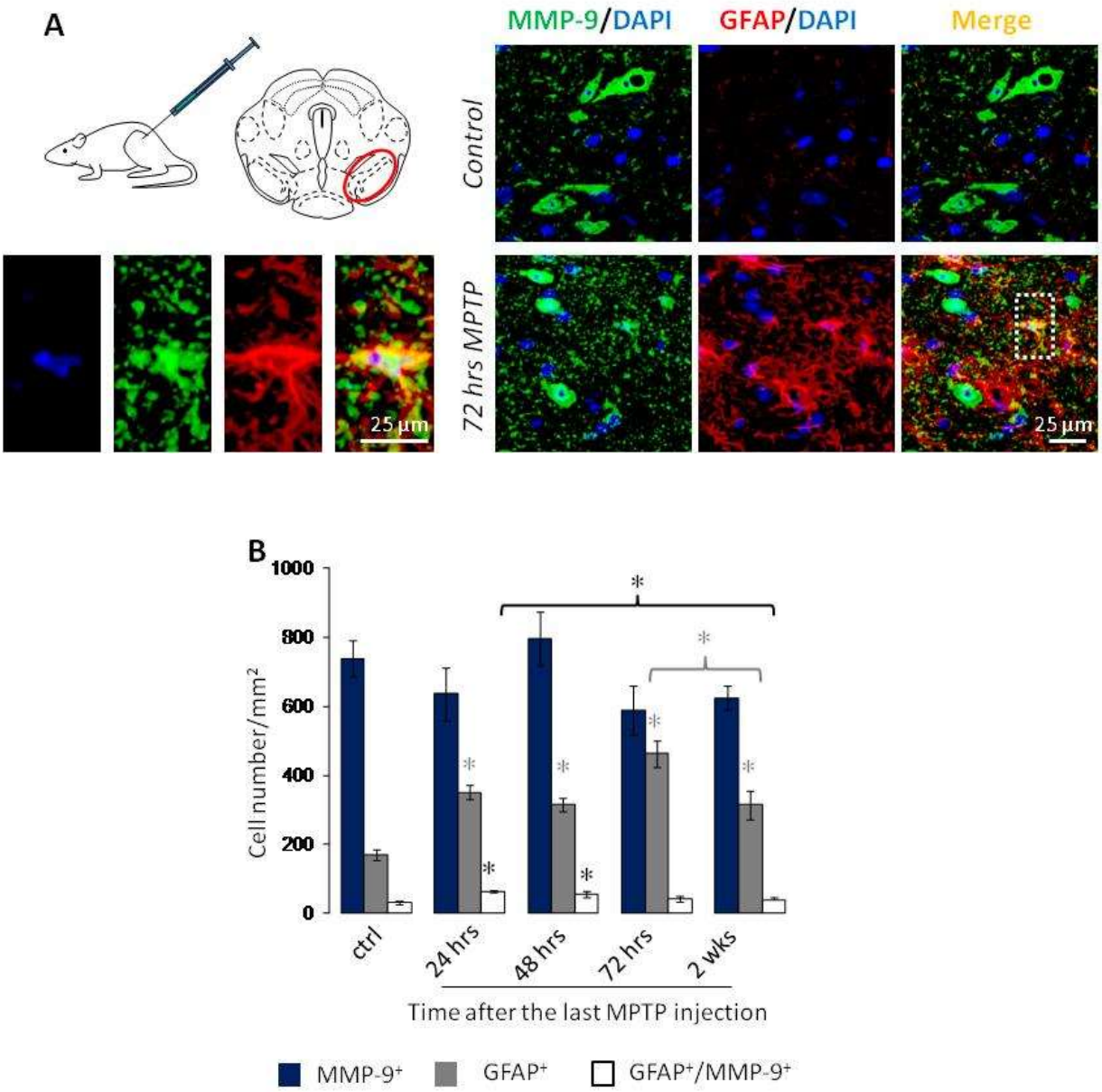

Fig. 11. Confocal images of MMP-9/GFAP double immunofluorescence and relative quantitative stereological analysis in the SN*pc* of control and MPTP-treated mice. A). After MPTP injection, both size and number of cell processes of astrocytes increase. On the left hand side, the enlargement of the boxed area evidencing a detail of the co-localization between MMP-9 and GFAP, is shown. Nuclei were counterstained with DAPI (blue) B) Stereological quantification of MMP-9$^+$ (blue bars), GFAP$^+$ (gray bars) and MMP-9$^+$/GFAP$^+$ cells (white bars) reveals that MPTP treatment determines a significant increase in both GFAP$^+$ and MMP-9$^+$/GFAP$^+$ cells number. n = 3-4 animals/experimental group; bars represent the mean ± s.e.m. of the cell number/mm^2; *p ≤ 0.05 calculated by the one way ANOVA (Duncan's test).

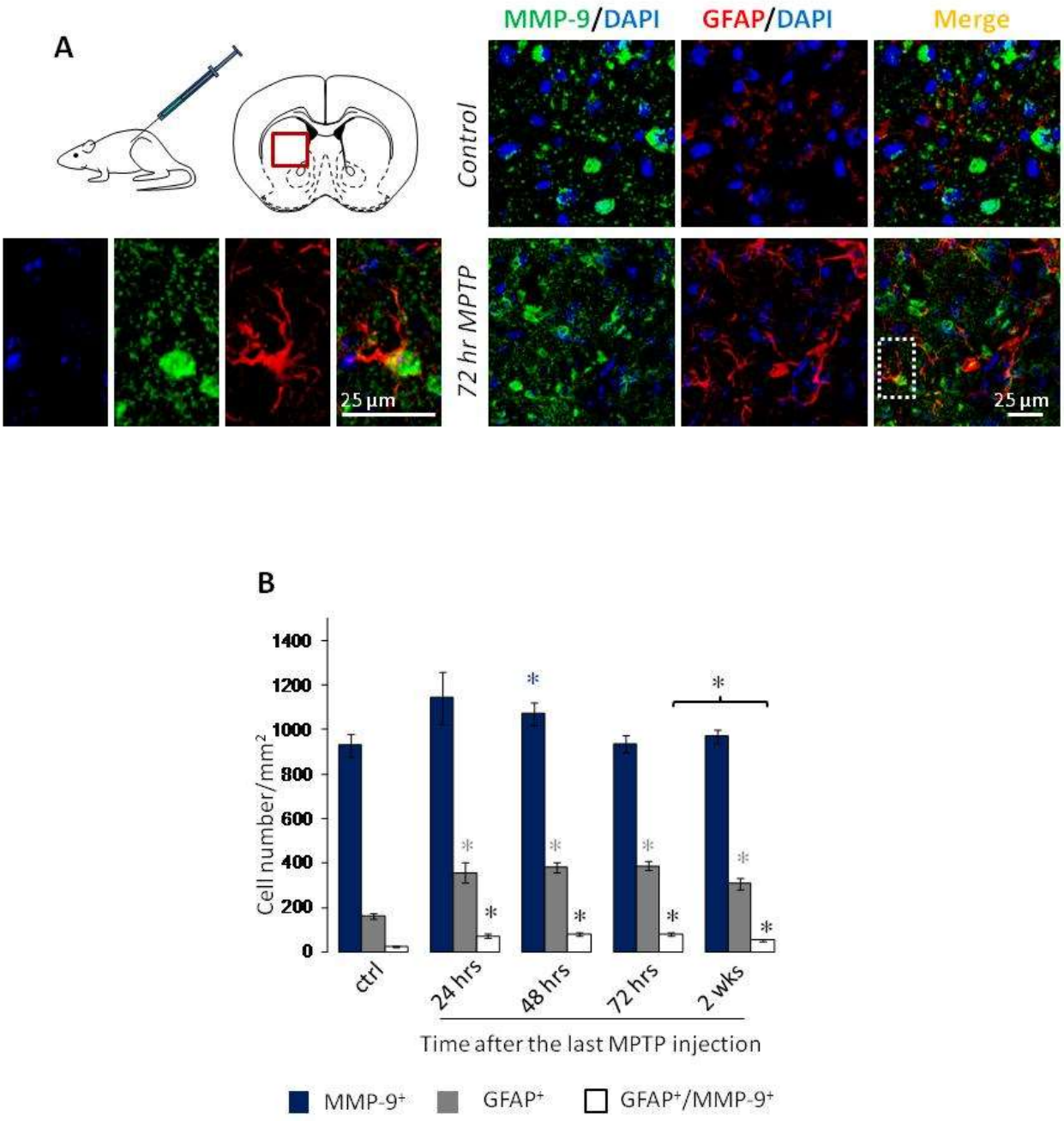

Fig. 12. Confocal images of MMP-9/GFAP double immunofluorescence (A) and relative quantitative stereological analysis (B) in the striatum of control and MPTP-treated mice. A) After MPTP treatment, a prominent astrogliosis is observed (red channel). The enlargement, at the left side, of the boxed area shows MMP-9 co-localization with a $GFAP^+$ cell body. Often puncta of MMP-9 immunoreactivity are present along the characteristic processes of activated astrocytes (arrows in the merge panel of the MPTP group). Nuclei are counterstained in blue with DAPI. (B) Stereological quantification of $MMP\text{-}9^+$ (blue bars), $GFAP^+$ (gray bars) and $MMP\text{-}9^+/GFAP^+$ cells (white bars) reveals that MPTP treatment determines a significant increase in both $GFAP^+$ and $MMP\text{-}9^+/GFAP^+$ cells number. n = 3-4 animals/experimental group; bars represent the mean ± s.e.m. of the cell number/mm^2; *$p \leq 0.05$ calculated by the one way ANOVA (Duncan's test).

MMP-9/ lectin Griffonia Simplicifolia (GSA) co-localization in the SNpc and striatum of control and MPTP-injected mice

Microglia are the main modulators of inflammation in brain and in the mouse MPTP model of parkinsonism, it has been demonstrated that activated microglial cells undergo morphological changes (Depino et al., 2003). We, therefore, investigates whether MMP-9 was expressed and/or modulated by MPTP-activated microglia, by staining sections of both SN*pc* and striatum of control and treated mice with a classical microglia marker, the *Griffonia Simplicifolia* Lectin I, Isolectin B4 (GSA) (Pott Godoy, 2008), alone and in combination with MMP-9 immunofluorescence. Fluorescent microscopy analysis (Fig. 13A, SN*pc*; Fig. 14A, striatum) revealed that MPTP treatment triggered microglia activation in the entire nigro-striatal pathway. In both control mouse SN*pc* and striatum, GSA staining was generally weak, mainly as associated to small cells characterized by few, thin processes (Fig. 13A, SN*pc*; Fig. 14A, striatum; arrows in red channel panels). After MPTP injections, the intensity of the GSA staining increased and microglial cells assumed an amoeboid-like feature, with a round-shaped perikaryon with short, thick and stout processes (Fig. 13A, SN*pc*; Fig. 14A, striatum; red channel). The quantitative stereological study conducted in both areas (Fig. 13B, SN*pc* and 14B, striatum), showed that, in our model, microglia activation was associated to a significant increase in the number of GSA^+ cells, by early after the treatment (24 hrs). The number of positive cells further increased up to 72 hrs post-injection and then significantly decreased, compared to this date, after 2 wks, although remaining higher than control. Even if microglia activation was observed along the entire nigro-striatal dopaminergic pathway, in the SN*pc* this phenomenon appeared exacerbated, probably because of the contiguity with dying neurons.

In control mice, we rarely found microglial cells immunopositive for MMP-9; however, the number of MMP-9^+/GSA^+ double labelled cells significantly increased, respect to control, after MPTP treatment, in both SN*pc* (Fig. 13 B) and striatum (Fig. 14B). Interestingly, while in the striatum of all MPTP experimental groups the number of MMP-9^+ microglial cells was always higher than that in control mouse striatum, (Fig. 14B) in the SN*pc* it was significantly higher only 48 hrs and 72 hrs after the last MPTP injection, dates in which neuronal loss reached its peak (Fig. 13B). However, as for astrocytes, stereological quantification performed in both areas (Fig. 13B, SN*pc* and 14B, striatum) outlined as microglia was only a minority of the totality of MMP-9^+ cells.

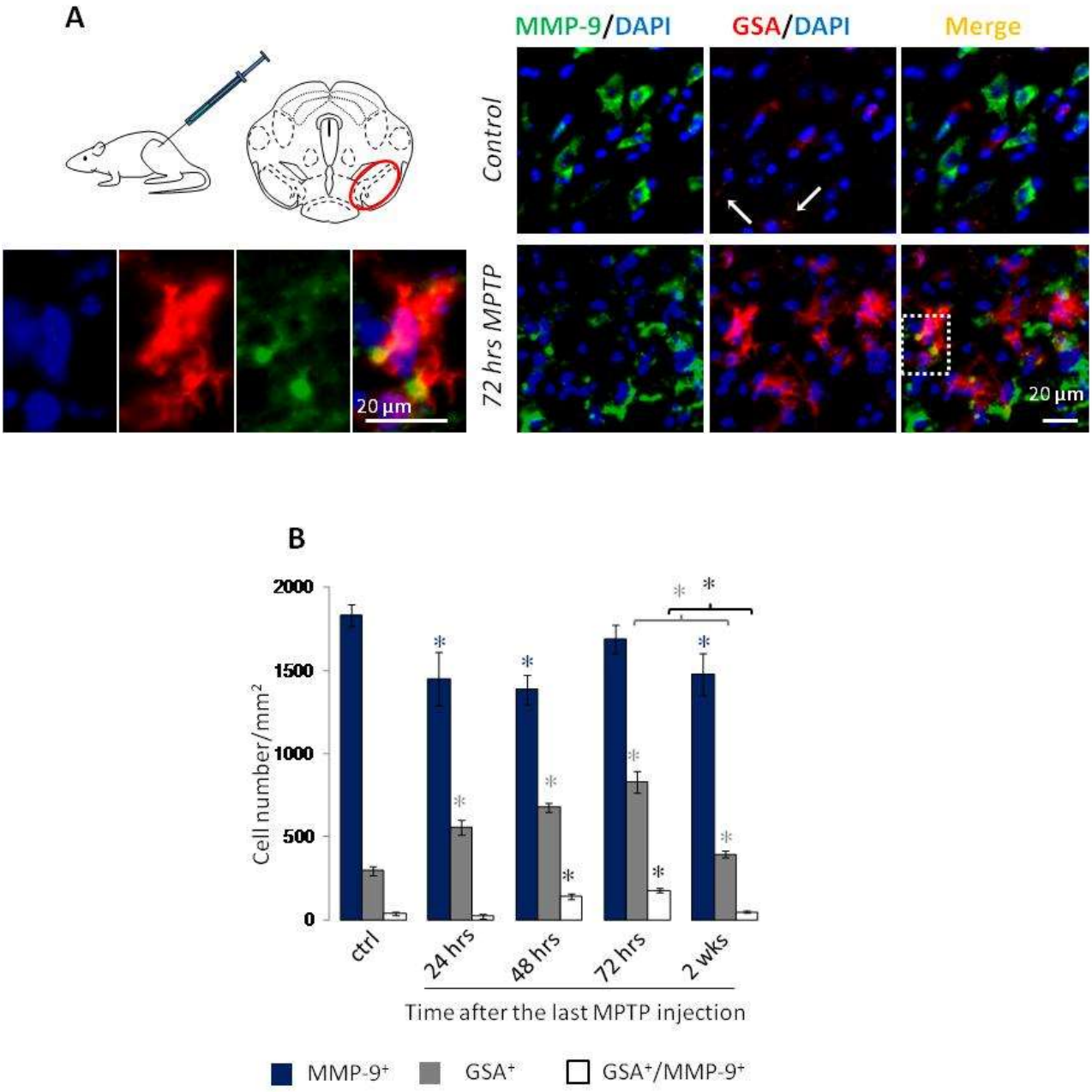

Fig. 13. GSA staining combined with MMP-9 immunofluorence in the SN*pc* of control and MPTP-injected mice and relative quantitative stereological analysis. A) Sections of SN*pc* immunolabeled for MMP-9 (green) combined with GSA staining (red). In control mice, microglia is weakly stained by GSA and is characterized by small perikarya with a few, thin processes (arrows in red channel panel). After MPTP treatment, microglia switches to an activated phenotype, characterized by increased cell size with thick and stout processes. Double immunopositive cells were more often found respect to control (enlargement of the boxed area, at the left hand side). Nuclei were counterstained with DAPI (blue) B) Stereological quantification of MMP-9$^+$ (blue bar), GSA$^+$ (gray bar) and MMP-9$^+$/GSA$^+$ (white bars) cells reveals a significant increase in the number of both GSA$^+$ and MMP-9$^+$/GSA$^+$ cells after MPTP injection (48-72 hrs). n = 3-4 animals/experimental; bars represent the mean ± s.e.m. of the cell number/mm^2; *p ≤ 0.05 calculated by the one way ANOVA (Duncan's test).

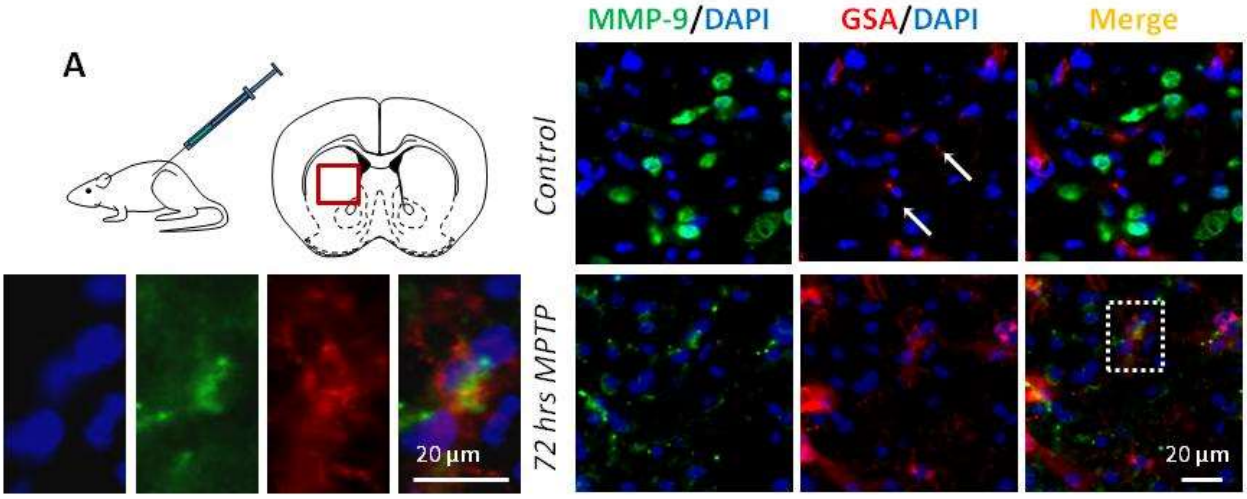

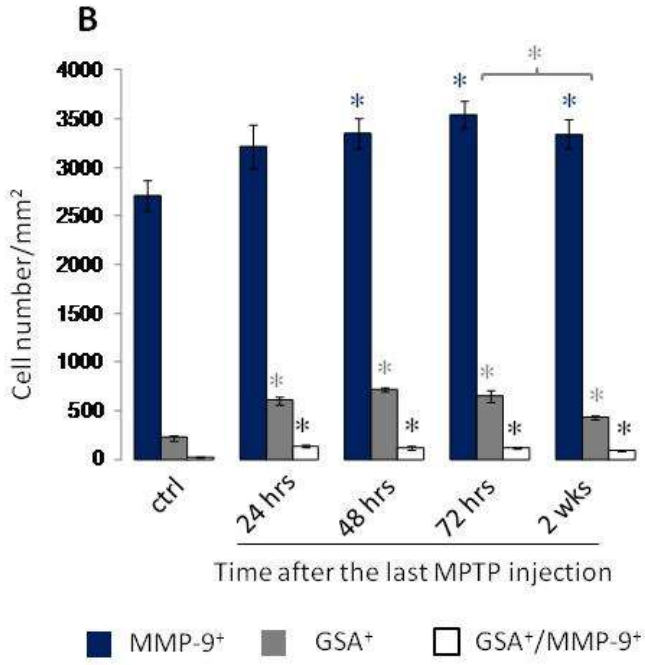

Fig. 14. GSA staining combined with MMP-9 immunofluorence in the striatum of control and MPTP-injected mice (A) and relative quantitative stereological analysis (B). A) In control mice, MMP-9 (green) poorly co-localizes with GSA^+ (red) cells. After MPTP treatment, microglia takes the typical activated morphology, and the number of double positive cells increases respect to control. As shown in the enlargement of the boxed area at the left hand side, MMP-9 clumps of staining in GSA^+ cells are frequently polarized. Arrows in the red channel indicate cells with the typical inactive microglial morphology. Nuclei are counterstained with DAPI (blue). B) Stereological quantification of MMP-9^+ (blue bar), GSA^+ (gray bar) and MMP-9^+/GSA^+ (white bars) cells reveals that MPTP treatment determines a significant increase in the number of both GSA^+ and MMP-9^+/GSA^+ cells along the entire period of observation. n = 3-4 animals/experimental group; bars represent the mean ± s.e.m. of the cell number/mm^2; *$p \leq 0.05$ calculated by the one way ANOVA (Duncan's test).

MMP-9/MRP co-localization in the SNpc and striatum of control and MPTP-injected mice

In order to complete our study, we investigated the level of co-localization between MMP-9 and MRP, an OL marker. In both SN*pc* and striatum of control mice, OLs were characterized by a small cell size with a few or no evident branches processes (Fig. 15A, SN*pc*; Fig. 16A, striatum). In MPTP-treated mice, confocal analysis revealed a series of important OL morphological changes during the critical period of dopaminergic neuron death. Actually, after toxin treatment, OL cell body size increased compared to control, showing a higher number of processes with increased thickness, which could also reach higher levels of arborization (Fig. 15A, SN*pc*; Fig. 16A, striatum; red channel). Altogether, these features are usually related to an OL activation, also known as oligodendrogliosis. OL activation has been described in several neurodegenerative diseases, but its role in PD is unknown, as data on both post-mortem PD human brains and on PD animal models are not conclusive (Takagi, 2007; McGeer and McGeer, 2008). We, therefore, decided to first characterize in detail this phenomenon and, because of the novelty of the results, we will describe them in a separated session of this thesis.

MMP-9/MRP co-localization was investigated by confocal analysis. In the nigro-striatal pathway of control mice, MMP-9 rarely co-localized with MRP, however, following MPTP treatment, the number of MMP-9^{+}/MRP^{+} significantly increased by 24 hrs after the last injection, remaining higher than control up to 72 hrs. Two weeks after MPTP treatment, while the number of MMP-9^{+}/MRP^{+} in the SN*pc* returned to control levels (fig. 15B) after the one in the striatum remained higher than control (Fig. 16B). As a general observation, MMP-9^{+}/MRP^{+} cells appeared smaller and morphologically less characterized than the neighboring MMP-9^{-}/MRP^{+}. As for astrocytes, MMP-9

staining never filled the entire OL cytoplasm, being characteristically distributed in patches and small puncta (Fig. 15A, SN*pc*; Fig 16A, striatum; enlargement of boxed areas, at the left-hand side).

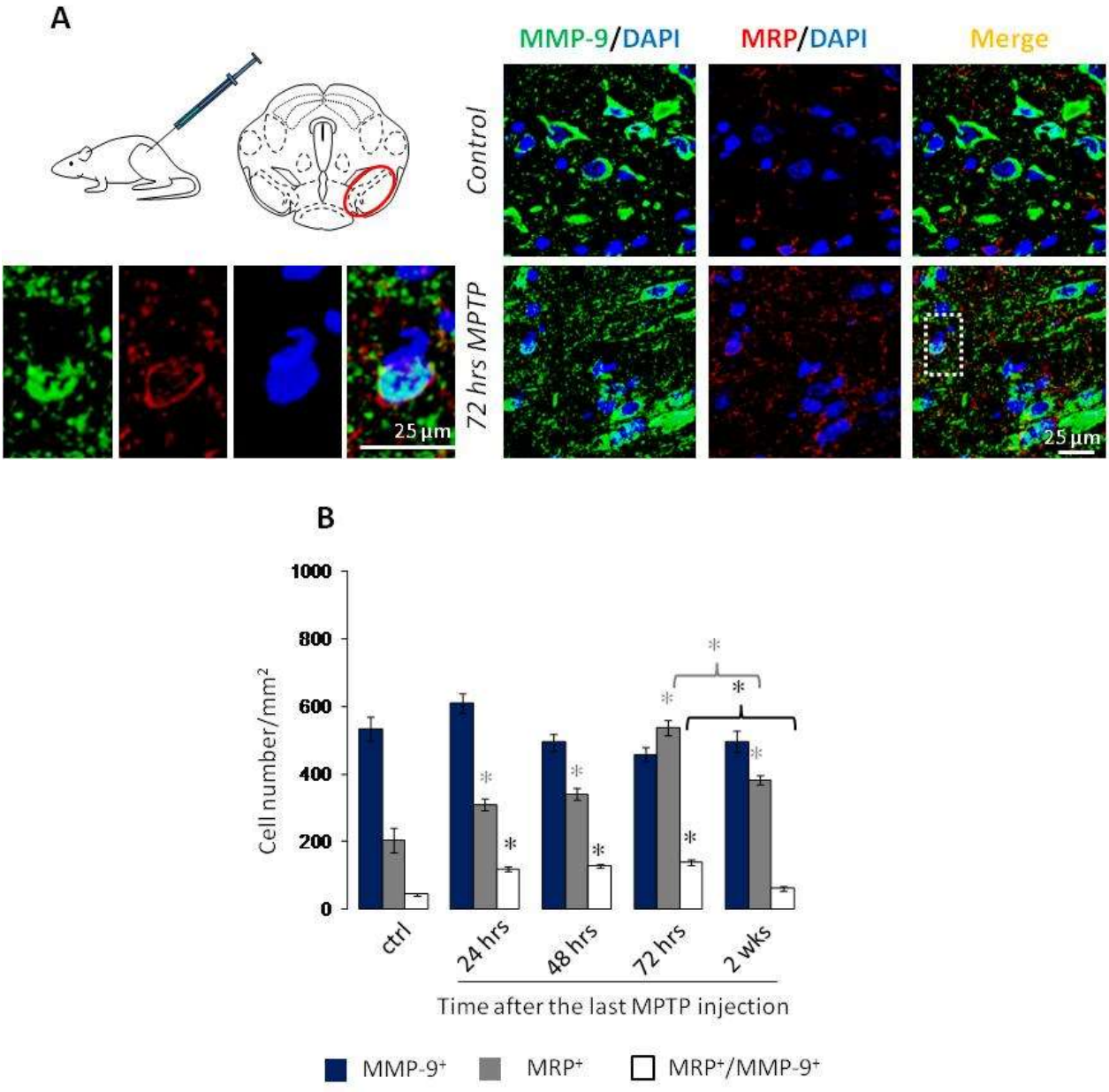

Fig. 15. Confocal images of MMP-9/MRP co-localization in the SN*pc* of both control and MPTP-injected animals (A) and relative stereological quantification (B). (A) In control mice, MMP-9 (green) rarely co-localizes with MRP (red). In MPTP-treated mice, double immunopositive cells are more frequently encountered and often the staining for the two proteins is localized in different cytoplasmatic compartments (enlargement of the boxed area at the left hand side). After MPTP treatment, MRP staining increases and OL morphology switches to an activated state. Nuclei are counterstained with DAPI (blue). B) Stereological quantification of MMP-9$^+$ (blue bar), MRP$^+$ (gray bar) and MMP-9$^+$/MRP$^+$ (white) cells reveals a significant increase in both MRP$^+$ and MMP-9$^+$/MRP$^+$ cell number after MPTP treatment respect to control. The number of double immunopositive cells returns to control levels after 2 wks.

n = 3-4 animals/experimental group; bars represent the mean ± s.e.m. of the cell number/mm^2; *p ≤ 0.05 calculated by the one way ANOVA (Duncan's test).

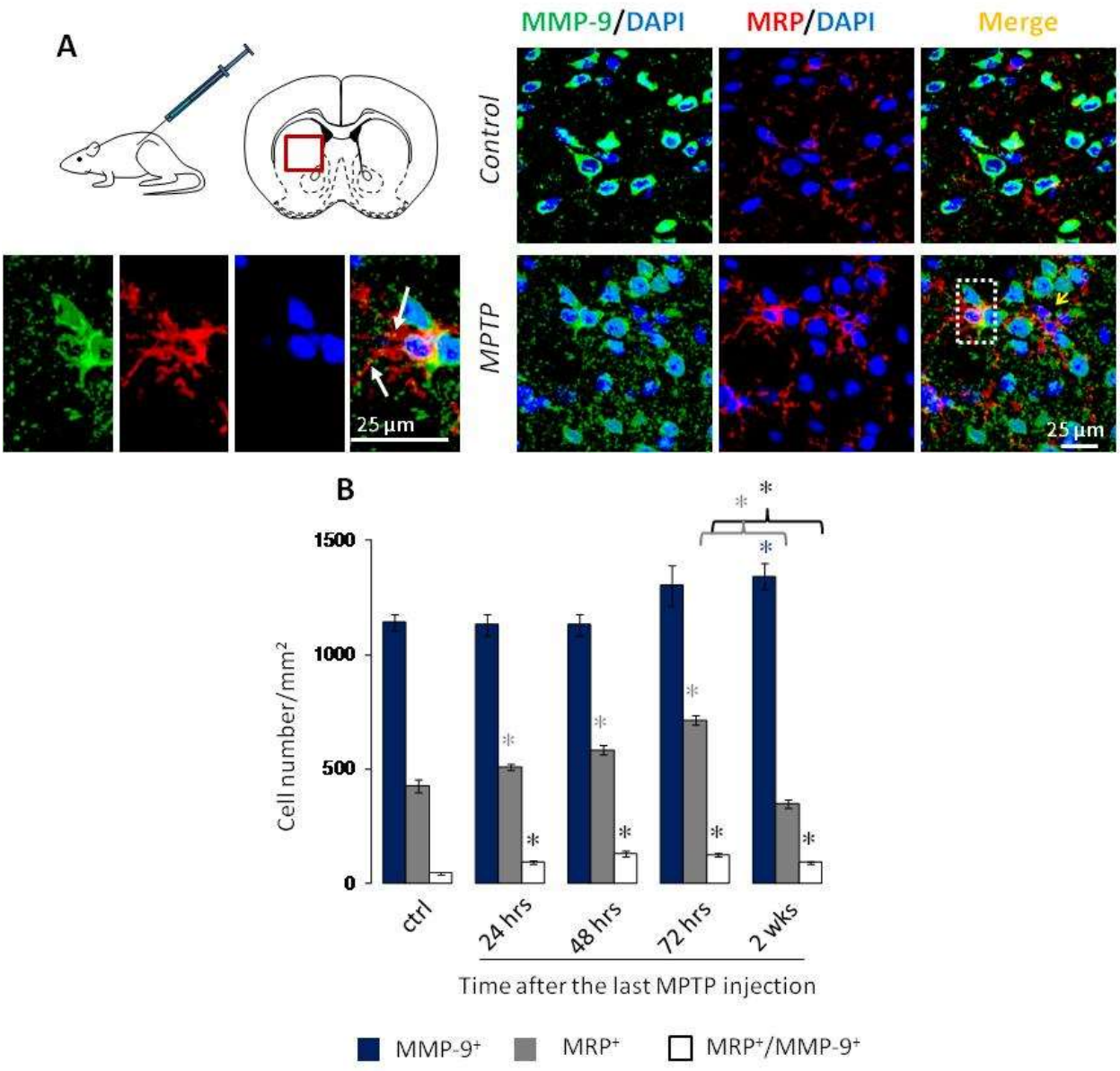

Fig. 16. Confocal images of MMP-9/MRP co-localization in the striatum of control and MPTP-injected mice (A) and relative stereological quantification (B). A) In the striatum of control mice, MMP-9 (green)/MRP (red) co-localization is almost null, and MRP$^+$ cells are characterized by small cell body with a few, thin processes. In MPTP-treated mice, the number of double immunopositive cells increase respect to control, concomitantly with a prominent. oligodendrogliosis. MMP-9 immunostaining co-localizes with both small and poorly activated OLs (yellow arrow in A), but numerous MMP-9$^+$ puncta are be observed along process arborizations after MPTP treatment (arrows in merge panel). Nuclei were counterstained with DAPI (blue). B) Stereological quantification of MMP-9$^+$ (blue bars), MRP$^+$ (gray bars) and MMP-9$^+$/MRP$^+$ (white bars) cells show a significant increase in both MRP$^+$ and MMP-9$^+$/MRP$^+$ cell number after MPTP treatment with respect to control. MMP-9$^+$/MRP$^+$ cell number, returns to control levels 2 wks after the last MPTP injection. n = 3-4 animals/experimental group; bars represent the mean ± s.e.m. of the cell number/mm^2; *p ≤ 0.05 calculated by the one way ANOVA (Duncan's test).

MMP-9 immunolocalization and stereological analysis in control and parkinsonian monkeys, alone and in combination with cell specific markers

If from one side, the mouse model of parkinsonism had the advantage of a fast analysis of the cellular and molecular processes related to the nigro-striatal pathway degeneration, on the other hand, the use of monkeys was extremely important for better understanding the role that inflammatory processes and glial cell reaction, along with MMP-9 activation, may have in the long-term disease progression, as it occurs in humans. At this purpose, monkey brain sections were immunolabeled for MMP-9 alone and in combination with either NeuN, GFAP or MBP, and then analyzed at the confocal microscope. This allowed us, along with a quantitative stereological analysis, to describe accurately the pattern of MMP-9 expression in the non-human primate model. For this part of the study, only brain sections from monkey striatum were available, which however were the most useful considering the cellular pattern of expression of MMP-9 in mice.

MMP-9/NeuN co-localization in the striatum of control and MPTP-injected monkeys

In the striatum of control and parkinsonian monkeys, MMP-9 immunolabeling largely co-localized with the neuronal marker NeuN (Fig. 17A, caudate; Fig. 17B, putamen; enlargement of boxed areas at the left-hand side) although, as observed in the mouse brain, MMP-9^- neurons were also present. MPTP treatment induced an increase in MMP-9 immunolabeling in both caudate and putamen, respect to control, at both cellular (number of immunopositive cells) (Fig. 17A,B, A' and B') and extracellular (Fig. 17A,B) levels. This increase paralleled that in the number of $NeuN^+$/$MMP\text{-}9^+$ double labeled neuron (Fig. 17A',B'). The total number of $NeuN^+$ neurons, instead, remained comparable to control, indicating new MMP-9 expression by striatal neurons,

which were previously immunonegative. A large MMP-9^{+}NeuN^{-} population, constituted by cells with a glial morphology (Fig. 17A,B) and that was not observed in control monkey striatum, was also distinguishable.

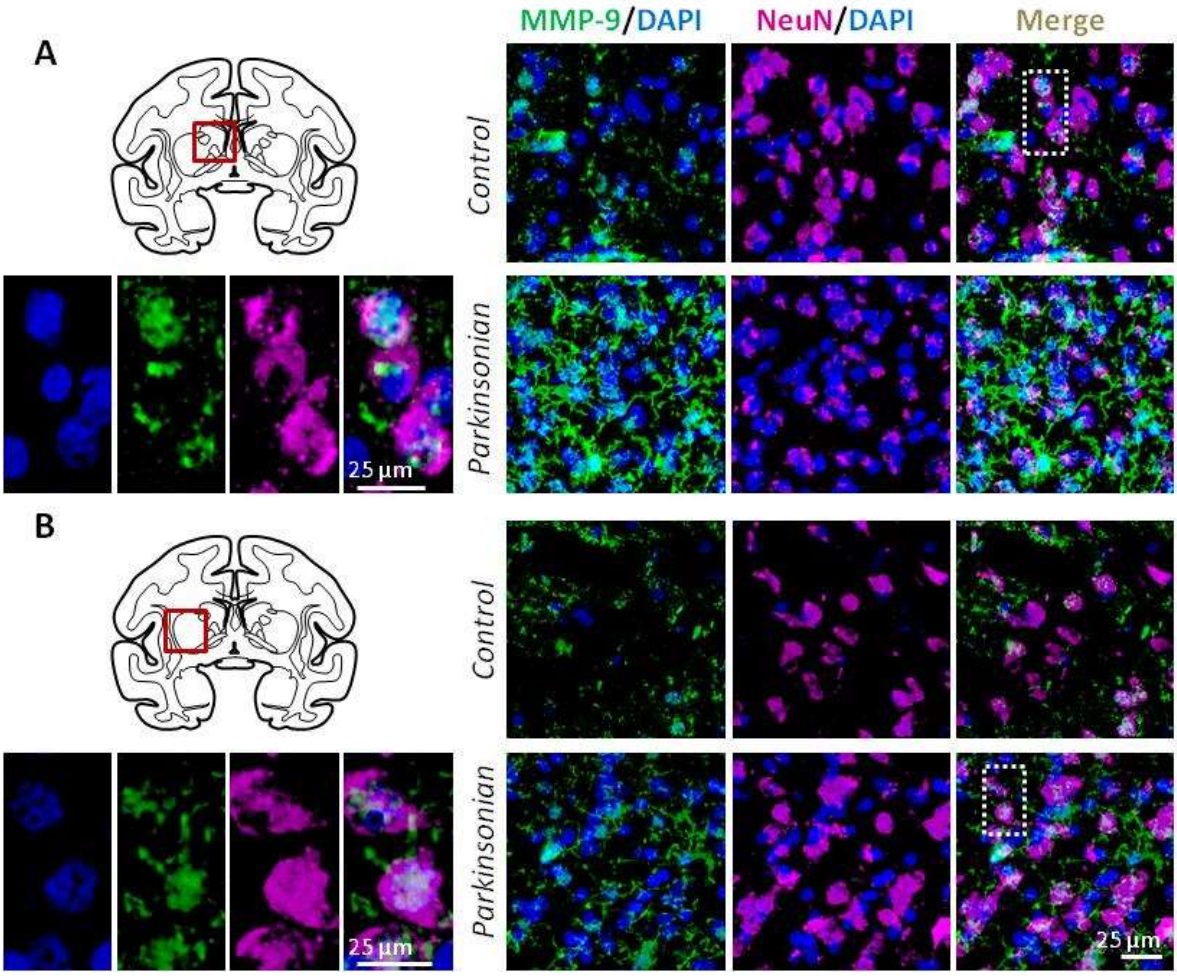

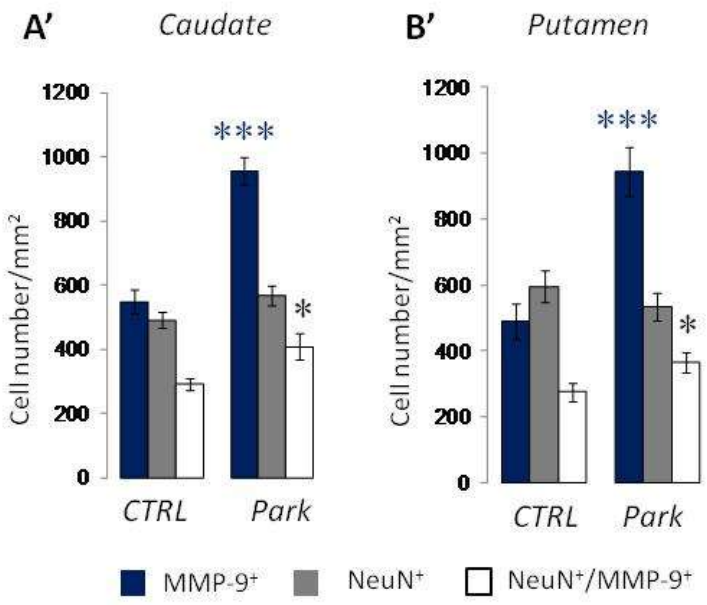

Fig. 17. MMP-9/NeuN co- immunolocalization in the caudate (A) and putamen (B) of control and MPP-treated monkeys and relative stereological quantification (A' and B'). MMP-9 (green) staining in both control and treated animals co-localizes with NeuN (violet). On the left hand side, the enlargements of the boxed area are shown. In parkinsonian monkeys, MMP-9 staining increases respect to control and it is largely associated with non-neuronal cells characterized by a glial morphology. Nuclei are counterstained with DAPI (blue). A',B') Caudate (A') and putamen (B') stereological quantifications of MMP-9$^+$ (blue bars), NeuN$^+$ (gray bars) and MMP-9$^+$/NeuN$^+$ (white bars) cells. Control group: n = 3 animals; Parkinsonian group: n = 5. Histograms represent the mean ± s.e.m. of the number of cells/mm^2; *p≤0.05, ***p≤0.001 calculated by the student's *t* test.

MMP-9/GFAP co-localization in the striatum of control and MPTP-injected monkeys

Double MMP-9/GFAP immunolabeling was performed on striatum sections (Fig. 18A, caudate; Fig. 18B, putamen; enlargement of boxed areas at the left-hand side) of both control and MPTP-treated monkeys to ascertain MMP-9 expression by astrocytes. Section examination at a confocal microscope showed a massive increase in activated astrocytes after MPTP treatment respect to control, in both striatal areas. Astrocyte activation was characterized by an increase in both cell size and number of cell processes of GFAP$^+$ cells (Fig. 18A, caudate; Fig. 18B putamen red channel). Besides morphological changes, quantitative stereology performed on random photographic fields of the striatum, disclosed a significant increase in the number of GFAP$^+$ cells (Fig 18A',B') in parkinsonian monkeys respect to control. Immunolabeling was

preferentially localized in both cell bodies (enlargement of the boxed areas of Fig. 18A,B, at the left- hand side) and processes (arrows in Fig. 18A,B and enlargement of the boxed areas, at the left- hand side) of activated astrocytes. In general astroglia represented only a small percentage of the MMP-9^{+} cells, in both control and parkinsonian monkeys, although MPTP treatment significantly increased this value (Fig. 18A',B').

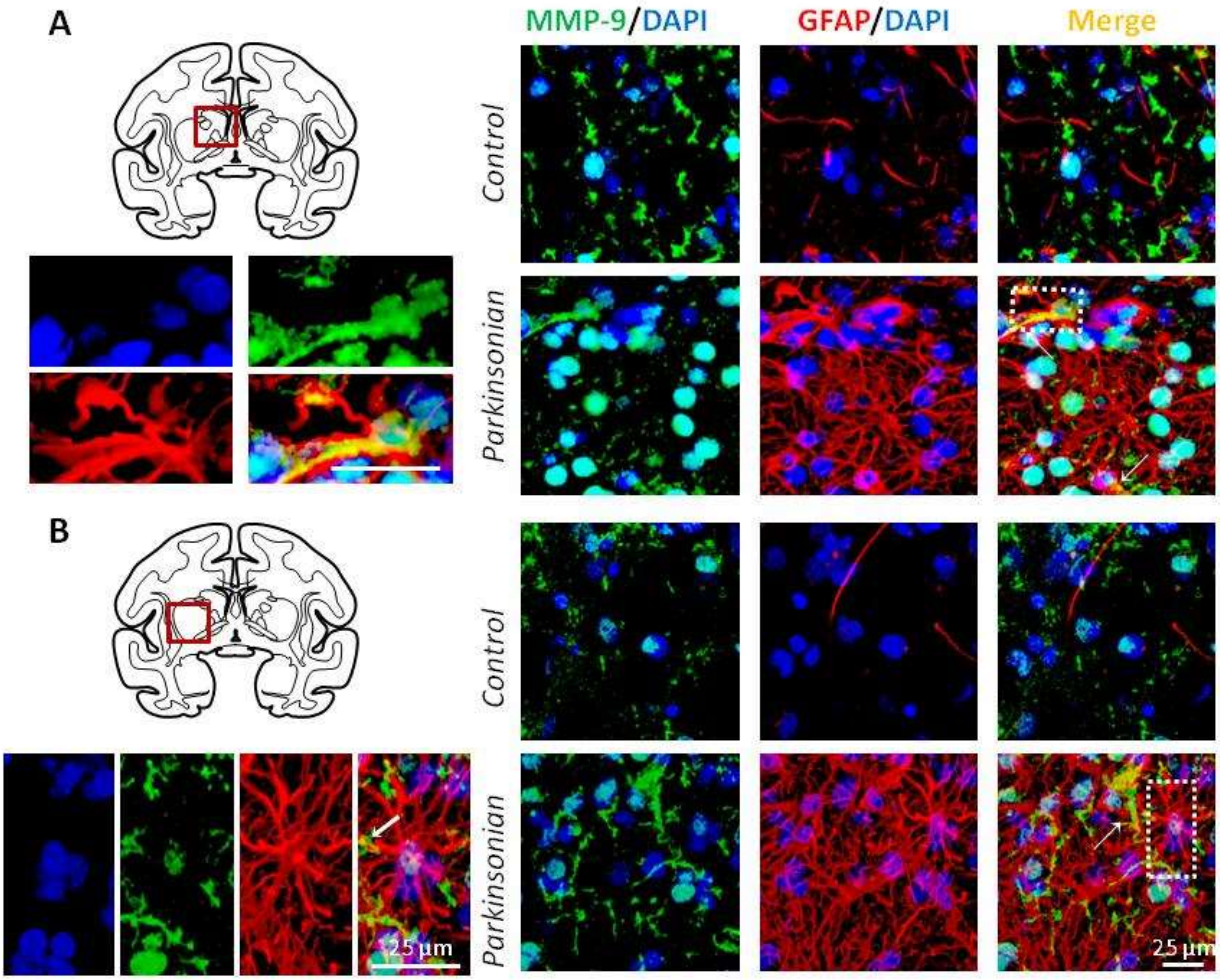

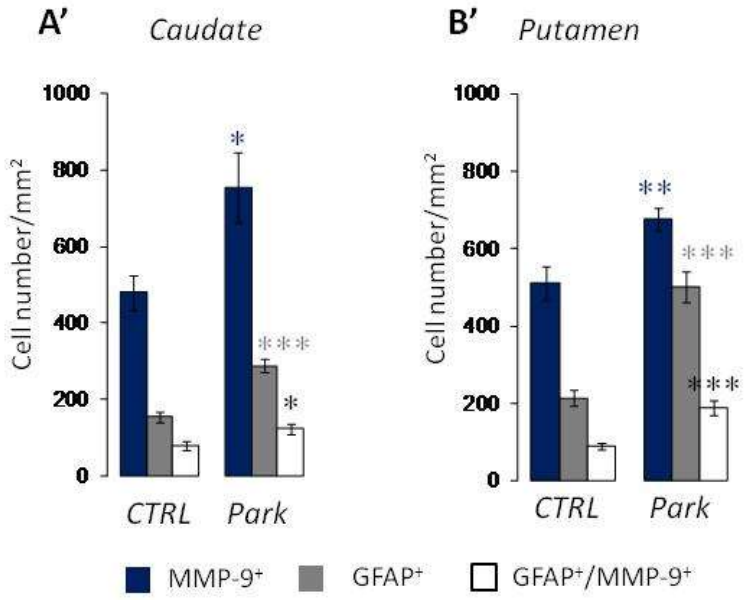

Fig. 18. MMP-9/GFAP co-immunolocalization in the caudate (A) and putamen (B) of control and MPP-treated monkeys and relative stereological quantification (A',B'). In control animals, GFAP staining (red) is weak and it is associated with small-sized cells with a few, thin processes. In parkinsonian monkeys, years after intoxication, a prominent astroglial reaction is still present. Activated astrocytes present increased cell sizes and numerous, thick, complex processes. The number of MMP-9$^+$ (green)/GFAP$^+$ (red) cells is low in both control and treated monkeys. MMP-9 staining associates to cell bodies (enlargements of the boxed area at the left hand side) and/or to cell processes (arrows) of activated astrocytes. Nuclei were counterstained with DAPI (blue). A',B') Caudate (A') and putamen (B') stereological quantifications of MMP-9$^+$ (blue bars), GFAP$^+$ (gray bars) and MMP-9$^+$/GFAP$^+$ (white bars) cells. Control group: n = 3 animals; Parkinsonian group: n = 5. Histograms represent the mean ± s.e.m.; *p≤0.05, **p≤0.01, ***p≤0.001 calculated by the student's *t* test.

MMP-9/ MBP co-localization in the striatum of control and MPTP-injected monkeys

Finally, we performed double immunolabeling for MMP-9 and MBP, an OL marker, on sections of striatum of both control and parkinsonian monkeys. In both caudate (Fig. 19A and enlargement of the boxed area, at the left-hand side) and putamen (Fig. 19B and enlargement of the boxed area, at the left-hand side) of control monkeys, MBP immunoreactivity appeared as a weak extracellular staining with only a few, small immunopositive cells. In the same areas of parkinsonian monkeys, the extracellular staining was more intense than control and several MBP$^+$ cells showed an increase in their cell size. As in the case of mice, these signs could be ascribed to the condition of oligodendrogliosis. An accurate description of these aspects is reported in the next

paragraphs of this session. Quantitative stereological analysis (Fig. 18A', caudate; Fig. 18B', putamen) showed a significant increase, in MPTP-injected monkeys respect to control, in both MBP^+ cells, confirming OLs activation, and double $MBP^+/MMP\text{-}9^+$ cells, making these cells the second major cell population after neurons expressing MMP-9.

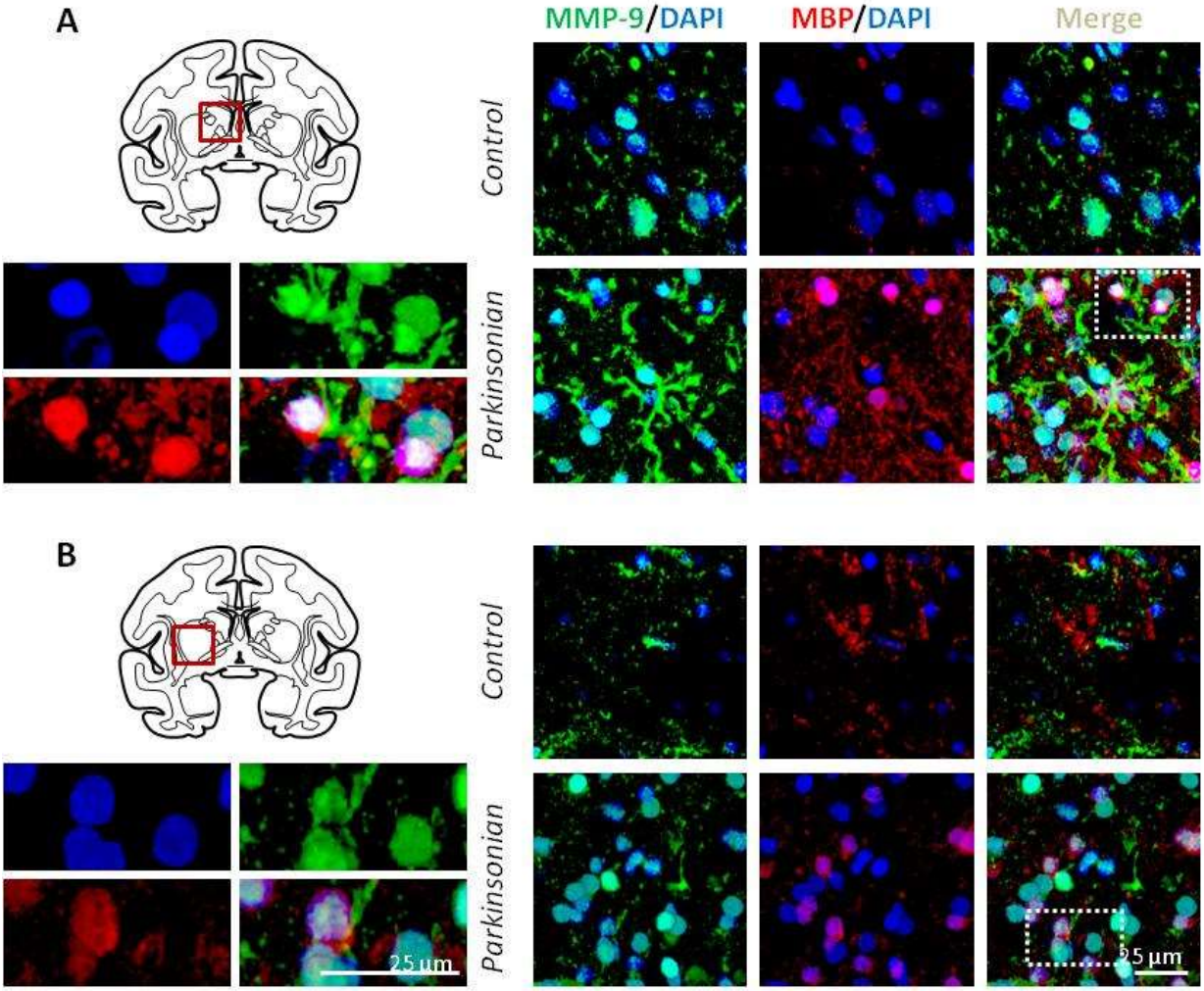

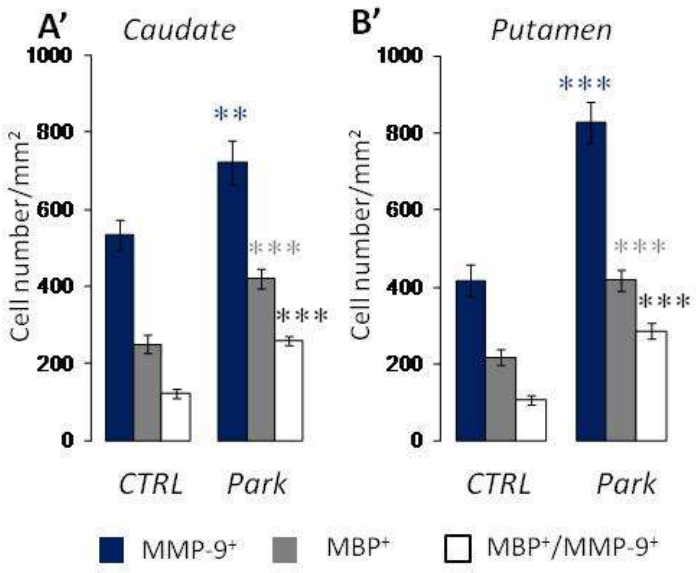

Fig. 18. MMP-9/MBP co-immunolocalization in both caudate (A) and putamen (B) of control and MPTP-treated monkeys and relative stereological quantification (A',B'). MBP staining (red) in controls animals is weak and mainly localized extracellularly. In parkinsonian monkeys, years after the intoxication, it is still possible to observe a sustained MBP cellular and extracellular staining, indicating active OL reaction. The number of MMP-9$^+$ (green)/GFAP$^+$(red) cells is low in control monkeys, but it clearly increase in MPTP-treated monkeys, in both striatal regions. On the left hand side, enlargements of the boxed areas representing MMP-9/MBP co-localization are shown. Nuclei are counterstained with DAPI (blue). A',B') Caudate (A') and putamen (B') stereological quantifications of MMP-9$^+$ (blue bars), MBP$^+$ (gray bars) and MMP-9$^+$/MBP$^+$ (white bars) cells. Control group: n = 3 animals; Parkinsonian group: n = 5. Histograms represent the mean ± s.e.m. of the number of cells/mm^2; **p≤0.01, ***p≤0.001 calculated by the student's *t* test.

Myelin Damage and Oligodendrogliosis in MPTP-induced Parkinsonism

To date, it is unknown whether and with which progression axons of MPTP-affected neurons undergo degeneration and/or structural remodeling, which also involve modification in their myelin sheath, and whether oligodendrocytes take part in any of these events. In this result session, we will report evidences of myelin alteration and oligodendrogliosis after acute and chronic MPTP treatment in mice and monkeys, respectively. We decided to treat this topic separately from the other body of results as these findings highlight that early axonal damage and oligodendrogliosis may be an aspect as important as neglected in the pathogenesis of parkinsonism.

MPTP acute treatment induces axonal and myelin damage in the mouse striatum

At the aim to identify possible ultrastructural axonal alterations induced by MPTP intoxication we performed a comparative electron microscopy analysis of the striatum of both control and MPTP-treated mice (Fig. 19). In control animals, axons displayed what we can describe as a normal morphology (19A-C). Myelinated striatal axons were numerous (Fig. 19A), characteristically heterogeneous in shape, size and thickness of their myelin sheaths and running intermixed with several unmyelinated fibers (Fig. 19B, C). Myelin sheaths were well preserved, with the typical high electron-density, surrounding concentrically the axonal cylinder with alternate regions of compact and loose myelin (Fig. 19C). Axoplasms occupied most of the intra-myelin space, in which spatially organized microtubules, neurofilaments, different types of vesicles and mitochondria were recognizable (Fig. 19C).

Seventy-two hours after acute MPTP intoxication, striatal axons appeared less in number and more sparsely distributed compared to control (Fig. 19A'), with spaces between one another possibly occupied by glial cell processes (Fig. 19B'). High magnification showed a number of prominent alterations, i.e. numerous axons were surrounded by a dramatically destructured myelin sheath, containing large vacuoles in the periaxonal and intermyelinic space caused by a consistent splitting of the myelin lamellae (Fig. 19B'-C'). In the majority of cases, vacuoles bulged from one side of the broken myelin sheath, compressing the inner axon against the opposite side of the sheath (Fig. 19C'), which determined axonal atrophy and axoplasm disorganization. At points, myelin breakdown could also occur (Fig. 19C'), which could cause exit of the axoplasm to the interstitial space (Fig. 19C'). Two weeks after the last MPTP injection, striatal axons, at least the myelinated ones, appeared fewer and more loosely arranged

respect to the 72 hrs time point (Fig. 19A''). This was accompanied by a reduction in the frequency and volume of the intra-myelin vacuoles (Fig. 19B''-C''), remarking the observation that severity and extension of vacuolizations were highest at early stages (72 hrs) after MPTP treatment. After 2 weeks, myelinated axons were enveloped by thin myelin sheaths. In the majority of cases they were organized in loose myelin lamellae, suggesting the formation of new myelin sheaths, or contained small residual vacuoles, possibly identifying sites of repair of previously damaged myelin coats (Fig. 19C"). Usually, the analysis at this time point did not reveal the presence of dystrophic axons.

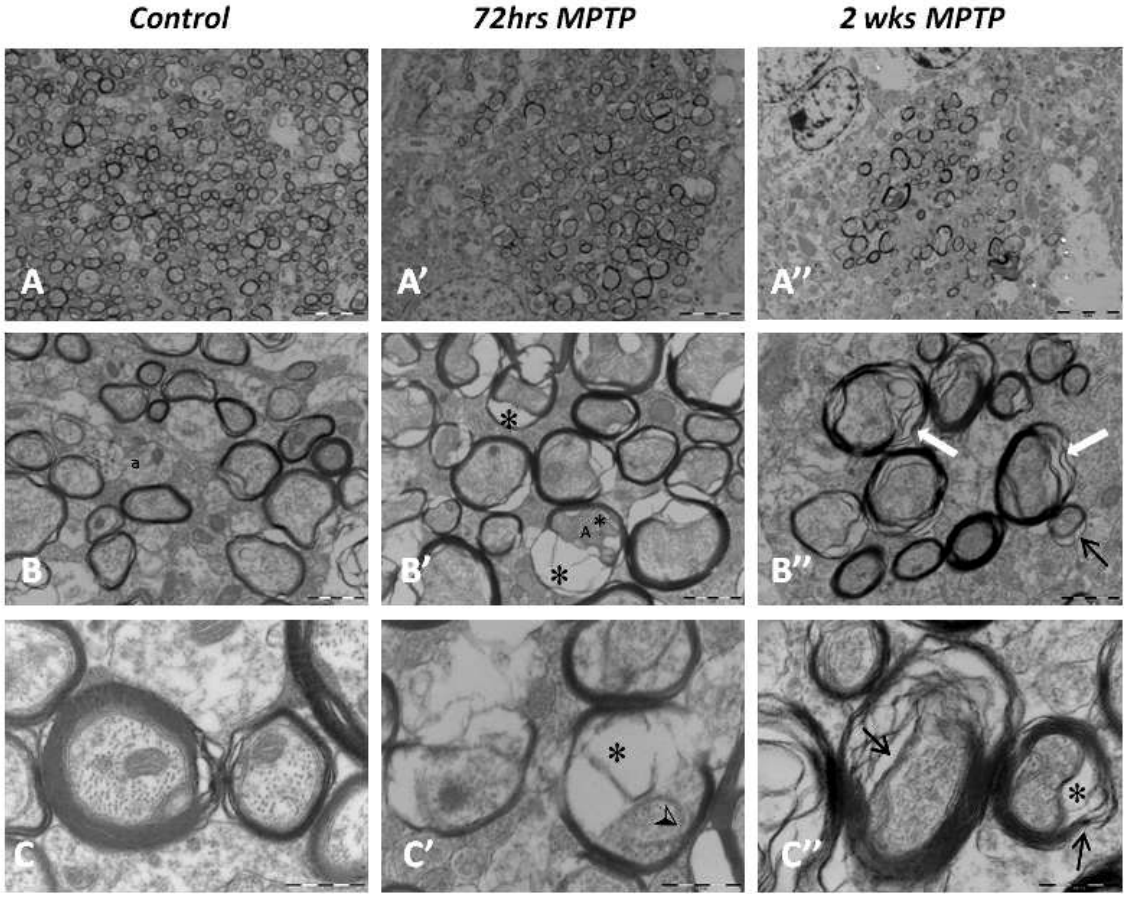

Fig. 19. Electron micrographs showing myelin ultrastructural alterations following acute MPTP-treatment in mice. (A-C) Control mice. A) In control mice striatum, myelinated axons are numerous and characterized by different calibres, shape and myelin thickness. B-C) Healthy unmyelinated (some of them indicated by a) and myelinated axons are intermixed, the latter being surrounded by the typical multilamellar structure, which alternate loose and compact regions. (A'-C') Mouse striatum 72 hours after MPTP injection. A') Early after MPTP treatment, myelinated axons in the striatum appear less than in control and are loosely arranged. B'-C') A high degree of myelin vacuolization is observed. Vacuoles are mainly characterized by the splitting and breakdown of the myelin lamellae (*) in both the periaxonal and intermyelinic spaces. Vacuolated myelin sheaths often surround dystrophic axons (A*), which remained compressed against one side of the myelin coat. Myelin coat can break at points (arrows)

determining the exit of the inner axoplasm (arrowheads in C'). Boxed area in B' is enlarged in C'. (A''-C'') Mouse striatum 2 weeks after MPTP injection. (A'') Myelinated axons are reduced respect to those in the striatum of control and 72 hours MPTP treated mice. (B''-C'') Intra-myelin vacuoles persist (*), but much reduced in volume with respect to 72 hrs treated mice. Thin (arrow) and loosely arranged myelin sheaths, composed by only few myelin leaflets (white arrows), are commonly found. Scale bars: 5 µm (A-A''), 1µm (B-B''), 500 nm (C-C'')

Axonal damage induced by MPTP treatment in mice was associated with a transient oligodendrogliosis in both SNpc and striatum

Since OLs are engaged in the production, maintenance and repair of myelin in the CNS, we performed a stereological study of their number and morphology. We, therefore, immunolocalized at the confocal microscope specific MRPs in the mouse striatum and SN*pc*, in order to establish whether myelin alterations observed in the striatal axons at the electron microscope, could be associated with changes in the OLs state (Fig. 20). After MPTP treatment, confocal analysis (Fig. 20A-C, SN*pc*; Fig. 20A'-C', striatum), combined with stereological evaluation of the immunopositive cells, showed a significant increase, compared to control mice, in the number, average area and total area of the MRP^+ cells in both SN*pc* (Fig. 20D-F) and striatum (Fig. 20D'-F'), which suggested OL activation. Active OLs were characterized by hypertrophic cell bodies, thickened proximal processes and elevated arborization of the distal processes (Fig. 20A, A' control; Fig. 20B, B', 72 hrs MPTP). All these parameters corresponded to a remarkable enlargement in OL cell body size, as indicated by the significant increase in both average and total areas per photographic field occupied by immunopositive cells (Fig. 20E-F, SN*pc*; Fig. 20E'-F', striatum). Two weeks after MPTP treatment, confocal (Fig. 20C, C') and stereological (Fig. 20D-F; 20D'-F') analyses showed a significant decrease, respect to the 72 hrs-MPTP experimental group, in the number and cell body size (average and total area per field) of OLs, in both SN*pc* (Fig. 20C; 20D-F) and striatum (Fig. 20C'; 20D'-F'). Moreover, all the values relative to this group were significantly lower compared with, or equal to, control, suggesting a reversion of the

process. The only difference was observed in the number of MRP^+ cells in the SN*pc*, which remained significantly higher than in control mice. Both series of images confirm the MPTP induced striking changes in shape and size of OLs. All these changes inversely correlated with TH immunoreactivity in the dopaminergic pathway (Fig. 21 A-F, for SN*pc* and Fig. 21 A'-F', for striatum) which showed a significant decrease 72 hrs after the last MPTP injection and a partial, but significant, recovery after 2 wks, in

both SN*pc* and striatum.

Fig. 20. Transient oligodendrogliosis in the SN*pc* and striatum of MPTP treated mice. (A-C, A'-C') Confocal analysis of MRP immunolabeling (red) in the SN*pc* and striatum of control (A, A') and MPTP-treated mice (B, B', 72 hrs; C, C', 2 wks). Seventy-two hours after MPTP injection (B,B') a prominent oligodendrogliosis is observed when compared to control animal (A,A'), which is drastically reduced after 2 weeks (C,C'). Cell nuclei are counterstained in blue with DAPI. (D-F; D'-F') Stereological analysis shows that OL cell number (D, SN*pc* and D', striatum) and average cell body size (E, SN*pc* and E' striatum) are significantly increased in 72 hrs MPTP-treated mice respect to control. A similar increase is observed in the total area per photographic filed occupied by MRP^+ cells (F, SN*pc*, F', striatum). All these values significantly decrease after 2 wks from MPTP treatment. n = 4-5 animals/experimental group. Histograms are the mean ± s.e.m. of the examined parameters; *p ≤ 0.05, calculated by the one way ANOVA (Duncan's test).

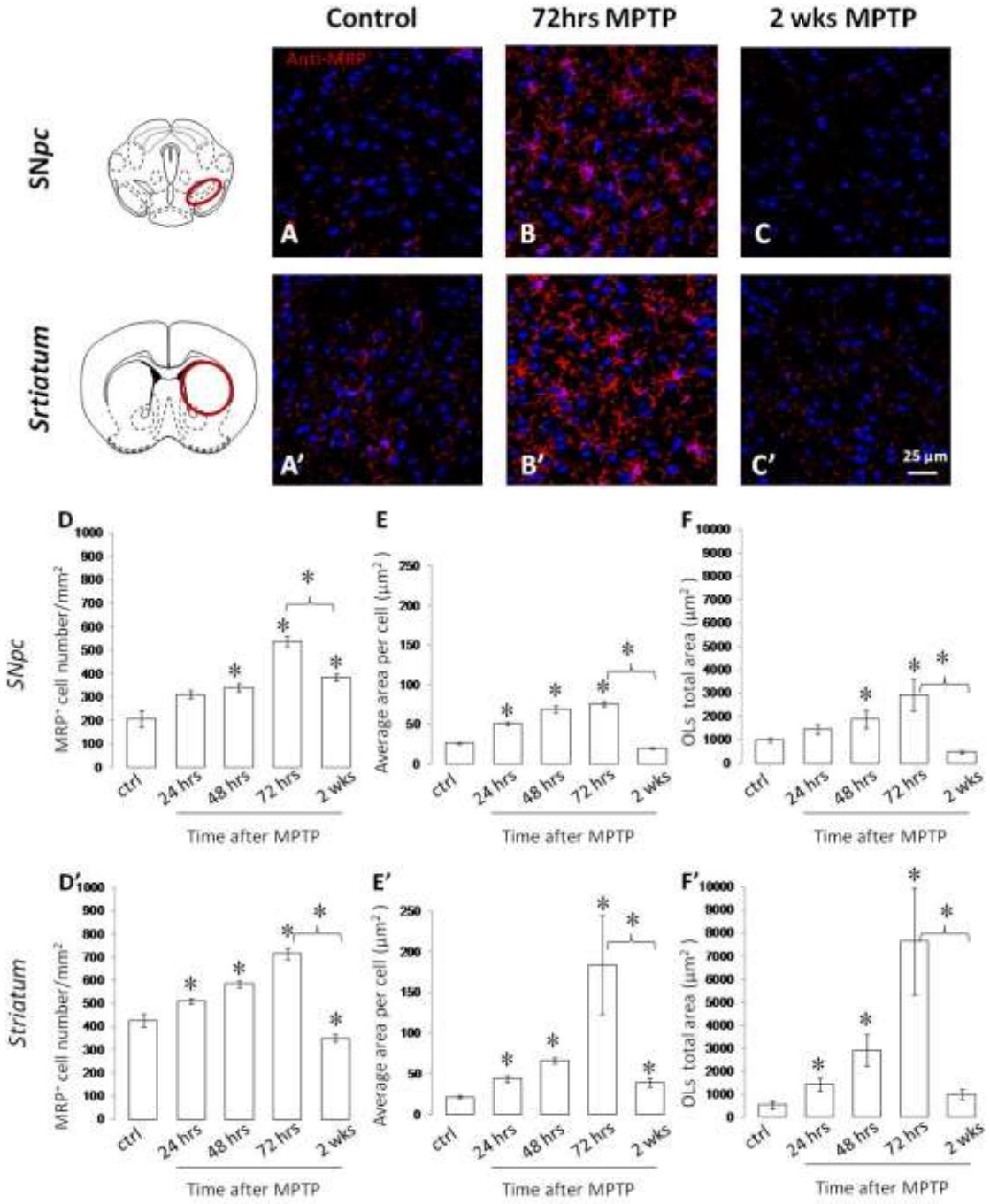

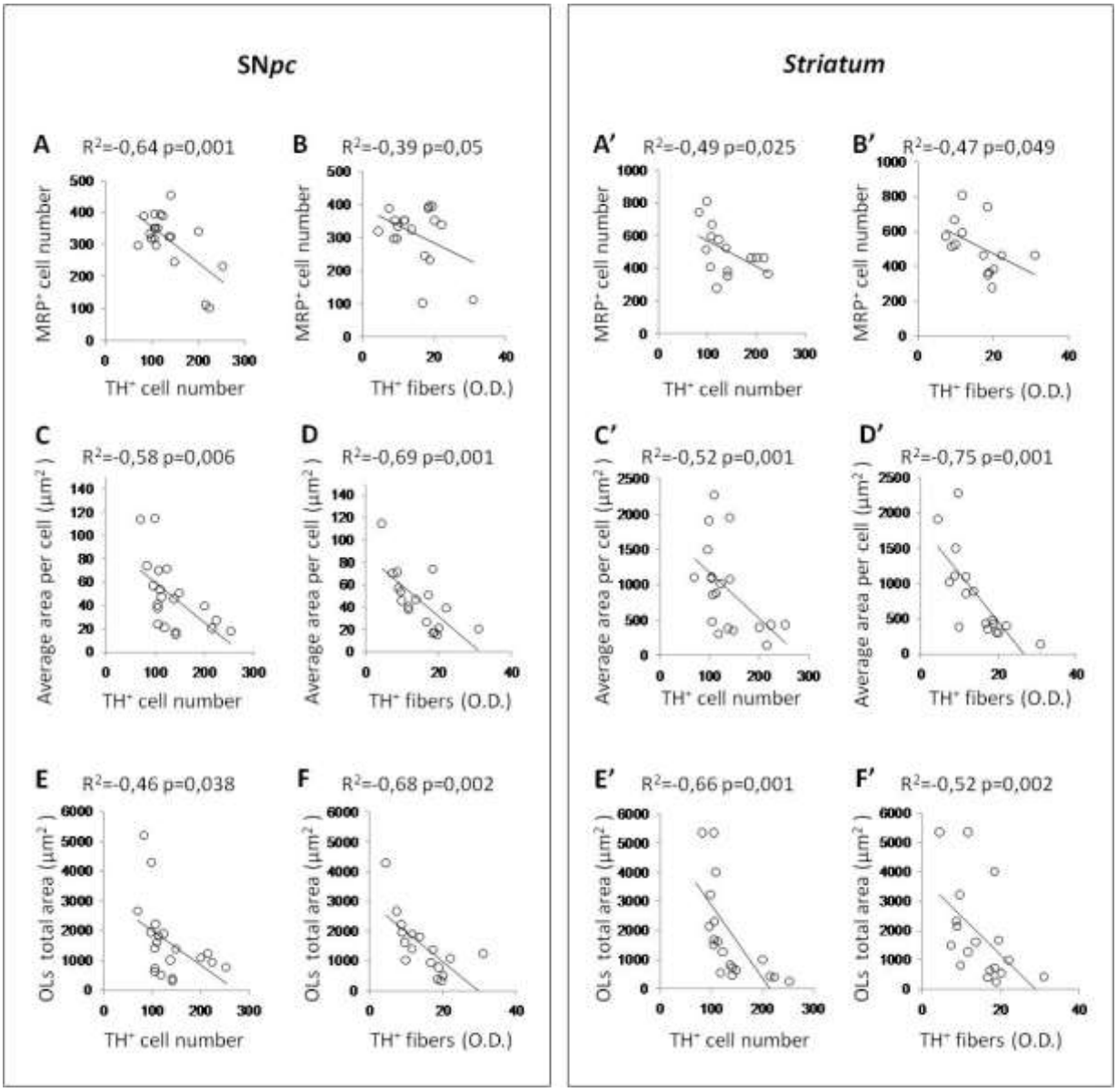

Fig. 21. In mice, the level of MPTP-induced oligodendrogliosis is inversely correlated to the loss of the dopaminergic neurons and fibers of the nigro-striatal pathway. MPTP treatment in mice induces a transient oligodendrocytosis, evaluated by counting the number of MRP^+ cells (A, B, A', B'), their average cell body size area (in μm^2) (C, D, C', D') and the total area occupied by OLs (E, F, E', F'), which is inversely proportional to the levels of TH immunostaining observed in both SN*pc* and striatum. These refer to both the number of TH^+ cell (A, C, E and A', C', E') and optical density of the TH^+ fibers (B, D, F and B', C', F'). Pearson correlation coefficient R^2 and the correspondent p values are indicated in each correlation graph. n = 15-20.

A persistent oligodendrogliosis was observed in the striatum of parkinsonian monkeys two years after receiving MPTP treatment

On the basis of the results obtained in mice, we analyzed whether OLs activation could persist years after the last MPTP injection in a chronic model of parkinsonism. A confocal microscope and stereological analysis was carried out on sections of monkey

striatum (subdivided in caudate and putamen) immunolabeled for MBP (Fig. 22). Parkinsonian monkeys showed a striking and significant increase in the number of MBP^+ cells in both caudate (Fig. 22A-B', confocal images; Fig. 22C, cell count) and putamen (Fig. 22E-F', confocal images; Fig. 22G, cell count) respect to control monkeys. OLs also showed an evident increase in their cell body size, as we observed in mice 72 hrs after the MPTP treatment. However, because of the strong increase in the extracellular MBP staining, we were technically unable to measure the area occupied by MBP^+ cells, as discussed in the methods section. Notably, we found an inverse correlation between the number of OLs, quantified in the caudate and the putamen of each monkey, and both the number of surviving dopaminergic neurons in the SN*pc* (Fig. 22D, caudate; Fig. 22H, putamen) and their TH^+ axon projections to both areas of the striatum (Fig. 22D', caudate; Fig. 22H', putamen).

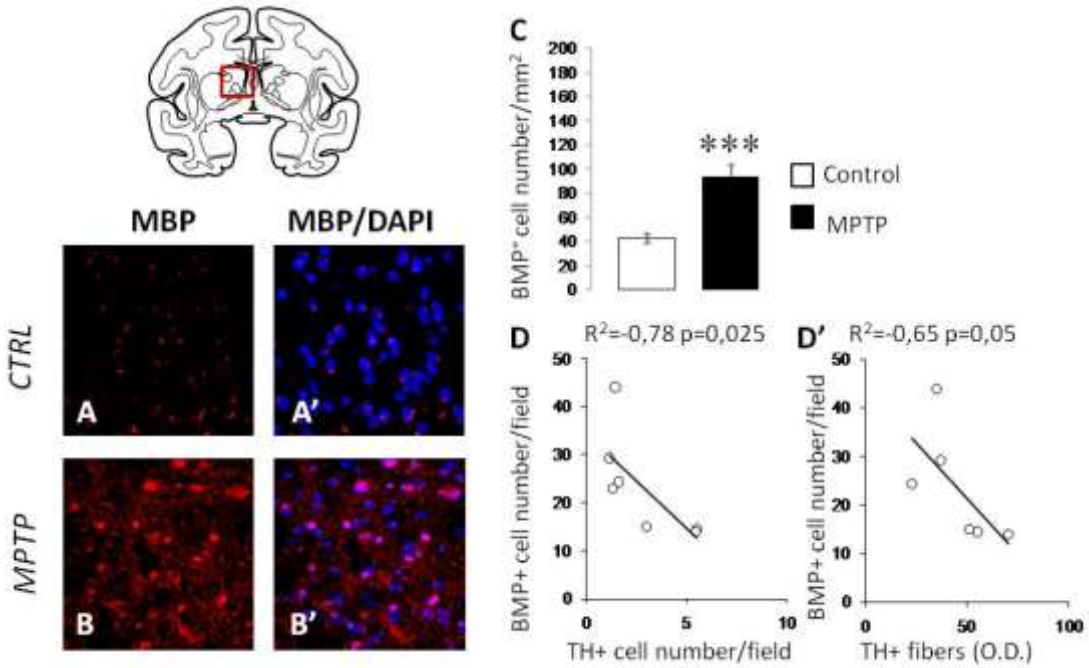

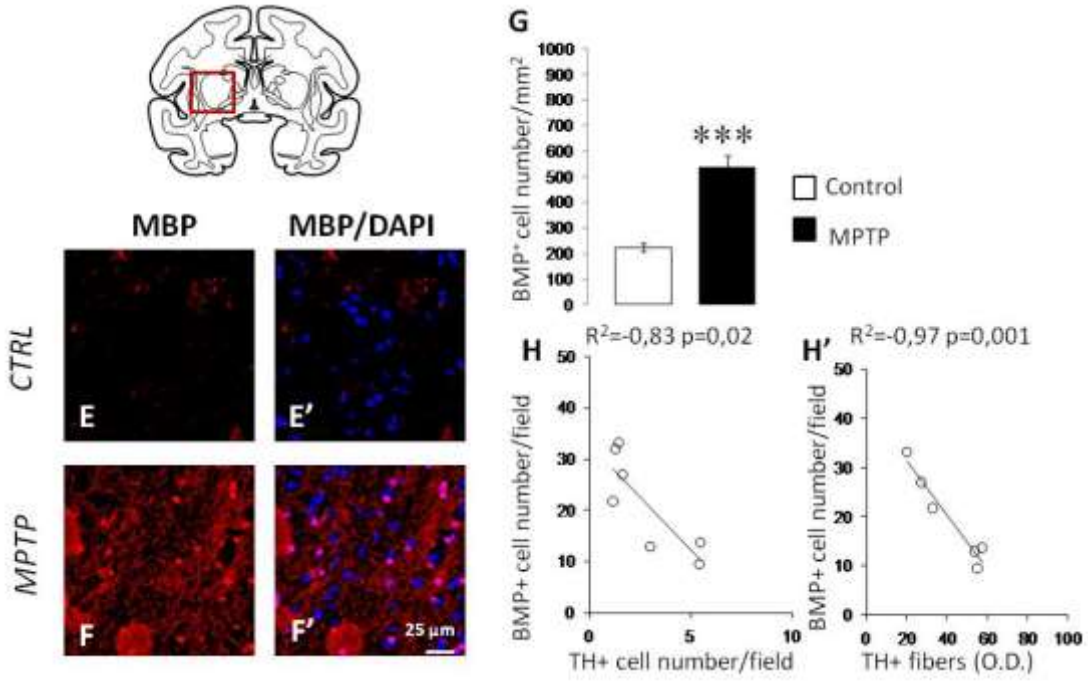

Fig. 22. Persistent oligodendrogliosis in parkinsonian monkeys' striatum. Representative pictures of confocal analysis are shown in (A-B') for the caudate and in (E-F') for the putamen. A striking increase, respect to control, in MBP immunolabeling (red) is still observed two years after MPTP treatment (B-B', F-F'). Cell nuclei are counterstained in blue with DAPI. (C-D' and G-H') Stereological analysis conducted on the confocal images reveals a significant increase in the number of OLs in parkinsonian monkey caudate (C) and putamen (G) compared to control animals. (D, D' and H, H') The increase in MBP^+ cells is inversely proportional to the number of TH^+ neurons counted in the SN*pc* (D, caudate; H, putamen) and to the optical density associated with the TH immunolabeling of the dopaminergic axons projecting to both caudate (E') and putamen (H'). Control group: n = 3 monkeys; parkinsonian group: n = 5 monkeys. The histograms in D and I represent the mean ± s.e.m. of the BMP^+ cell number; ***$p \leq 0.001$, calculated by the student's *t* test. The Pearson correlation coefficient R^2 is indicated in each of the correlation graphs (D, D', H, H').

DISCUSSION

In recent years, many experimental evidences described the involvement of the two major extracellular proteolytic pathways in brain, the MMP and the PAs/plasmin system, in different neurodegenerative diseases (Akenami, 1999; Lorenzl S, 2002; Lorenzl S, 2003; Melchor, 2003; Lovrecic, 2008; Sokolowska, 2009; Rosenberg, 2009; Bonneh-Barkay and Wiley, 2009; Mille JP, 2010). These proteases play important roles in a number of processes, which require remodeling of the ECM. MMPs can degrade all ECM proteins and several other substrates, including growth factors, cell membrane receptors and adhesion molecules. Because of this versatility, MMPs are implicated in

pathological and physiological processes very different from one another, such as cell migration, apoptosis, angiogenesis and inflammation (Sternlicht and Werb, 2001; Dzwonek, 2004; Yong VW, 2005; Ethell and Ethell, 2007; Agrawal, 2008; Candelario-Jalil, 2009). Although a role for MMPs has been widely accepted in several neuropatholgies, their involvement in PD is still poorly investigated and elusive. Similarly, involvement of the PAs/plasmin system in this pathology is still completely unexplored. Plasmin, generated by cleavage of plasminogen by means of either tPA and uPA, is a serine protease with a large number of substrates. As MMPs, the PAs/plasmin system is involved in numerous brain physiological and pathological processes and the two systems may also act in combination, being the activation of some of the MMPs even operated by plasmin (Teesalu, 2002; Yepes and Lawrence, 2004; Pang, 2004; Sheehan and Tsirka, 2005; Reijerkerk, 2008). Alltogether, these data prompted us to investigate the role that MMPs and the PAs/plasmin proteolytic system may play, singularly or in combination, in the pathogenesis and/or progression of parkinsonism. At this aim, we used two major PD animal models, i.e. mice and monkeys, acutely and chronically treated with MPTP, respectively.

Acute and chronic MPTP intoxication resolves in two different parkinsonian syndromes: why it is important considering both of them

Investigations on *post mortem* brain tissues of PD patients and MPTP chronically-treated monkeys provide a fixed image of advanced stages of PD or parkinsonism, which does not allow to unravel early or dynamic neurodegenerative events. The MPTP rodent model of parkinsonism (Vernice & Przedborski, 2007) well overcome this limit, allowing a point-to-point analysis of the cellular and molecular processes associated

with the progressive degeneration of the nigro-striatal pathway. In this thesis, we have shown, by TH immunohistochemistry, that early after (1 d) MPTP injection both the number of DA neurons in the SN and the intensity of TH immunolabeling in the striatum decreases significantly respect to control. However, in both areas of the nigrostriatal pathway, a partial recovery of the immunolabeling is seen after two weeks, suggesting that a number of affected neurons in the SN does not degenerate, but recover at later stages, possibly regenerating their damaged axons and re-innervate the striatum to some extent. This hypothesis is based on the fact that a decrease in TH immunolabeling does not necessarily indicate a generalized loss of DA neurons. In fact, TH is the rate limiting enzyme of the catecholamine synthesis, and its level of expression is strictly related to neuronal activity. Therefore, MPTP induces neuronal intoxication, which can or cannot evolve in a death process, but that surely imply a reduction in neuronal activity. All these phenomena are flanked by a prominent and transient gliosis (micoglia and astroglia), which reaches its highest peak in coincidence with the depression of the nigro-striatal pathway, as it occurs in PD. What we observe in mice acutely intoxicated with MPTP, however, is extremely different from the irreversible death process that a chronic treatment provokes in both human (Langston, 1999) and monkeys (Kolata, 1983; Langston, 1984). The same study reported in this thesis performed on brain sections of monkey sacrificed years after receiving MPTP, indicates that in primates the massive loss of dopaminergic neurons and fibers is progressive and it is always associated with a neuroinflammatory reaction.

Therefore, when compared with parkinsonian monkeys, the MPTP mouse model lacks one of the principal features characterizing the PD, i.e. the perpetuation throughout years of both neuronal death (Jenner, 1998; Carvey, 2006) and gliosis (McGeer, 1988; Hurley, 2003; Barcia, 2004). To date, it is still unknown whether glial

cells are actively involved in the progression of the dopaminergic neuron death. Indeed, both a neuroprotective and a deleterious role have been proposed (Hirsch, 2003). The observation of an activated glia phenotype, which is maintained over several years after MPTP intoxication in monkeys, suggests that some re-activation mechanisms may operate. Several studies describe a persistent release of pro-inflammatory cytokines within the CNS and the blood stream as a crucial factor in the perpetuation of the inflammatory glial reaction (Barcia, 2005; Godoy, 2008; Reale, 2009; Scalzo, 2009). In contrast with primates, mice do not show such persistent increase in the levels of cytokines in the blood, which may be consistent with a transient glial activation. Actually, previous reports have shown that MPTP-treated mice merely show a transient increase in pro-inflammatory cytokines after 24 hrs-72 hrs (Hebert, 2003; Brochard, 2009; Kurkowska-Jastrzebska, 2009; Luchtman, 2009), dates in which we detected the highest levels of gliosis.

Discrepancies between MPTP-induced parkinsonism in primates and rodents might be due to species differences and/or differences in the MPTP intoxication protocol. However, we believe very useful comparing results obtained with the two different models of parkinsonism, as we do not exclude that uncovering the mechanisms, which determine the "self-limiting" character of the neuronal death and neuroinflammation in mice, may be the key for identifying some of the factors responsible for its progression in primates.

Which are the extracellular proteases positively modulated in parkinsonism?

In the first part of the study we screened for changes in mRNA and protein levels of components of the PAs/plasmin system and of some of the MMP family (MMP-2,

MMP-9 and MMP-3, which are the most expressed in brain) in MPTP-induced parkinsonian mice.

In the brain, plasminogen activators, and in particular tPA, are constitutively expressed by neurons in regions involved in learning and memory (hippocampus), emotional states (amigdala), motor learning (cerebellum) and autonomic and endocrine functions (hypothalamus). In all these regions, tPA is involved in the regulation of synaptic plasticity and neuronal activity, either trough activation of plasmin cascade (Sallés and Strickland, 2002; Madani, 2003; Melchor and Strickland, 2005) or by a direct modulatory effect on glutamatergic and dopaminergic pathways (Nicole, 2001; Matys and Strickland, 2003; Samson and Medcalf, 2006). It is, therefore, concivable that any insult, damage or toxin, leading to a massive neuronal death, could down-regulate PAs and plasminogen expression and/or activity, as we observed in both SN and striatum of MPTP-treated mice. The significant increase in tPA mRNA levels observed only in the SN 1hr after MPTP injection, is not contradictory with the depression of all other components of this enzymatic pathway. In fact, tPA mRNA may be under translational control, i.e. once transcribed it is stabilized and stored in neurons, being its expression regulated by its binding to the *cytoplasmic polyadenylation element binding* (CPEB) protein, which leads to the tPA mRNA polyadenylation and a subsequent rapid increase in tPA protein synthesis (Shin, 2004). Therefore, we suppose that soon after MPTP treatment, tPA m-RNA transcription is increased in response to the toxin and that the transcripts are stored in the cytoplasm and not immediately translated. However, the progressive neuronal loss prevails on both tPA mRNA and protein, thus determining a global depression of the tPA/plasmin system.

The analysis of both m-RNA and protein levels of MMP-2, MMP-3 and MMP-9, indicates that the only protease strongly modulated and activated by MPTP treatment

is the MMP-9. In fact, MMP-9 expression, protein synthesis and enzymatic activation vary with a kinetics that overlaps the decrease in both number of TH+ neurons in the SN*pc* and loss of TH+ fibers in the striatum, as well as the prominent gliosis observed in both brain areas. This strongly suggests a crucial role for MMP-9 in both reaction of the nigro-striatal pathway to MPTP administration, which consists in an early dying-back of part of the SN*pc* neurons followed by partial rescue of dopaminergic pathway at later dates, and the simultaneous glial activation.

The specific up-regulation of MMP-9 following toxic insult is in accord with the literature, which reports MMP-9 as normally present in CNS, prevalently expressed by neurons at low levels and upregulated following injuries (Rosemberg, 2001; Lee, 2003; Jidday, 2005; Candelario-Jalil, 2009). MMP-2, the other gelatinase which share with MMP-9 similar substrates, is constitutively expressed in brain, mainly by glial cells (Del Zoppo, 2007), and its levels may increase in some types of diseases associated with inflammation, when it often concentrates in the cerebrospinal fluid (CSF) (Rosenberg, 2002). MMP-3, along with MMP-9, is one of the major inducible MMP during neuroinflammation (Gurney, 2006; Kim, 2007; McClain, 2009; Candelario-Jalil, 2009; Cho, 2009; Moon, 2009; Yamada, 2010). Our findings relative to MMP-3, did not reveal changes in its m-RNA levels in parkinsonian mice respect to control. However, before speculating about this matter, some considerations are mandatory. First of all, our results are relative only to mRNA levels, which may not necessarily change in accord with the proteic ones. Second, results obtained by real time RT-PCR are remarkably variabile from on animal and the other within the same group and signal detection required a high number of cycles. Third, Western immunoblot analysis performed with different primary antibodies was unsuccesfull in giving convincing MMP-3 immunopositive bands. Altogether, these points suggest that low levels of

MMP-3 mRNA and protein are limiting for a reliable detection in our experimental system. In effect, studies by other groups, illustrating a role of MMP-3 in neurodegenerative and neuroinflammatory processes, have all been performed on either cell cultures, or animal models different than ours, by using other experimental paradigms of neuroinflammation (Kim, 2007; McClain, 2009).

By immunohystochemistry we show that MMP-9 is mainly expressed by neurons along the entire nigro-striatal pathway of both control and MPTP-treated mice and monkeys. Although in both species the percentage of glial cells (microglia, astrocytes, OLs) expressing MMP-9 in control conditions is low, MPTP treatment determines its significant increase in both SN*pc* and striatum (Fig. 23). These results are in accord with numerous studies demostrating that, in the CNS, endothelial cells, astrocytes, neurons, and microglia synthetize both MMP-2 and MMP-9, although MMP-9 expression appears to depend on the experimental conditions and treatments (Yong, 2005; Yin, 2006; Del Zoppo, 2007; Liu, 2007; Rylski, 2008; Wilczynski, 2008; Frontczak-Baniewicz, 2009; Michaluk, 2009; Candelario-Jalil, 2009; Lehmann, 2009; Walker and Rosenberg, 2010).

An interesting aspect emerging by our studies is that while in monkeys the increase in MMP-9 expression by neuronal and glial cells persists years after the toxic insult (Fig. 24), correlating with the progressive loss of TH immunoreactivity, in the mouse model of acutely-induced parkinsonism the increased expression of MMP-9 in glial cells is transient, reverting in the majority of cases to control levels after two weeks from MPTP treatment (Fig. 23). This data is in accord with the observed remission of gliosis and partial recovery of neurons and fibers expressing TH at later dates (2 weeks).

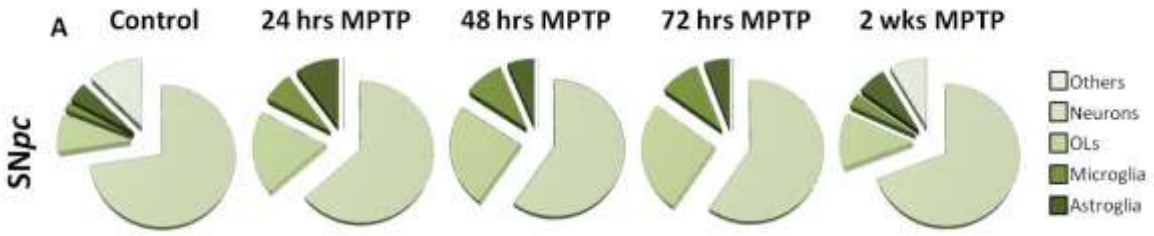

SN*pc*	ctrl	24 hrs	48 hrs	72 hrs	2 wks
Neuron	75,9±3,9	66,7±4	63,6±3,2	71,4±4,1	68,6±3
OLs	8,6±0,3	20,3±1,2*	26,3±1,3*	30,6±1,3*	12,6±1,1
Astrocytes	4,5±0,9	10,6±0,7*	6,8±0,4	7±0,8	6,6±1,6
Microglia	1,9±1,3	7,5±3,2*	10,4±3,4*	10,9±3,6*	3,1±1,6

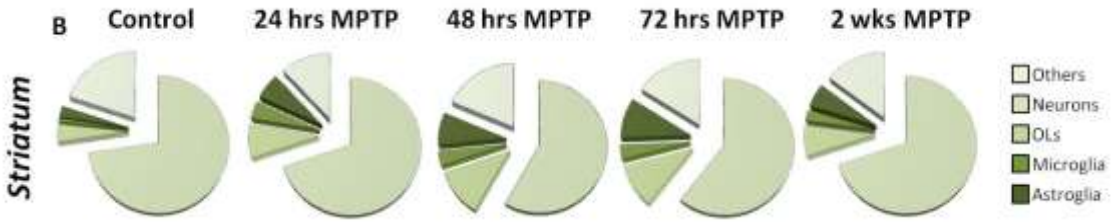

Striatum	ctrl	24 hrs	48 hrs	72 hrs	2 wks
Neuron	73,5±2,2	72,5±5,8	58,2±4,6*	60,5±4,2	69,9±3,2
OLs	4,2±0,4	7,9± 0,4*	11,5±0,8*	10,4±0,7*	12,6±0,7*
Astrocytes	2,5±0,3	6,2±0,5*	8±0,9*	9,7±1*	5,6±0,6*
Microglia	0,8±0,2	4,1±0,8*	3,6±1,3*	3,4±0,4*	2,6±0,2*

Fig. 23 A,B. Percentages of the different cell types expressing MMP-9 in the SNpc (A) and striatum (B) of control and MPTP-injected mice, evaluated by stereological quantification, at the confocal microscope, of MMP-9 immunopositive cells. MMP-9 is mainly expressed by neurons. The percentage of MMP-9 immunopositive neurons in both SN*pc* and striatum decreases significantly after MPTP treatment, whereas that of all types of MMP-9^+ glial cells increases. The increase is more prominent for oligodendrocytes (Ols) in the striatum. All percentages return to almost control level afet two weeks. *p ≤ 0.05, calculated by the one way ANOVA (Duncan's test).

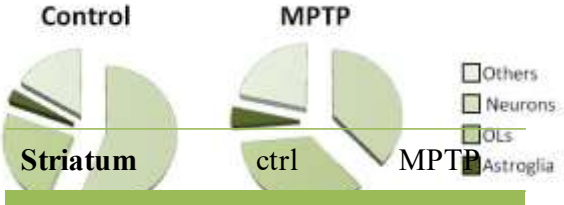

Striatum	ctrl	MPTP
Neuron	56,2±0,6	37,6±0,4**
OLs	24,2±0,3	36,05±0,3***
Astrocytes	16,8±0,2	36,7±0,3*

Fig. 24. Percentages of the different cell types expressing MMP-9 in the striatum of control (A) and parkinsonian monkeys (B) evaluated by stereological quantification at the confocal microscope of MMP-9 immunopositive cells. MMP-9 is mainly expressed by neurons and oligodendrocytes (Ols), in both control and parkinsonian monkeys. In the MPTP-treated group, the percentage of neurons immunopositive for MMP-9 decreases to a 20%, while MMP-9^{+} Ols and astrocytes increase. *p≤0.05, **p≤0.01, ***p≤0.001 calculated by the student's *t* test.

Alltogether, the results obtained in both mice and monkeys suggest that MMP-9 may exert functions tightly correlated with both glial cell reaction to MPTP intoxication and neuronal death. Therefore, here we propose a dual role of MMP-9 in experimentally-induced parkinsonism: one related to the early response of SNpc neuron to MPTP intoxication, implying loss of part of the dopaminergic neurons, neuroinflammation, oligodendrogliosis and dopaminergic neuron axon degeneration, and the other coincident with the possible recovery of survived neurons and the partial dopaminergic re-innervation of the striatum.

The injury phase

The adherence of cells to the ECM provides survival signals through mechanisms that include activation of cell surface receptors, as integrins. Integrins, especially the β1 subtype, regulate the activation of the PI3K/Akt pathway through the interaction with the integrin-linked kinase (ILK), and their loss induces apoptotic cell death both *in vitro* and *in vivo* by disrupting survival signaling (Saito, 2003; Bouchard, 2007).Early after MPTP intoxication, the most significant consequence in the SN*pc* is the loss of large part of dopaminergic neurons.This occurs primarily by block of the mitochondrial respiration by this specific neurotoxin, but a concert of other mechanisms cannot be excluded, especially in association with the perpetuation of neuronal death years after

intoxication (i.e. in monkeys), when the toxic molecule is no longer present in the organism. Recently, several lines of evidence have demonstrated that active MMP-9 is responsible for the shedding of adhesion molecules from the cell surface, thus disrupting cell-cell and cell-ECM signaling. This may resolve in an apoptoic signaling within cells (Gary and Mattson, 2001; Tagaya, 2001; Lee, 2004; Gyung, 2009), or promote cell plasticity (Luo, 2005; Takács, 2010). In particular, Gyung and colleagues showed *in vivo* that β1 integrin is probably a direct target of MMP-9 and that its disruption is responsible for the apoptotic death of hippocampal cells after pilocarpine-induced *status epilepticus* (Gyung, 2009). Moreover, experiments both *in vitro* and *in vivo*, demonstrated that a selective MMP-9 inhibitor prevents the loss of β1 integrin from the surface of hippocampal neurons and rescues from seizure-induced apoptotic cell death (Gyung, 2009). Based on the results obtained in our experimental models, we hypothesize that following the primary action of MPTP on the block of the mitochondrial electronic chain in the dopaminergic neurons of the SN*pc*, affected/dying neurons may release factors, among which MMP-9, which could stimulate neighboring glial cells by cleaving cell surface reptors, activating chemotactic factors and/or degrading ECM to favor cell migration toward the sites of injury. Moreover, MMP-9 expression by glial cells themselves increases, possibly amplifying their amoebid migration. Increased MMP-9 release, may ultimately contribute to the dopaminergic neuronal loss by cleaving, for example, the β1 integrin and triggering an apoptotic pathway. However, the ultimate mechanism by which MPTP induces dopaminergic neuron death is still unclear, as recent studies in primates failed to show activated caspase-3 or fluoro-jade positive dopaminergic neurons long after MPTP insult (Garrido-Gil, 2009).

In our experimental models, MMP-9 could also exert its action on the basal lamina and tight junction proteins (TJPs) of endothelial cells (ECs) and, therefore, cooperate to the opening of the blood-brain barrier (BBB), which allows peripheral immune-cells to enter the CNS (Rosenberg, 2007; Jin, 2010). As an example, after cerebral ischemia, MMP-9 activity is responsible for the second BBB opening, which generally occurs 24-48 hrs after the initial opening, exhacerbating blood vessels damage. As a matter of fact, treatment with specific MMP inhibitors or with MMP-neutralizing antibodies decreases infart size and prevents BBB breakdown after focal ischemic stroke (Rosemberg, 1998; Amantea, 2007; Rosemberg, 2009). Moreover, in a MMP-9 knockout mouse model of focal ischaemic lesion, damage to the BBB and size of infarct area are decreased (Gasche, 2001). Physiologically, BBB opening is a protective mechanism during CNS infections, which allows peripheral immune-cells to enter the brain and to attack noxious microorganisms. However, when the cause of barrier brackdown is not an infectious agent, the inflammatory response contributes to tissue damage (Candelario-Jalil, 2009). Several studies on PD patients and animal models suggest a pathogenic linkage between BBB disruption and dopapminergic neuron death (Faucheu, 1999; Barcia, 2004; Kortekaas, 2005; Yasuda, 2007; Rite, 2007; Chen, 2008). That BBB undergoes alterations in PD and parkinsonism was also indirectly confirmed by the observation of infiltrating peripheral immune-cell in dopaminergic areas of both PD patients and parkinsonism animal models (McGeer, 2003; McGeer and McGeer, 2008; Kurkowska-Jastrzebska, 2009; Brochard, 2009). Several line of evidence raise also the possibility that in inflammatory states MMP-9 released by ECs may be important for the extravasation of peripheral blood monocytes and leukocytes, as the enzyme degrades collagen type IV and entactin, both of which are major components of the blood capillary basement membrane (Nguyen, 2005;

Kolaczkowska, 2006; Nguyen, 2006; Higashida, 2010). In addition, expression of MMP-9 by monocytes could be envisioned as part of the program of monocyte/macrophage differentiation after exposure to a variety of inflammatory stimuli (Zhang, 1998; Vos, 2000; Serra, 2010). Because these evidences, we consider that ECs, as well as peripheral blood monocytes/leukocytes, may represent the fraction of MMP-9+ cells that we defined as "others" and that in our co-immunolocalization studies were immunonegative for all the specific cell markers used.

As already highlighted, in both MPTP-intoxicated mice and monkeys, microglia and astroglia undergo prominent activation. These results are in accord with several experimental evidences, in both SN*pc* and striatum of MPTP treated mice, showing that during inflammation microglia proliferates and gradually changes its morphology from small-sized, quiescent and ramified (resting state) to amoeboid (activated state) (Giulian, 1991; Kreutzberg, 1996; Stence, 2001; Hirsch and Hunot, 2009). Moreover, Barcia and colleagues previously demonstrated that microglia activation is still present several years after the interruption of MPTP treatment, in both SN*pc* and striatum of the same monkeys used in this study (Barcia, 2004; Barcia, 2010). In the brain of both parkinsonian mice and monkeys (Barcia, 2004; Barcia, 2010) a prominent and localized astroglia activation is appreciated. Astrogliosis can be easily evaluated by both increase in the number of GFAP+ cells and morphological changes, in which the star-shaped astrocytes, characteristic of control conditions, transform into reactive cells with large-sized perikarya from which numerous thick processes emanate (Wilhelmsson, 2006; Anastasia, 2009; Hirsch and Hunot, 2009). Our results evidenced that in the mouse model both microglia and astroglia activation are transient, following a typical "inverted-U" trend: i.e. glial activation reaches a maximum by 48-72 hrs after MPTP acute injection and drastically reverts at the end of the observation time (2 weeks).

Interstingly, MMP-9 synthesis by microglia and astroglia is positively correlated to the kinetics of glial cell activation, increasing concomitantly to the onset of gliosis and decreasing at lated dates. Accordingly, in monkeys, where the chronic MPTP treatment induces a persistent glial activation, MMP-9 synthesis remains significantly higher than control. Altogether, these results suggest that MMP-9 is somehow related with the events promoting the switch of glial cells from an inactive to an activated state. As

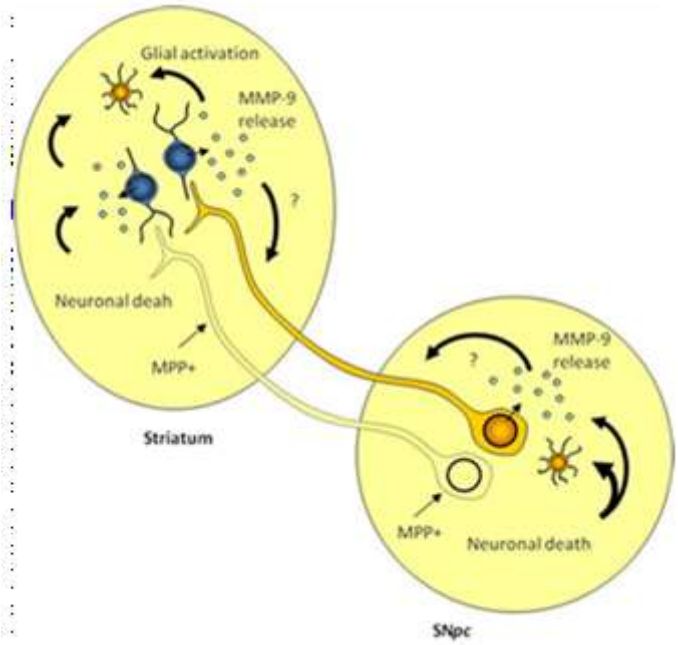

proposed earlier in the Discussion and shown in the drawing of Fig. 25, MMP-9 may be released at first by intoxicated dopaminergic neurons in the SN*pc* and by their axons in the striatum. This would, in turn, facilitate the arrival of glial cells to the affected areas, a process that itself may benefit from prodution and site-specific release of MMP-9 by glial cells (see below).

Fig. 25. Prosposed role of MMP-9 in glial cell activation after MPTP intoxication. MMP-9, sinthetised mainly by neurons, contributes to glia activation. In turn, MMP-9 released by activated glial cells, along with other factors, may trigger a reverberating inflammatory process, which ultimately increases loss of DA neuron.

A survey of the literature on rodents suggests that microglial cells and/or astrocytes may provide a source of MMP-9 when stimulated by pro-inflammatory cytokines (Rivera, *The MIT press* pag. 53-86; Yong, 2005; Ben Hur, 2006; del Zoppo, 2007). Recently, *in vitro* studies have demonstrated that microglia and astroglia stimulated with α-synuclein release MMP-9, concomitantly to changes in their morphology (So, 2010; Lee, 2010). MMP-9 secreted by the stimulated microglia, in turn, activates microglia itself by activating the protease-activated receptor-1 (PAR-1) in an autocrine and/or paracrine manner (Lee, 2010). PARs are G protein-coupled receptors that signal in response to extracellular proteases. After the N-terminal extracellular domain of PAR-1 has been digested by proteases, the remaining domain acts as tethered ligand and generates intracellular signals (Vu, 1991). PAR-1 has been demonstrated to be located on the surface of microglial cells and the binding of PAR-1 to its ligand activates microglia (Suo, 2002). Lee and colleagues have also demonstrated that MMP-9 cleaves PAR-1 with a high efficacy and that blocking MMP-9 activity significantly suppresses the expression of iNOS, TNF-α, IL-1β and ROS production by microglia, producing an effect similar to that exherted by the PAR-1 specific inhibitor (Lee, 2010). These results indicate a role for MMP-9 in the perpetuation of microglia activation. The same authors also reported that inhibition of MMP-9 suppresses microglia activation by LPS *in vitro* (Woo, 2008), suggesting that the enzyme may indeed play a role as a mediator of inflammation and that PAR-1 is part of a mechanisms of MMP-mediated microglial activation.

It's well-known that in response to brain injury, both microglia and astroglia migrate and accumulate at the sites of damage, which represent an important step in the regulation of inflammation and neuronal degeneration/regeneration. Supported by numerous evidences (Machida, 1989; del Zoppo, 2007; Choi, 2010; Shin, 2010; Sbai,

2010), we believe that the increase in MMP-9 synthesis associated to glia activation after MPTP administration may mediate also migration of glial cells promoting advancement of lamellipodia, protusion of invadopodia, as well as regulation of chemotactic signals. Recent reports suggest that ATP, released by apoptotic cells, may also acts as chemotactic signal to recruit fagocytic cells into damaged areas, highlighting a crucial role of ATP *via* MMP-9 secretion in the regulation of an inflammatory phenotype in brain injury (Elliot, 2009; Choi, 2010). Sbai and colleagues demonstrated that MMP-9 and MMP-2 have a different intracellular vesicular distribution in LPS-activated astrocytes. Specifically, MMP-9, but not MMP-2, was localized in vesicles positive for the lysosomal-associated membrane protein-2 (LAMP-2) (Sbai, 2010). Moreover, time-lapse live-cell imaging revealed that these MMP-9+ lysosomal vesicles move to, and fuse with, the plasma membrane at the podosomes of activated astrocytes. Because it has been demonstrated that these structures mediate cell migration and invasion by coordinating the reorganization of cytoscheleton and by focal degradation of the ECM *via* MMPs and/or serine proteases (Tu, 2008), the above mentioned results indicate that MMP-9 gelatinolytic activity is involved in the regulation of reactive astrocytes migration.

Our results show that in parkinsonian primate, microglia and astroglia activation persists in association with both their MMP-9 production and progressive neuronal death years after the initial toxic insult. We, therefore, hypothesize that in this animal model, differently from mice, pathophysiological mechanisms, involving MMP-9 and directed to maintain the inflammatory state, were not correctly modulated. In this case, the persistence of gliosis may become detrimental due to persistent release of potentially neurotoxic factors (i.e. ROS, cytokines) and by formation of an impenetrable glial scar, which would block any attempt of damaged axon re-growth, possibly triggering the

progression of neuronal death (Yong, 2005; Williams, 2007; Franklin and ffrench-Constant, 2008; Moore, 2010).

The repair phase

Our results demonstrate that acute MPTP intoxication in experimental parkinsonism in mice induces a prominent oligodendrogliosis within 72 hrs from toxin administration, which parallels the loss of 50-60% of the dopaminergic neurons in the SN*pc* and of their axons projecting to the striatum. This phenomenon, well characterized by confocal and stereological analysis, reflects different degrees of myelin sheath damage, clearly identified at the electron microscope, which range from intramyelinic oedema and swelling, to disruption of the myelin coat with consequent axonal atrophy and axoplasm extrusion, in the most severe cases. These myelin alterations associated to massive oligodendrogliosis along the entire dopaminergic pathway are exacerbated in the striatum. This may be related to the fact that MPP^+, the toxic product of MPTP metabolism in glial cells (Di Monte, 1992) is captured by dopaminergic axon terminals, where mitochondrial intoxication begins, and then are retrogradely transported to the cell body, progressively affecting the entire neuron. This peculiar mechanism of retrograde action is shared by other pathological situations consequent to the administration of different neurotoxins (Horton, 2009; Cliffer, 1998). Altogether, the evidences here presented support that dysfunction of dopaminergic axons and synapses in parkinsonism precedes that of dopaminergic neuron cell bodies and that probably the surviving dopaminergic neurons, with damaged axons, cannot properly function. In human PD, dopaminergic axons are severely affected (i.e. varicosities, disruption and shrinkage) (Duda, 2003; Kieburtz, 2007) and several authors have hypothesized that axonal degeneration may indeed precede neuronal apoptosis and protein aggregation (i.e. alpha-synuclein) in nerve fibers (Lewy neurites), suggesting that axon degeneration may be one of the initial causes of neuronal loss (Braak, 1999; Duda, 2002). However,

this may be something specific for humans, since no lewy pathology is observed in chronic parkinsonian monkeys (Halliday, 2009). One of the most intriguing aspects of our study, which may sustain this hypothesis, is that in mice, 2 wks after acute MPTP administration, we observed a partial recovery of TH immunoreactivity in both SN*pc* and striatum, concomitant to a reduction in the oligodendrogliosis and a partial rescue of the integrity of the myelin sheaths wrapping the remaining axons. This opens an important aspect concerning OL activation, which is their involvement in the initiation of a remyelinating process in the survived dopaminergic neurons (Levine, Reynolds, 1999; Reynolds, 2002; Franklin, 2008; Kitamura, 2010). Because an early step in fiber regeneration/remyelination is the production of extensive processes by oligodendrocytes to contact several axons, a requirement for MMP activity in remodelling the ECM seems likely (Hughes, 2002). In particular, MMP-9 could exert a crucial role, because its expression was often associated with OL activation in regenerative processes in CNS (Uhm, 1998; Larsen, 2003; Larsen, 2006). This hypothesis is improved by our results obtained in mice, which show as in the nigro-striatal pathway the MPTP-induced oligodendrogliosis is associated to an early and gradual increase in MMP-9 expression by OLs, which is significantly reverted 2 wks after the treatment, when OLs lose their activated state (Fig. 26).

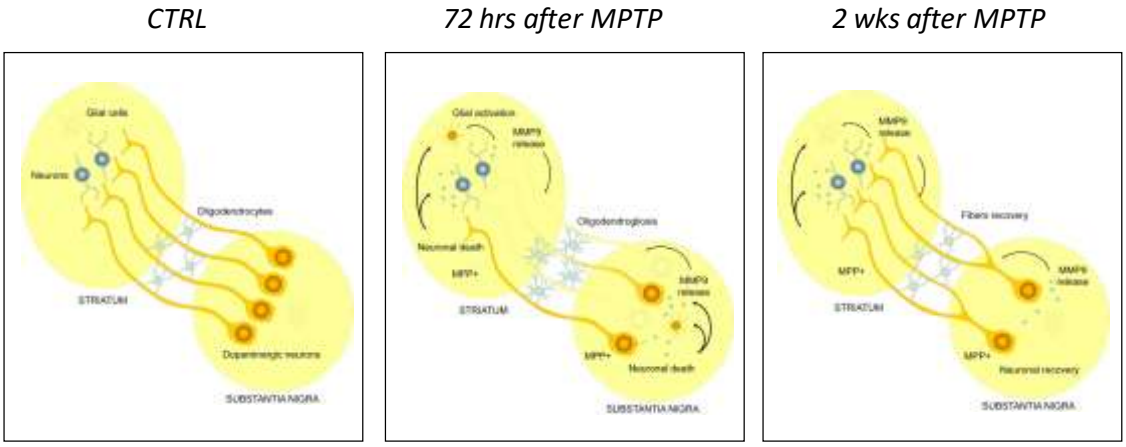

Fig. 26. MPTP acute PD model in mice. In control mice, neurons of SN*pc* project their axons to the striatum establishing the necessary connections for correct neural transmission. In the absence of damages, no evidences in glial activation are observed along the nigro-strial dopaminergic pathway. Following MPTP acute treatment, microglia and astrocytes, as well as oligodendrocytes, become activated. It is well known that MPTP induces a dying-back axonal damage in the striatum. In this scenario, the MMP-9 expression increases in both neurons and glial cells of both SN*pc* and striatum. The MMP-9 enzymatic activity may be crucial for the remodeling of the ECM and triggers oligodedrogliosis. We hypothesize that in the mouse model, in a final phase (2 wks), oligodendrocytes may contribute to a partial rescue of the affected dopaminergic neurons by favoring axonal re-growth, a processes in which MMP-9 could also have a role.

At this regard, Yong and colleagues described that OLs express MMP-9 to extend processes along an astrocyte ECM *in vitro* (Uhm, 1998). For tissue culture studies, OLs cultured from adult human or mouse brains are stripped of their processes during the cell isolation process, and the re-growth of processes provides a model of potential remyelinating capacity. The authors found that process re-extension by adult murine OLs is impaired in cells derived from MMP-9-null mice compared with the wild-type and that inhibitors of MMP-9 reduce cell process extension (Oh, 1999). These *in vitro* experiments were extended to models of remyelination in adult mice, in which a demyelinating insult was produced in the spinal cord by the lipid disrupting agent lysolecithin. The authors showed that after demyelization in adult mice the subsequent remyelination in MMP-9-null mice was retarded compared with that in tha wild-type animals (Larsen, 2003). The proposed role of MMP-9 in remyelination *in vivo* was attributed in part to the cleavage of NG2, a chondroitin sulfate proteoglican (CSPG) deposited into the ECM following injury, by MMP-9. In the absence of MMP-9, NG2 remains within the ECM and provids an inhibitory barrier that prevents the maturation of OLs into myelin forming cells (Larsen, 2003). On the other hand, MMP-9 is also implicated in the digestion of MBP, promoting demyelination in PNS (Chattopadhyay, 2007; Kobayashi, 2008). This activity could also be important for astrocytes, microglia and macrophages in order to remove myelin debris (Fancy, 2010; Franklin and Kotter, 2008; Nielsen, 2009). Pathological studies have revealed that chronically demyelinating

lesions in MS often fail to repair because of a failure in the differentiation of precursor cells responsible for remyelination, rather than a failure in their recruitment (Franklin and Kotter, 2008), as molecules accumulated in the myelin debris can inhibit OL differentiation (Hughes, 2002; Liu, 2008; Fancy, 2010).

Considering this scenario, in our mouse PD model, MMP-9 could take part in two series of events, as is summarized in the diagram of Fig. 27. First, early after the injury, it may favor axonal retration by damaged neurons, disassembling their myelin sheaths by digestion of MBP and/or of other proteins important for myelin stabilization, as dystroglycan (Chattopadhyay, 2007; Kobayashi, 2008; Shiryaev, 2009; Zhao, 2010). This in turn may induce a "dying-back" degeneration of neurons. In a second series of events, MMP-9 may support new terminal axon sprouting in those dopaminergic neurons which survived MPTP intoxication, promoting ECM remodeling and debris scavenging by appropriated cells (Webber, 2002; Larsen, 2003; Saxena and Caroni, 2007; Murray, 2008). All these processes will ultimately bring to a partial reinnervation of the striatum, as suggested by the recovery of TH immunolabeling in both SNpc and striatum, as well as the ultrastructural analysis conducted at the electron microscope. Also the observation that after a critical period of abut 72 hrs, mice apparently recover their motor skills, conforts this hypotheis.

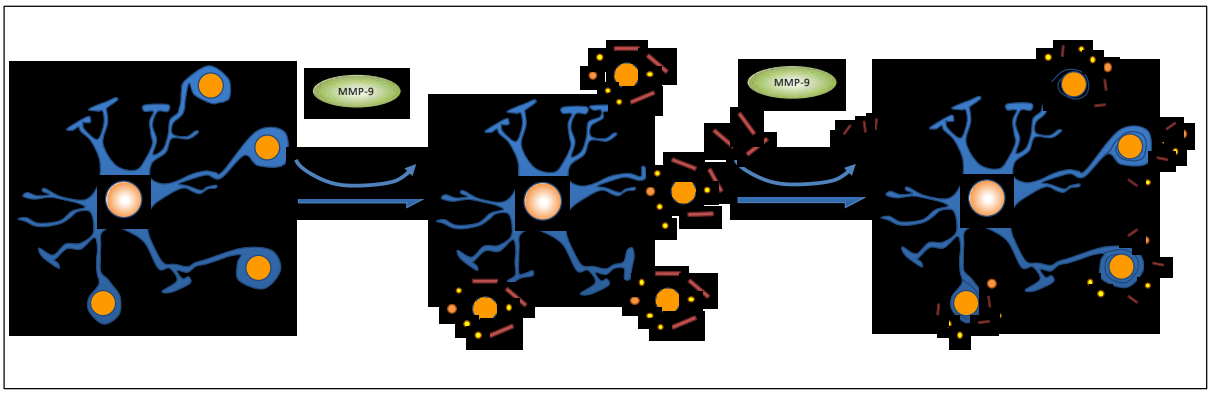

Fig. 27. MMP-9 regulates myelin. In response to a nocive stimulus MMP-9 could be involved in both myelin disruption and reparing. Early after injury, the increase in MMP-9 levels may have a significant role in the fragmentation of MBP, or of other proteins important for myelin stabilization, triggering the disorganization of the myelin sheets around axons and favouring its retraction. On the other hand, following demyelination, in the adult mouse SNC, MMP9 regulates remyelination. One mechanism through which this could be achieved is the clearance of proteoglycans, which constitute an inhibitory barrier for oligodendrocytes maturation and their subsequent reformation of myelin. The enzyme can also remove from sites of CNS injury some oligodendrocyte myelin glycoproteins and ECM proteogycans, which inhibit the new axonal growth.

The results we obtained in the monkey model of chronic MPTP administration differ, but do not contradict, those described in the mouse model. Two years after the establishment of stable parkinsonism, in the monkey striatum, both number and size of OLs are still higher than control, being the oligodendrogliosis more prominent in those monkeys with a more severe dopaminergic depletion. As shown the diagram in Fig. 28, OL activation and their MMP-9 synthesis is perpetuated along the years and, differently from mice, there is no partial rescue of the nigro-striatal dopaminergic system.

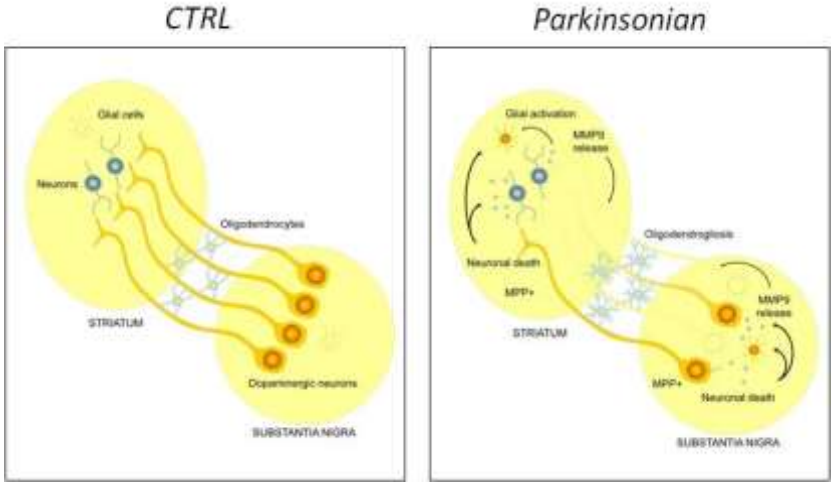

Fig. 28. MPTP chronic PD model in non-human primates. The diagram represents the alterations observed in the striatum of parkinsonian primates, years after the interruption of MPTP treatment. Features of oligodendrogliosis and both astroglia and microglia activation are still present, concomitant with the persistance of MMP-9 protein levels higher than controls. In the MPTP chronic PD the absence of a phase of gliosis regression and DA system recovery, observed in mice, suggests that the perpetuation of the neuroinflammatory processes may sustain the characteristic progression of the parkinsonian syndrome.

Therefore, we hypothesize that, in the chronic model of experimental parkinsonism, the initial neuronal damage may activate oligodendrogliosis and a cascade of glia-mediated inflammatory signals able to perpetuate themselves and probably induce progressive neuronal loss (Czlonkowska, 2001; Brochard, 2009; Saijo, 2009). In this situation, the persistence of an inflammatory stimulus years after MPTP injections (Barcia, 2004; McGeer, 2003), may promote the formation of a glial scar at sites of axon degeneration, imposing a barrier to a possible regeneration (Smith-Thomas, 1994; Fidler, 1999; Silver and Miller, 2004; Rolls, 2009) and creating a hostile environment in which OL activity may become ineffective compared with acute lesions (Foote and Blakemore, 2005; Setzu, 2006; Goldschmidt, 2009). In this context, the persistent expression of MMP-9 could be advocated to the high number of inflammatory cells, present at the injury sites. The chronic inflammation observed in monkeys respect to the transient inflammatory state characteristic of parkinsonian mice entails a series of differences in gene expression by the different cell types involved in the process, which might determine whether MMP-9 has a beneficial or detrimental function in this PD models. Probably, in primate parkinsonism, lack of mechanisms able to regulate a discreet and local MMP-9 expression, may affect both remodelling and repair processes after the initial phase of the injury, as it occurs in mice.

Our studies emphasize that myelin degeneration may play an important role in parkinsonism, but its function and mechanisms in the human disease needs to be further investigated. Very little has been reported on the involvement of OLs in PD. Previous investigations have shown the presence of complement-activated OLs in the SN*pc* in only a few cases of PD (Yamada, 1991). However, its relation with the disease remains unclear and it has been largely overlooked by researchers (McGeer and McGeer, 2008). In this innovative aspect, the possible role of MMP-9 needs to be further investigated in

order to open a window on new specific therapeutic strategies aimed at preventing, or minimize, axonal degeneration.

Conclusion and future directions

In this thesis we demonstrated *in vivo* an upregulation of the MMP-9 in MPTP-induced parkinsonism in mice and monkeys. However, how does MMP-9 achieve it effects and what are its specific roles are awiting further elucidation. Indeed, our data give us a precious background on which speculating a series of functions in different moments of the nigro-striatal pathway response to MPTP intoxication and of the development of a neuroinflammatory response. More indicative results are expected from the use of mice knock-out for MMP-9 activity (Wang, 2000; Asahi, 2001). MMP9-null mice and their corresponding wild-type mice have already been treated with MPTP in order to observe, by immunohistochemistry for the different neuronal and glial cell-specific markers, already utilized throughout this work of thesis, whether the absence of this enzymatic activity attenuates, or exacerbates, the dopaminergic neuron death and/or the neuroinflammatory response to the toxic insult. Clarify this point will be also useful for the interpretation of the results obtained in monkeys. In fact, *post-mortem* analysis of parkinsonian monkeys provide a final picture of this neuropathology, which could just suggest that glial activation, neuronal loss and increased MMP-9 expression are connected, but without giving hints on the original cause of the entire process. Conversely, the mouse model give us a dynamic experimental system, in which after a critical stage (48-72 hrs) a partial rescue of the nigro-striatal dopaminergic pathway is observed. Once clarified all the unresolved queries in mice, we will able to focus our research on parkinsonian monkeys, hoping to shed a light on a possible role for MMP-9 in human PD.

REFERENCES

Adibhatla RM et al., Brain extracellular matrix in neurodegeneration. *CNS Neurol Disord Drug Targets*. (2008), 7(3):243-53

Agrawal SM et al., MMPs in the central nervous system: where the good guys go bad. *Semin Cell Dev Biol* (2008), 19: 42-51

Akenami FO et al., Tissue plasminogen activator gene expression in multiple sclerosis brain tissue. *J Neurol Sci*. (1999), 165(1):71-6

Albrecht, P. J. et al. Astrocytes produce CNTF during the remyelination phase of viral-induced spinal cord demyelination to stimulate FGF-2 production. *Neurobiol. Dis.* (2003), 13:89–101;

Allan SM et al., Interleukin-1 and neuronal injury. *Nat Rev Immunol* (2005), 5:629–640

Amantea D et al., Early upregulation of matrix metalloproteinases following reperfusion triggers neuroinflammatory mediators in brain ischemia in rat. *Int Rev Neurobiol* (2007), 82:149-169

Anastasia A et al., Enriched environment protects the nigrostriatal dopaminergic system and induces astroglial reaction in the 6-OHDA rat model of Parkinson's disease. *J. Neurochem*. (2009), 109:755-7,65

Anthony D. C. et al., Matrix metalloproteinase expression in an experimentally-induced DTH model of multiple sclerosis in the rat CNS. *J. Neuroimmunol*. (1998), 87:62–72

Appel SH, CD4+ T cells mediate cytotoxicity in neurodegenerative diseases. J *Clin Invest.* (2009), 119(1):13-5

Asahi M et al., Effects of matrix metalloproteinase-9 gene knock-out on the proteolysis of blood-brain barrier and white matter components after cerebral ischemia. *J Neurosci*. (2001), 21(19):7724-32

Badie B et al., Interferon-gamma induces apoptosis and augments the expression of Fas and Fas ligand by microglia in vitro. *Exp Neurol* (2000); 162:290–296

Balistreri et al., TLR4 polymorphisms and ageing: implications for the pathophysiology of age-related diseases. *J Clin Immunol*. (2009), 29(4):406-15

Bandtlow CE and al., Proteoglycans in the developing brain: new conceptual insights for old proteins. *Physiol Rev* (2000), 80:1267–1290

Barcia C et al, Evidence of active microglia in substantia nigra pars compacta of parkinsonian monkeys 1 year after MPTP exposure. *Glia* (2004), 46:402–409

Barcia C et al., Blood vessels and Parkinsonism. Frontiers in Bioscience (2004), 9:277-282

Barcia C et al., Increased plasma levels of TNF-alpha but not of IL1-beta in MPTP-treated monkeys one year after the MPTP administration. *Parkinsonism Relat Disord* (2005), 11: 435-9

Barcia C et al., IFN-γ signaling, with the synergistic contribution of TNF-α, mediates cell specific microglial and astroglial activation in experimental models of Parkinson's disease (2010), submitted

Bauer S. et al, The neuropoietic cytokine family in development, plasticity, disease and injury. *Nat Rev Neurosci.* (2007), 8:221-232

Beal MF, Experimental models of Parkinson's disease. *Nat Rev Neurosci*. (2001), 2(5):325-34

Ben Hur T et al., Cytokine-mediated modulation of MMPs and TIMPs in multipotential neural precursor cells. J Neuroimmunol (2006), 175(1/2):12-18

Benarroch EE, Tissue plasminogen activator: beyond thrombolysis. *Neurology* (2007), 69(8):799-802

Benner EJ et al., Nitrated alpha-synuclein immunity accelerates degeneration of nigral dopaminergic neurons. *PLoS One*. (2008), 3(1):e1376

Benveniste EN et al., Differential modulation of astrocyte cytokine gene expression by TGF-beta. *J Immunol*. 1994, 153(11):5210-21

Betarbet R et Greenamyre JT, Parkinson's disease: animal models. *Handb Clin Neurol*. (2007), 83:265-87

Björkqvist M, Wild EJ, Tabrizi SJ, Harnessing immune alterations in neurodegenerative diseases. *Neuron.* (2009), 15;64(1):21-4

Block ML, Zecca L, Hong JS, Microglia-mediated neurotoxicity: uncovering the molecular mechanisms. *Nat Rev Neurosci*. (2007), 8(1):57-69

Bonneh-Barkay D and Wiley CA, Brain extracellular matrix in neurodegeneration. *Brain Pathol.* (2009), 19(4):573-85

Bouchard et al., Fak/Src signaling in human intestinal epithelial cell survival and anoikis: differentiation state-specific uncoupling with the PI3-K/akt-1 and MEK/Erk pathways. *J. Cell. Physiol*. (2007), 212:717-728

Bove J. et al., Proteasome inhibition and PD modeling, *Ann. Neurol.* (2006), 60:260-264

Braak H et al., Extensive axonal Lewy neurites in Parkinson's disease: a novel pathological feature revealed by alpha-synuclein immunocytochemistry. *Neurosci letters.* (1999), 265(1):67-9

Braak H et al., Idiopathic Parkinson's disease: possible routes by which vulnerable neuronal types may be subject to neuroinvasion by an unknown pathogen. *J Neural Transm*. (2003), 110(5):517-36

Braak H et al., Development of alpha-synuclein immunoreactive astrocytes in the forebrain parallels stages of intraneuronal pathology in sporadic Parkinson's disease. *Acta Neuropathol.* (2007), 114(3):231-41

Breidert T et al., Protective action of the peroxisome proliferator-activated receptor gamma agonist pioglitazone in a mouse model of Parkinson's Diesease. *J Neurochem* (2002), 82:615-24

Bridges LC and Bowditch RD, ADAM-integrin interactions: potential integrin regulated ectodomain shedding activity. *Curr Pharm Des* (2005), 11:837–847

Brochard V et al., Infiltration of CD4+ lymphocytes into the brain contributes to neurodegeneration in a mouse model of Parkinson disease. *J Clin Invest* (2009), 119:182-92

Brückener G et al, Cortical areas abundant in extracellular matrix chondroitin sulphate proteoglycans are less affected by cytoskeletal changes in Alzheimer's disease. *Neuroscience* (1999), 92(3):791-805

Candelario-Jalil E et al., Diverse roles of matrix metalloproteinases and tissue inhibitors of metalloproteinases in neuroinflammation and cerebral ischemia. *Neuroscience* (2009), 158(3):983-94

Carvey PM, Progressive dopamine neuron loss in Parkinson's disease: the multiple hit hypothesis. *Cell Transplant.* (2006), 15(3):239-50

Castaño A et al., The degenerative effect of a single intranigral injection of LPS on the dopaminergic system is prevented by dexamethasone, and not mimicked by rh-TNF-alpha, IL-1beta and IFN-gamma. *J Neurochem*. (2002), 81(1):150-7.

Chattopadhyay S et al., Cytokine regulation of MMP-9 in peripheral glia: implications for pathological processes and pain in injured nerve. *Brain Behav Immun*. (2007), 21(5):561-8

Chen, X. et al., Caffeine protects against MPTP-induced bloodbrain barrier dysfunction in mouse striatum. *J. Neurochem.* (2008), 107:1147-1157

Chia-Jen Siao & Stella E. Tsirka, Tissue plasminogen activator mediates microglial activation via its finger domain through Annexin II. *J of Neurosci* (2002), 22:3352-3358

Chintala SK et al., Deficiency in matrix metalloproteinase gelatinase B (MMP-9) protects against retinal ganglion cell death after optic nerve ligation. *J Biol Chem* (2002), 277:47461–47468

Cho Y et al., Doxycycline is neuroprotective against nigral dopaminergic degeneration by a dual mechanism involving MMP-3. *Neurotox Res.* (2009), 16(4):361-71

Choi DH et al., A novel intracellular role of matrix metalloproteinase-3 during apoptosis of dopaminergic cells. *J Neurochem* (2008), 106:405-15

Choi MS et al., ATP induced microglia cell migration through non-transcriptional activation of matrix metalloproteinase-9, *Arch Pharm Res* (2010), 2:257:265

Cliffer KD et al., Physiological characterization of Taxol-induced large-fiber sensory neuropathy in the rat. *Ann Neurol.* (1998), 43(1):46-55

Correale and Villa, The neuroprotective role of inflammation in nervous system injuries. *J Neurol*. (2004), 251(11):1304-16

Crocker SJ et al., The TIMPs tango with MMPs and more in the central nervous system. J Neurosci Res (2004), 75:1–11

Czlonkowska A et al., Role of inflammatory factors in neurodegeneration. *Neurol Neurochir Pol* (2001), 31:13-22

Damier P et al.,Glutathione peroxidase, glial cells and Parkinson's disease. *Neuroscience.* (1993), 52(1):1-6

Danzer KM et al., Different species of alpha-synuclein oligomers induce calcium influx and seeding. *J Neurosci.* (2007), 27(34):9220-32

Dauer W and Przedborski S, Parkinson’s disease: mechanisms and models. *Neuron* (2003), 39:196-221

Del Zoppo GJ et al., Microglial activation and matrix protease generation during focal cerebral ischemia. *Stroke* (2007), 38(2 Suppl):646-51

Di Monte DA et al., Role of astrocytes in MPTP metabolism and toxicity. *Annals of the New York Academy of Scie*nces. (1992), 648:219-28

Di Virgilio et al., P2X(7): a growth-promoting receptor-implications for cancer. Purinergic Signal. (2009), 5(2):251-6

Dickson DW et al., Microglia and cytokines in neurological disease, with special reference to AIDS and Alzheimer's disease. *Glia*. (1993), 7(1):75-83

Dityatev A and Schachner M., Extracellular matrix molecules and synaptic plasticity. *Nat Rev Neurosci* (2003), 4:456–468

Dityatev A et al., Extracellular matrix in plasticity and epileptogenesis. *Neuron Glia Biol.* (2008), 4:235-47

Duda JE et al., Novel antibodies to synuclein show abundant striatal pathology in Lewy body diseases. *Annals Neurol*. (2002), 52(2):205-10

Duda JE. Parkinson's Disease: The Life Cycle of the Dopamine Neuron. *Princeton, New Jersey, USA. Proceedings. Annals of the New York Academy of Sciences* (2003), 991:1-360

Dumin, J. A. et al. Pro-collagenase-1 (matrix metalloproteinase-1) binds the α2β1 integrin upon release from keratinocytes migrating on type I collagen. *J. Biol. Chem.* (2001), 276:29368–29374

Dzwonek J, Rylski M and Kaczmarek L, Matrix metalloproteinases and their endogenous inhibitors in neuronal physiology of the adult brain. *FEBS Lett* (2004), 567: 129-135

Elliot MR et al., Nucleotides released by apoptotic cells act as find me signal to promote phagocytic clearance. *Nature* (2009), 461:282-286

Ethell IM and Ethell DW, Matrix metalloproteinases in brain development and remodelling: synaptic functions and targets. *J Neurosci Res* (2007), 85: 2813-2823

Faissner A et al., Contributions of astrocytes to synapse formation and maturation - Potential functions of the perisynaptic extracellular matrix. *Brain Res Rev.* (2010), 63(1-2):26-38

Fancy SP et al., Overcoming remyelination failure in multiple sclerosis and other myelin disorders. *Exp Neurol.* (2010), 225(1):18-23

Faucheux, B. A. et al., Blood vessels change in the mesencephalon of patients with Parkinson's disease. Lancet (1999), 353:981-982

Ferger B et al., Genetic ablation of tumor necrosis factor-alpha (TNF-alpha) and pharmacological inhibition of TNF-synthesis attenuates MPTP toxicity in mouse striatum. *J Neurochem*. (2004), 89(4):822-33

Fidler PS et al., Comparing astrocytic cell lines that are inhibitory or permissive for axon growth: the major axon-inhibitory proteoglycan is NG2. *J Neurosci.* (1999), 19(20):8778-88

Foote, A. K. & Blakemore, W. F., Inflammation stimulates remyelination in areas of chronic demyelination. Brain (2005), 128:528–539

Forno LS, Neuropathologic features of Parkinson's, Huntington's, and Alzheimer's diseases. *Ann N Y Acad Sci.* (1992), 11;648:6-16

Franklin R and Kotter MR, The biology of CNS remyelination: the key to therapeutic advances. *J Neurol.* (2008)a, 255 Suppl 1:19-25

Franklin RJ et al., Remyelination in the CNS: from biology to therapy. *Nature reviews* (2008)b, 9(11):839-55

Garrido-Gil et al., 1-Methyl-4-phenyl-1,2,3,6-tetrahydropyridine exposure fails to produce delayed degeneration of substantia nigra neurons in monkeys. *J Neurosci Res* (2009), 87: 586-972

Gary and Mattson, Integrin signaling via the PI3-kinase-Akt pathway increases neuronal resistance to glutamate-induced apoptosis. *J Neurochem* (2001), 76:1485-1496

Gasche Y et al., Matrix metalloproteinase inhibition prevents oxidative stress-associated blood-brain barrier disruption after transient focal cerebral ischemia. *J Cereb Blood Flow Metab* (2001), 21: 1393–400

Gasser T, Molecular pathogenesis of Parkinson disease: insights from genetic studies. *Expert Rev Mol Med.* (2009), 11:e22

Gendelman HE, et al. Innate and acquired immunity in neurodegenerative disorders. *J Leukoc Biol* (1999), 65:407–408

Gerhard A et al., In vivo imaging of microglial activation with [11C](R)-PK11195 PET in idiopathic Parkinson's disease. *Neurobiol Dis*. (2006), 21(2):404-12

Giulian, D. et al., Microglial mitogens are produced in the developing and injured mammalian brain. *J. Cell. Biol.* (1991), 112:323-333

Glass C.K., Mechanisms underlying inflammation in neurodegeneration. *Cell* (2010), 140(6):918-34

Godoy MC et al., Central and systemic IL-1 exacerbates neurodegeneration and motor symptoms in a model of Parkinson's disease. *Brain* (2008), 131: 1880-94

Goldschmidt T et al., Remyelination capacity of the MS brain decreases with disease chronicity. *Neurology* (2009), 72(22):1914-21

Gu Z et al., A highly specific inhibitor of matrix metalloproteinase-9 rescues laminin from proteolysis and neurons from apoptosis in transient focal cerebral ischemia. *J Neurosci* (2005), 25:6401– 6408

Gu, Z. et al. S-nitrosylation of matrix metalloproteinases: signaling pathway to neuronal cell death. *Science* (2002), 297:1186–1190

Gualandris A et al., Membrane depolarization induces calcium-dependent secretion of tissue plasminogen activator. *J Neurosci* (1996), 16:2220–2225

Guix FX et al., The physiology and pathophysiology of nitric oxide in the brain. *Prog Neurobiol* (2005), 76:126–152

Gurney KJ et al., Blood-brain barrier disruption by stromelysin-1 facilitates neutrophil infiltration in neuroinflammation. Neurobiol Dis. (2006), 23(1):87-96

Gyung Kim W et al., The role of MMP-9 in integrin-mediated hippocampal cell death after pilocarpine-induced status epilecticus. *Neurobiol of dis* (2009), 36:169-180

Halliday G et al., No Lewy pathology in monkeys with over 10 years of severe MPTP Parkinsonism. *Mov Disord.* (2009), 24(10):1519-23

Hanisch UK, Microglia as a source and target of cytokines. *Glia*. (2002), 40(2):140-55

Harry GJ et al., The type 1 interleukin 1 receptor is not required for the death of murine hippocampal dentate granule cells and microglia activation. *Brain Res* (2008), 1194:8–20

Harry GJ et al., Tumor necrosis factor p55 and p75 receptors are involved in chemical-induced apoptosis of dentate granule neurons. *J Neurochem* (2008), 106:281–298

Hebert G et al., Time-course of the expression of inflammatory cytokines and matrix metalloproteinases in the striatum and mesencephalon of mice injected with 1-methyl-4-phenyl-1,2,3,6-tetrahydropyridine, a dopaminergic neurotoxin. *Neurosci Lett* (2003), 349: 191-5

Herrera AJ et al., The single intranigral injection of LPS as a new model for studying the selective effects of inflammatory reactions on dopaminergic system. *Neurobiol Dis.* 2000, 7(4):429-47

Herrero MT et al., Does neuromelanin contribute to the vulnerability of catecholaminergic neurons in monkeys intoxicated with MPTP? Neuroscience. (1993)a, 56(2):499-511

Herrero MT et al., Neuromelanin accumulation with age in catecholaminergic neurons from Macaca fascicularis brainstem. *Dev Neurosci.* (1993)b, 15(1):37-48

Higashida T et al., The role of hypoxia-inducible factor-1α, aquaporin-4, and matrix metalloproteinase-9 in blood-brain barrier disruption and brain edema after traumatic brain injury. *J Neurosurg.* (2010), in press

Hirsch EC et al., Glial cells and inflammation in Parkinson's disease: a role in neurodegeneration? *Ann Neurol*. (1998), 44(3 Suppl 1):S115-20

Hirsch et al., The role of glial reaction and inflammation in Parkinson's disease. *Ann NY Acad Sci* (2003), 991:214–228

Hirsch EC and Hunot S, Neuroinflammation in Parkinson's disease: a target for neuroprotection? *Lancet Neurol* (2009), 8:382–97

Horton M et al., Pathological evidence of vacuolar myelinopathy in a child following vigabatrin administration. *Journal of child neurology.* (2009), 24(12):1543-6

Hughes PM et al., Comparison of matrix metalloproteinase expression during Wallerian degeneration in the central and peripheral nervous systems. *Neuroscience* (2002), 2:273-287

Hurley SD et al., Microglial response poorly correlated with neurodegeneration following chronic, low-dose MPTP-administration in monkeys. *Exp Neurol* (2003), 189:659–668

Husemann et al., Scavenger receptors in neurobiology and neuropathology: their role on microglia and other cells of the nervous system. *Glia* (2002), 40(2):195-205

Hwang J. J et al., Activation of the Trk signaling pathway by extracellular zinc. Role of metalloproteinases. *J. Biol. Chem.* (2005), 280:11995–12001

Ito A. et al. Degradation of interleukin 1β by matrix metalloproteinases. *J. Biol. Chem.* (1996), 271:14657–14660

Javitch JA et al, Parkinsonism inducing neurotoxin, N-methyl-4-phenyl-1,2,3,6-tetrahydropyridine: uptake of the metabolite N-methyl-4-phenylpyridinium by dopamine neurons explain selective toxicity. *Proc. Natl. Acad. Sci. USA* (2000), 82:2173-2177

Jenner P et al., Understanding cell death in Parkinson's disease. *Ann Neurol* (1998), 44:72–84

Jenner P, Functional models of Parkinson's disease: A valuable tool in the development of novel therapies. *Ann of Neurol* (2008), 64:16-29

Jidday JM et al., Leucocyte derived matrix metalloproteinase-9 mediates blood brain barrier breakdown and is pro-inflammatory after transient focal cerebral ischemia. *Am J Physiol Heart Circ Physiol* (2005), 289:H558-H568

Jin R, Yang G, Li G., Molecular insights and therapeutic targets for blood-brain barrier disruption in ischemic stroke: critical role of matrix metalloproteinases and tissue-type plasminogen activator. *Neurobiol Dis*. (2010), 38(3):376-85

Kastner A et al., Is the vulnerability of neurons in the substantia nigra of patients with Parkinson's disease related to their neuromelanin content? *J Neurochem*. (1992), 59(3):1080-9

Kattenmann H., Triggering the brain's pathology sensor. *Nat Neurosci.* (2006), 9(12):1463-4)

Kattenmann H., Neuroscience: the brain's garbage men. *Nature* (2007), 446(7139):987-9

Kaushal V et al., Mechanisms of microglia-mediated neurotoxicity in a new model of the stroke penumbra. *J Neurosci* (2008), 28:2221–2230. 281–298

Kieburtz K, Ravina B. Why hasn't neuroprotection worked in Parkinson's disease? *Nature clinical practice* (2007), 3(5):240-1

Kim YS et al., Matrix metalloproinase-3: a novel signaling proteinase from apoptotic neuronal cells that activates microglia. *J Neurosci* (2005), 25:3701-11

Kim YS et al., A pivotal role of matrix metalloproteinase-3 activity in dopaminergic neuronal degeneration via microglial activation. *FASEB J.* (2007), 21(1):179-87

Kitamura Y et al., The 6-hydroxydopamine-induced nigrostriatal neurodegeneration produces microglia-like NG2 glial cells in the rat substantia nigra. *Glia* (2010), 58(14):1686-700

Kobayashi H et al., MMPs initiate Schwann cell-mediated MBP degradation and mechanical nociception after nerve damage. *Mol Cell Neurosci.* (2008), 39(4):619-27

Kolaczkowska E et al., Gelatinase B/matrix metalloproteinase-9 contributes to cellular infiltration in a murine model of zymosan peritonitis. *Immunobiology* (2006), 211(3):137-48

Kolata G, Monkey model of Parkinson's disease. *Science* (1983), 220(4598):705

Kortekaas R et al., Blood-brain barrier dysfunction in parkinsonian midbrain in vivo. *Ann. Neurol.* (2005), 57, 176-179

Kreutzberg, G. W. Microglia: a sensor for pathological events in the CNS. *Trends. Neurosci*. (1996), 19:312-318

Kurkowska-Jastrzebska I et al., The inflammatory reaction following 1-methyl-4-phenyl-1,2,3,6-tetrahydropyridine intoxication in mouse. *Exp Neurol* (1999), 156:50-61

Kurkowska-Jastrzebska I et al., Anti-myelin basic protein T cells protect hippocampal neurons against trimethyltin-induced damage. *Neuroreport* (2007), 18:425–429

Kurkowska-Jastrzebska I et al., Decreased inflammation and augmented expression of trophic factors correlate with MOG-induced neuroprotection of the injured nigrostriatal system in the murine MPTP model of Parkinson's disease. *Int Immunopharmacol* (2009), 9: 781-91

Langston JW et al., Chronic parkinsonism in humans due to a product of meperidine-analog synthesis. *Science* (1983), 219: 979-980

Langston JW et al., MPTP-induced parkinsonism in human and non-human primates: clinical and experimental aspects. *Acta Neurol Scand Suppl*. (1984), 100:49-54

Langston JW et al., Evidence of active nerve cell degeneration in the substantia nigra of humans ears after 1-methyl-4-phenyl-1,2,3,6-tetrahydropyridine exposure. *Ann Neurol* (1999), 46:598–605

Larsen PH. et al., Matrix metalloproteinase-9 facilitates remyelination in part by processing the inhibitory NG2 proteoglycan. *J. Neurosci.* (2003), 23:11127–11135

Larsen PH et al., Myelin formation during development of the CNS is delayed in matrix metalloproteinase-9 and -12 null mice. *J Neurosci.* (2006), 26(8):2207-14

Lee EJ et al., {alpha}-synuclein activates microglia by inducing the expression of matrix metalloproteinases and the subsequent activation of protease-activated receptor-1. *J immunol* (2010), 185:615-623

Lee HJ et al., Clearance and deposition of extracellular alpha-synuclein aggregates in microglia. *Biochem Biophys Res Commun*. (2008), 372(3):423-8

Lee SR et al., Induction of caspase-mediated cell death by matrix metalloproteinases in cerebral endothelial cells after hypoxia-reoxygenation. *J. Cereb. Blood Flow Metab* (2004), 24:720-727

Lee WJ et al., Induction of MMP-9 in lipopolysaccharide-stimulated primary astrocytes is mediated by extracellular signal-regulated protein kinase1/2. *Glia* (2003), 41:15-24

Lefebvre d'Hellencourt C. et al., Molecular profiles of mRNA levels in laser capture microdissected murine hippocampal regions differentially responsive to TMT-induced cell death. *J Neurochem* (2005), 93:206–220

Lehmann HC et al., Matrix metalloproteinase-2 is involved in myelination of dorsal root ganglia neurons. *Glia* (2009), 57(5):479-89

Levine JM, Reynolds R. Activation and proliferation of endogenous oligodendrocyte precursor cells during ethidium bromide-induced demyelination. *Experimental neurol* (1999), 160(2):333-47

Levin J et al., Increased α-synuclein aggregation following limited cleavage by certain matrix metalloproteinases. *Exp Neurol* (2009), 215:201-208

Li Q et al., Matrilysin shedding of syndecan-1 regulates chemokine mobilization and transepithelial efflux of neutrophils in acute lung injury. *Cell* (2002), 111:635– 646)

Liu R et al., Regulation of axonal regeneration following the central nervous system injury in adult mammalian. *Neurosci Bull.* (2008), 24(6):395-400

Liu W et al., Differential expression of tissue inhibitor of metalloproteinases-3 in cultured astrocytes and neurons regulates the activation of matrix metalloproteinase-2. *J Neurosci Res*. (2007), 85(4):829-36

Liu Y. et al, Gene transfere of a reserpine-sensitive mechanism of resistance to N-methyl-4-phenyl-1,2,3,6-tetrahydropyridine. *Proc. Natl. Acad. Sci. USA* (1992), 89:9074-9078

Lo EH et al., Extracellular proteolysis in brain injury and inflammation: role for plasminogen activators and matrix metalloproteinases. *J Neurosci Res* (2002), 69:1–9

Lorenzl S et al., Expression of MMP-2, MMP-9, and MMP-1 and their endogenous counterregulators TIMP-1 and TIMP-2 in postmortem brain tissue of Parkinson's disease. *Exp Neurol* (2002), 178:13-20

Lorenzl S et al., Tissue inhibitors of matrix metalloproteinases are elevated in cerebrospinal fluid of neurodegenerative diseases. *J Neurol Sci* (2003), 207(1-2):71-6

Lorenzl S et al., Matrix metalloproteinase-9 is elevated in 1-methyl-4-phenyl-1,2,3,6-tetrahydropyridine-induced parkinsonism in mice. *Neuromolecular Med* (2004), 5(2):119-32

Lovrecic L et al., PAI and TPA gene polymorphisms in multiple sclerosis. *Mult Scler.* (2008), 14(2):243-7

Luchtman DW et al., Behavior, neurotransmitters and inflammation in three regimens of the MPTP mouse model of Parkinson's disease. *Physiol Behav* (2009), 98: 130-8

Luo J., The role of matrix metalloproteinases in the morphogenesis of the cerebellar cortex. *Cerebellum*. (2005), 4(4):239-45

Machida C. et al., NGF induction of the gene encoding of the protease transin accompanies neuronal differentiation in PC12 cells. *Cell* (1989), 2:1587-1596

Madani R et al., Emotions are building up in the field of extracellular proteolysis. *Trends Mol Med* (2003)a, 9:183–185

Madani R et al., Impaired explorative behavior and neophobia in genetically modified mice lacking or overexpressing the extracellular serin protease inhibitor neuroserpin. *Mol. Cell. Neurosci.* (2003)b, 23(3):473-494

Marin C et al., Motor complications in Parkinson's disease and the clinical significance of rotational behavior in the rat: have we wasted our time? *Exp Neurol* (2006), 197(2):269-74

Matias-Roman S et al., Membrane type 1-matrix metalloproteinase is involved in migration of human monocytes and is regulated through their interaction with fibronectin or endothelium. *Blood* (2005), 105:3956–3964

Matusevicius D. et al. Multiple sclerosis: the proinflammatory cytokines lymphotoxin-alpha and tumour necrosis factor-alpha are upregulated in cerebrospinal fluid mononuclear cells. *J Neuroimmunol* (1996), 66:115–123

Matys T and Strickland S., Tissue plasminogen activator and NMDA receptor cleavage. *Nat Med* (2003), 9:371-373

McAllister AK and van de Water J, Breaking boundaries in neural-immune interactions.

McClain JA et al., Increased MMP-3 and CTGF expression during lipopolysaccharide-induced dopaminergic neurodegeneration. *Neurosci Lett.* (2009), 460(1):27-31

McCoy MK et al., Blocking soluble tumor necrosis factor signaling with dominant-negative tumor necrosis factor inhibitor attenuates loss of dopaminergic neurons in models of Parkinson's disease. *J Neurosci*. (2006), 26(37):9365-75

McGeer PL et al, Rate of cell death in parkinsonism indicates active neuropathological process. *Ann Neurol.* (1988)a, 24(4):574-6

McGeer PL et al., Reactive microglia are positive for HLA-DR in the substantia nigra of Parkinson's and Alzheimer's disease brains. *Neurology* (1988)b, 38:1285–1291

McGeer et al., Presence of reactive microglia in monkey substantia nigra years after 1-methyl-4-phenyl-1,2,3,6-tetrahydropyridine administration, *Ann Neurol* (2003), 54:599-604

McGeer et al., Inflammation and neurodegeneration in Parkinson's disease, *Parkinsonism Relat Disord* (2004), 1:S3-7

McGeer PL and McGeer EG, Glial reaction in Parkinson's disease. *Mov Disord* (2008), 23:474-483

McQuibban G et al., Inflammation dampened by gelatinase A cleavage of monocyte chemoattractant protein-3. *Science* (2000); 289:1202–1206)

Melchor JP et al., The possible role of tissue-type plasminogen activator (tPA) and tPA blockers in the pathogenesis and treatment of Alzheimer's disease. *J Mol Neurosci.* (2003), 20(3):287-9

Melchor JP and Strickland S Tissue plasminogen activator in central nervous system physiology and pathology. *Thromb Haemost* (2005), 93:655–660

Michaluk P and Kaczmarek L, Matrix metalloproteinase-9 in glutamate-dependent adult brain function and dysfunction.Cell death and differentiation (2007), 14:1255-1258

Michaluk P et al., Matrix metalloproteinase-9 controls NMDA receptor surface diffusion through integrin beta1 signaling. *J Neurosci.* (2009), 29(18):6007-12

Mille JP et al., Matrix metalloproteinases are modifiers of huntingtin proteolysis and toxicity in Huntington's disease. *Neuron* (2010), 67(2):199-212

Miller G., Neuroscience. The dark side of glia. *Science* (2005), 308:778-78

Milligan ED et al, Pathological and protective roles of glia in chronic pain. *Nat Rev Neurosci*. (2009), 10:23-36

Mitsui S et al., Mosaic serine proteases in the mammalian central nervous system. *Front Biosci.* (2008), 13:1991-2000

Mogi M et al., Interleukin-1 beta, interleukin-6, epidermal growth factor and transforming growth factor-alpha are elevated in the brain from parkinsonian patients. *Neurosci Lett.* (1994)a, 180(2):147-50

Mogi M et al., Tumor necrosis factor-alpha (TNF-alpha) increases both in the brain and in the cerebrospinal fluid from parkinsonian patients. *Neurosci Lett*. (1994)b, 165(1-2):208-10

Moon M et al., Neuroprotective effect of ghrelin in the 1-methyl-4-phenyl-1,2,3,6-tetrahydropyridine mouse model of Parkinson's disease by blocking microglial activation. *Neurotox Res.* (2009), 15(4):332-47

Moore CS et al., How factors secreted from astrocytes impact myelin repair. *J Neurosci Res.* (2010), in press

Morawski M et al., Neurons associated with aggrecan-based perineuronal nets are protected against tau pathology in subcortical regions in Alzheimer's disease. *Neuroscience* (2010), 169(3):1347-63

Mount MP et al., Involvement of interferon-gamma in microglial-mediated loss of dopaminergic neurons. *J Neurosci*. (2007), 27(12):3328-37

Mun-Bryce S et al., Stromelysin-1 and gelatinase A are upregulated before TNF-alpha in LPS-stimulated neuroinflammation. *Brain Res* (2002), 933(1):42-9

Murray LM et al., Loss of translation elongation factor (eEF1A2) expression in vivo differentiates between Wallerian degeneration and dying-back neuronal pathology. *Journal of anatomy*, (2008), 213(6):633-45

Nagase H et al., Structure and function of matrix metalloproteinases and TIMPs. *Cardiovasc Res* (2006), 69:562–573

Nagatsu T, Sawada M, Inflammatory process in Parkinson's disease: role for cytokines. *Curr Pharm Des*. (2005), 11(8):999-1016

Napoli I. and Neumann H., Microglial clearance function in health and disease. *Neuroscience* (2009), 158(3):1030-1038

Narassimahan K., Brain's guard cells show their agility. *Nature Neurosci* (2005), 8(6):752-8

Neufeld G et al., Vascular endothelial growth factor (VEGF) and its receptors. *FASEB J* (1999), 13:9–22

Newman, T. A. et al., T-cell- and macrophage-mediated axon damage in the absence of a CNS-specific immune response: involvement of metalloproteinases. *Brain* (2001), 124:2203–2214

Nguyen J et al., Inhibition of matrix metalloproteinase-9 by interferons and TGF-beta1 through distinct signalings accounts for reduced monocyte invasiveness. *FEBS Lett.* (2005), 579(25):5487-93

Nguyen JH et al., Matrix metalloproteinase-9 contributes to brain extravasation and edema in fulminant hepatic failure mice. *J Hepatol.* (2006), 44(6):1105-14

Nicole O. et al., neuroprotection mediated by glial cell line-derived neurotrophic factor: involvement of a reduction of NMDA-induced calcium influx by the mitogen-activated protein kinase pathway. *J Neurosci* (2001), 21(9): 3024-3033

Nielsen HH et al., Enhanced microglial clearance of myelin debris in T cell-infiltrated central nervous system. *J Neuropathol Exp Neurol*. (2009), 68(8):845-56

Noble L. J et al., Matrix metalloproteinases limit functional recovery after spinal cord injury by modulation of early vascular events. *J. Neurosci*. (2002), 22:7526–7535

O'Callaghan J.P, Glial fibrillary acidic protein and related glial proteins as biomarkers of neurotoxicity. *Exp. Opin. Drug Safety* (2005), 4:433-442

Obeso JA et al., Missing pieces in Parkinson's disease puzzle. *Nature Medicine* (2010), 16:653-661

Ogier C et al., Matrix metalloproteinase-2 (MMP-2) regulates astrocyte motility in connection with the actin cytoskeleton and integrins. *Glia* (2006), 54:272–284

Oh, L. Y. et al. Matrix metalloproteinase-9/gelatinase B is required for process outgrowth by oligodendrocytes. *J. Neurosci*. (1999), 19:8464–8475

Overall, C. M. et al. Protease degradomics: mass spectrometry discovery of protease substrates and the CLIP-CHIP, a dedicated DNA microarray of all human proteases and inhibitors. *Biol. Chem.* (2004), 385:493–504

Page-McCaw A et al., Matrix metalloproteinases and the regulation of tissue remodeling, *Nature Reviews Molecular Cell Biology* (2007), 8:221-233

Parks WC et al., Matrix metalloproteinases as modulators of inflammation and innate immunity. *Nature Rev. Immunol.* (2004), 4:617–629

Pawate S et al., Redox regulation of glial inflammatory response to lipopolysaccharide and interferon-gamma. *J Neurosci Res* (2004), 77:540–551

Porter S et al., The ADAMTS metalloproteinases. *Biochem J* (2005), 386:15–27

Pott Godoy MC et al., Central and systemic IL-1 exacerbates neurodegeneration and motor symptoms in a model of Parkinson's disease. *Brain* (2008), 131:1880-1894

Proost, P., Van Damme, J. & Opdenakker, G. Leukocyte gelatinase B cleavage releases encephalitogens from human myelin basic protein. *Biochem. Biophys. Res. Commun*. (1993), 192:1175–1181

Raines EW, Ross R. Compartmentalization of PDGF on extracellular binding sites dependent on exon-6-encoded sequences. *J Cell Biol* (1992), 116:533–54372

Ramsay RR et al, Energy-dependent uptake of N-methyl-4-phenyl-1,2,3,6-tetrahydropyridine by mitochondria. *J. Biol. Chem.* (1986), 261:7585:7587

Reale M et al., Peripheral cytokines profile in Parkinson's disease. *Brain Behav Immun* (2009)a, 23: 55-63

Reale M, Greig NH, Kamal MA, Peripheral chemo-cytokine profiles in Alzheimer's and Parkinson's diseases. *Mini Rev Med Chem*. (2009)b, 9(10):1229-41

Redwine, J. M. & Armstrong, R. C. In vivo proliferation of oligodendrocyte progenitors expressing PDGFαR during early remyelination. *J. Neurobiol.* (1998), 37:413–428

Reijerkerk A et al., Tissue-type plasminogen activator is a regulator of monocyte diapedesis through the brain endothelial barrier. *J Immunol* (2008), 181(5):3567-74

Reynolds R et al., The response of NG2-expressing oligodendrocyte progenitors to demyelination in MOG-EAE and MS. *J neurocytol* (2002), 31(6-7):523-36

Reynolds AD et al, Nitrated alpha-synuclein and microglial neuroregulatory activities. *J Neuroimmune Pharmacol.* (2008), 3(2):59-74

Rite, I et al., Blood brain barrier disruption induces in vivo degeneration of nigral dopaminergic neurons. *J. Neurochem.* (2007), 101:1567-1582

Rivera S et al., Matrix metalloproteinases and tissue inhibitors of metalloproteinases in neuronal plasticity and pathology. *The MIT press* pag. 53-86

Robin J. M. Franklin and Charles ffrench-Constant, Remyelination in the CNS: from biology to therapy. *Nature Reviews* (2008), 9:839-855

Roodveldt C et al., Immunological features of alpha-synuclein in Parkinson's disease. *J Cell Mol Med.* (2008), 12(5B):1820-9

Rosemberg et al., Matrix metallo proteinases and TIMPs are associated with blood-brain barrier opening after reperfusion in rat brain. *Stroke* (1998), 29:2189-2195

Rosemberg GA. et al., Immunohistochemistry of matrix metalloproteainases in reperfusion injury to rat brain: activation of MMP-9 linked to stromelysin-1 and microglia in cell coltures. *Brain Res* (2001), 893:104-112

Rosenberg GA., Matrix metalloproteinases in neuroinflammation. markedly upregulated in inflammation in many disease states. *Glia* (2002), 39(3):279-91

Rosenberg GA, Yang Y.,Vasogenic edema due to tight junction disruption by matrix metalloproteinases in cerebral ischemia. *Neurosurg Focus*. (2007), 22(5):E4

Rosemberg GA, Matrix metalloproteinases and their multiple roles in neurodegenerative diseases. *Lancet Neurol* (2009), 8: 205–16

Rylski M et al., Yin Yang 1 is a critical repressor of matrix metalloproteinase-9 expression in brain neurons. *J Biol Chem*. (2008), 283(50):35140-53

Saijo K et al., A Nurr1/CoREST pathway in microglia and astrocytes protects dopaminergic neurons from inflammationinduced death. *Cell* (2009), 137:47–59

Saito A et al., Oxidative stress affects the integrin-linked kinase signaling pathway after transient focal cerebral ischemia. *J. Cereb. Blood Flow Metab* (2003), 23:1010-1019

Sallés FJ and Strickland S, Localization and regulation of tissue plasminogen-activator-plasmin system in the hippocampus. *J. Neurosci*. (2002), 22:2125-2134

Samson M and Medcalf R, Tissue-type plasminogen activator: a multifaceted modulator of neurotransmission and synaptic plasticity. *Neuron* (2006), 50:673-678

Saxena S, Caroni P. Mechanisms of axon degeneration: from development to disease. *Progress in neurobiology.* (2007), 83(3):174-91

Sbai O et al., Differential vesicular distribution and trafficking of MMP-2, MMP-9 and their inhibitors in astrocytes. *Glia* (2010); 58:344-366

Scalzo P et al., Increased serum levels of soluble tumor necrosis factor-alpha receptor-1 in patients with Parkinson's disease. *J Neuroimmunol*. (2009), 216(1-2):122-5

Schwartz M et al., Innate and adaptive immune responses can be beneficial for CNS repair. *Trends Neurosci* (1999), 22:295–299

Serra R et al., Suppression of LPS-induced matrix-metalloproteinase responses in macrophages exposed to phenytoin and its metabolite, 5-(p-hydroxyphenyl-), 5-*phenylhydantoin*. *J Inflamm* (2010), in press

Serrats J. et al., Duals role of perivascular macrophages in Immune-to-brain signaling, *Cell* (2010), 65:94-106

Setzu, A. et al, Inflammation stimulates myelination by transplanted oligodendrocyte precursor cells. Glia (2006), 54:297–303;

Shin CY et al., Rapid, activity-induced increase in tissue plasminogen activator is mediated by metabotropic glutamate receptor-dependent mRNA translation. *J Neurosci* (2004), 24:9425–33

Shin SM et al., Urokinase-type plasminogen activator induces BV-2 microglial cell migration through activation of matrix metalloproteinase-9. *Neurochem res* (2010), 35:976-985

Shiryaev SA et al., Matrix metalloproteinase proteolysis of the myelin basic protein isoforms is a source of immunogenic peptides in autoimmune multiple sclerosis. *PLoS One*. 2009;4(3):e4952

Silver J, Miller JH. Regeneration beyond the glial scar. *Nature reviews*. (2004), 5(2):146-56; Rolls A et al., The bright side of the glial scar in CNS repair. *Nature reviews*. (2009), 10(3):235-41

Sithu SD et al., Membrane-type 1-matrix metalloproteinase regulates intracellular adhesion molecule-1 (ICAM-1)-mediated monocyte transmigration. *J Biol Chem* (2007), 282:25010–25019

Smith-Thomas LC et al. An inhibitor of neurite outgrowth produced by astrocytes. *Journal of cell science* (1994), 107 (Pt 6):1687-95

So HJ et al., Regulation of matrix metalloproteinase-9 and tissue plasminogen activator activity by alpha-synuclein in rat primary glial cells. *Neurosci letters* (2010), 469:352-356

Sofroniew MV et al, Astrocytes: biology and pathology. *Acta Neuropathol.* (2010), 119(1):7-35

Sokolowska B et al., Evaluation of matrix metalloproteinases in serum of patients with amyotrophic lateral sclerosis with pattern recognition method. *J Physiol Pharmacol.* (2009), 60 Suppl 5:117-20

Sriram K et al., Mice deficient in TNF receptors are protected against dopaminergic neurotoxicity: implications for Parkinson's disease. *FASEB J.* (2002), 16(11):1474-6

Sriram K et al., Deficiency of TNF receptors suppresses microglial activation and alters the susceptibility of brain regions to MPTP-induced neurotoxicity: role of TNF-alpha. *FASEB J.* (2006), 20(6):670-82

Stence N et al., Dynamics of microglial activation: a confocal time-lapse analysis in hippocampal slices. *Glia* (2001), 33:256-266

Sternlicht MD and Werb Z., How matrix metalloproteinases regulate cell behaviour. *Annu Rev Cell Dev Biol* (2001), 17: 463-516

Streit W.J., Microglia as neuroprotective, immunocompetent cells of the CNS. *Glia* (2002), 40:133-139

Streit WJ et al., Role of microglia in the central nervous system's immune response. *Neurol. Res.* (2005), 27:685-691

Suo Z et al., Participation of protease-activated-receptor-1 in thrombin induce microglia activation. *J Neurochem* (2002), 80:655-666

Tagaya M et al., Rapid loss of microvasvular inttegrin expression during focal brain ischemia reflects neuron injury. *J. Cereb. Blood Flow Metab* (2001), 21:835-846

Takács E et al., Matrix metalloproteinase-9 activity increased by two different types of epileptic seizures that do not induce neuronal death: a possible role in homeostatic synaptic plasticity. *Neurochem Int.* (2010), 56(6-7):799-809

Takagi S et al., Damage to oligodendrocytes in the striatum after MPTP neurotoxicity in mice. *J Neural Transm.* (2007), 114(12):1553-7

Tandé D et al., New striatal dopamine neurons in MPTP-treated macaques result from phenotypic shift and not neurogenesis. *Brain* (2006), 129:1194-200

Tansey MG et al., Neuroinflammatory mechanisms in Parkinson's disease: potential environmental triggers, pathways, and targets for early therapeutic intervention. *Exp Neurol.* (2007), 208(1):1-25

Taylor DL, et al. Stimulation of microglia metabotropic glutamate receptor mGlu2 triggers tumor necrosis factor α-induced neurotoxicity in concert with microglial-derived fas ligand. *J Neurosci* (2005), 25:2945–2964

Tedeschi B et al., Astrocytes produce interferon that enhances the expression of H-2 antigens on a subpopulation of brain cells. *J Cell Biol*. (1986), 102(6):2244-53

Teesalu T et al., Tissue plasminogen activator as a key effector in neurobiology and neuropathology. *Biochem Soc Trans.* (2002), 30(2):183-9

Thomas DM et al, The newly synthesized pool of dopamine determines the severity of methamphetamine-induced neurotoxicity. *J Neurochem*. (2008), 105(3):605-16

Tipton KF and Singer TP, Advances in our understanding of the mechanisms of neurotoxicity of MPTP and related compounds, *J. Neurochem*. (1993), 61:1191-1206

Tracey KJ. The inflammatory reflex. *Nature* (2002), 420:458–461

Tu C et al., Lysosomal cathepsin B participates in podosome-mediated extracellular matrix degradation and invasion via secreyted lysosomes in v-Src fibroblast. *Cancer Res* (2008), 68:9147-9156

Uhm, J. H et al., Oligodendrocytes utilize a matrix metalloproteinase, MMP-9, to extend processes along an astrocyte extracellular matrix. *Glia* (1998), 22:53–63

Van Den Steen PE et al., Gelatinase B/MMP-9 and neutrophil collagenase/MMP-8 process the chemokines human GCP-2/CXCL6, ENA-78/CXCL5 and mouse GCP-2/LIX and modulate their physiological activities. *Eur J Biochem* (2003), 270:3739 –3749

Verkhratsky A. et al, NMDA Receptors in glia. *Neuroscientist.* (2007), 13:28-37

Vernice Jackson-Lewis1 & Serge Przedborski, Protocol for the MPTP mouse model of Parkinson’s disease. *Nature Protocols* (2007), 2(1):141-151

Vos CM et al., Matrix metalloprotease-9 release from monocytes increases as a function of differentiation: implications for neuroinflammation and neurodegeneration. *J Neuroimmunol.* (2000), 109(2):221-7

Vu TK et al., Molecular cloning of a functional thrombin receptor reveals a novel proteolytic mechanism of receptor activation. *Cell* (1991), 64:1057-1068

Walker EJ and Rosenberg GA., Divergent role for MMP-2 in myelin breakdown and oligodendrocyte death following transient global ischemia. *J Neurosci Res.* (2010), 88(4):764-73

Wang X et al., Effects of matrix metalloproteinase-9 gene knock-out on morphological and motor outcomes after traumatic brain injury. *J Neurosci.* (2000), 20(18):7037-42

Webber C. A. et al, Metalloproteases and guidance of retinal axons in the developing visual system. *J. Neurosci.* (2002), 22, 8091–8100

Wilczynski GM et al., Important role of matrix metalloproteinase 9 in epileptogenesis. J Cell Biol. (2008), 180(5):1021-35; Frontczak-Baniewicz M et al., MMP2 and MMP9 in immature endothelial cells following surgical injury of rat cerebral cortex--a preliminary study. *Folia Neuropathol.* (2009), 47(4):338-4623–25

Wilhelmsson U et al, Redefining the concept of reactive astrocytes as cells that remain within their unique domains upon reaction to injury. *Proc. Natl. Acad. Sci. U.S.A.* (2006), 103:17513-17518

Williams A. et al., Astrocytes—friends or foes in multiple sclerosis? *Glia* (2007), 55:1300–1312

Wilms H et al., Activation of microglia by human neuromelanin is NF-kappaB dependent and involves p38 mitogen-activated protein kinase: implications for Parkinson's disease. *FASEB J.* (2003), 17(3):500-2

Woo MS et al., Inhibition of MMP-3 or MMP-9 suppress lipopolysaccharide-induced expression of proinflammatory cytokines and iNOS in microglia. *J Neurochem* (2008), 106:770-780

Xue M et al., Combination of thrombin and matrix metalloproteinase-9 exacerbates neurotoxicity in cell culture and intracerebral hemorrhage in mice. *J Neurosci* (2006), 26: 10281–10291

Yamada M et al., Gene disruption of caspase-3 prevents MPTP-induced Parkinson's disease in mice. *Biochem Biophys Res Commun.* (2010), in press

Yamada T et al., Relationship of Complement-Activated Oligodendrocytes to Reactive Microglia and Neuronal Pathology in Neurodegenerative Disease. *Dementia* (1991), 2:71-7

Yamaguchi Y. Lecticans, Organizers of the brain extracellular matrix. *Cell Mol Life Sci* (2000), 57:276–289

Yang L. et al., Target depletion of distinct tumor necrosis factor receptor subtypes reveals hippocampal neuron death and survival through different signal transduction pathways. *J Neurosci* (2002), 22:3025–3032

Yasuda, T. et al., Correlation between levels of pigment epithelium-derived factor and vascular endothelial growth factor in the striatum of patients with Parkinson's disease. *Exp. Neurol.* (2007), 206:308-317

Yong VW et al., Metalloproteinases in biology and pathology of the nervous system. *Nature Rev. Neurosci*. (2001), 2:502–511

Yong VW, Nature review (2005); Yin KJ et al., Matrix metalloproteinases expressed by astrocytes mediate extracellular amyloid-beta peptide catabolism. *J Neurosci.* (2006), 26(43):10939-48

Zalewska, T., Ziemka-Nalecz, M., Sarnowska, A. & Domanska-Janik, K. Involvement of MMPs in delayed neuronal death after global ischemia. *Acta Neurobiol. Exp. (Wars.)* (2002), 62:53–61

Zhang et al., Differential regulation of monocyte matrix metalloproteinase and TIMP-1 production by TNF-alpha, granulocyte-macrophage CSF, and IL-1 beta through prostaglandin-dependent and -independent mechanisms. *J Immunol.* (1998), 161(6):3071-6

Zhang K et al., HIV-induced metalloproteinase processing of the chemokine stromal cell derived factor-1 causes neurodegeneration. *Nat Neurosci* (2003), 6:1064 –1071

Zhang W et al., Aggregated alpha-synuclein activates microglia: a process leading to disease progression in Parkinson's disease. *FASEB J.* (2005), 19(6):533-42.

Zhao XL et al., MMP-mediated cleavage of beta-dystroglycan in myelin sheath is involved in autoimmune neuritis. *Biochem Biophys Res Commun.,* (2010), 392(4):551-6

Zorio E, Fibrinolysis: the key to new pathogenetic mechanisms. *Curr Med Chem*. (2008), 15(9):923-9

RINGRAZIAMENTI

“ Lodate il Signore, popoli tutti, voi tutte, nazioni, dategli gloria; perché forte è il suo amore per noi e la fedeltà del Signore dura in eterno. Alleluya!”.

Salmo 117.

Ringrazio la mia famiglia per avermi aiutato, spronato e sostenuta da ancora prima che venissi al modo e perchè continuerà a farlo per tutta la mia vita. Ad ognuno di voi, speciali ed unici, oggi dico *GRAZIE*. A mamma, per spendere tutte le sue forze per la famiglia. A papà, per essere un esempio di lealtà, responsabilità ed impegno nella vita privata e lavorativa. A mia sorella Maria Elena, perchè anche se siamo due, abbiamo un cuore solo. A mio cognato, Pierluigi, per partecipare sempre ai miei successi, lotte, lacrime ed allegrie con affetto fraterno. Al piccolo Francesco, seme di gioia e speranza per tutta la famiglia.

Grazie a la Fraternità Francescana di Betania, mio indispensabile sostegno spirituale. Grazie a Padre Pierluigi, Padre Igino, Padre Matteo, Padre Alberto, Padre Francesco e Padre Jesus per essere la splendida espressione terrena delle cure, le attenzioni e l’amore che Dio ha per me.

Ringrazio sinceramente la Prof. Egle De Stefano per aver vissuto insieme a me questi 4 anni di lavoro e difficoltà, senza mai perdere pazienza e fiducia, condividendo con me la passione per il nostro lavoro e l’amore per le piccole cose. Grazie a la Prof. Maria Trinidad Herrero, la mia tutor in Spagna, per avermi accolto per due anni nel suo laboratorio, mettendomi a disposizione le sue conoscenze ed offrendomi sempre un

sostegno sincero ed affettuoso. Grazie a tutti i “miei figlioletti prediletti”, Matteo, Tania, Angela, Ivan, Eleonora ed Ilaria, per avermi riempito il cuore del loro affetto che più di ogni cosa mi ha ripagato delle interminabili giornate passate in laboratorio. Grazie a la dott. Loredana Lombardi, per la sua presenza e disponibilità encomiabili. Grazie alla Prof. Paola Paggi, per averci sempre incitato a fare bene il nostro lavoro.

Grazie a tutte le persone speciali del laboratorio NECEX di Murcia. Grazie al dott. Francisco Ros Bernal, per le passeggiate, l’attenzione, l’affetto e la incontenibile simpatia, alla dott. Cristina Nombela Otero per la sua amicizia sincera, a Maria Angeles Carrillo per avermi offerto sempre un sorriso, una spalla su cui piangere e le sue preziose preghiere. Grazie con tutto il cuore ad Aurora Gomez, per avermi accolta nella sua famiglia come una sorella. Grazie alla dott. Marcela Bermudez perchè anime belle come le sue sono un regalo di Dio. Grazie a Jose Enrique Yuste per il suo buon umore, la simpatia e la forza e a Carmen Maria Ros per avermi sempre aiutato a sbrigare le questioni burocratiche. Infine, ringrazio sinceramente il dott. Carlos Barcia, mio padrino, mentore ed amico insostituibile, che sempre terrò nel cuore.

AGRADECIMIENTOS

"¡Alaben al Señor, todas las naciones, glorifíquenlo, todos los pueblos! Porque es inquebrantable su amor por nosotros, y su fidelidad permanece para siempre.¡Aleluya!".

Salmo 117.

Agradezco mi familia por haberme ayudado, animado y sustentado desde antes de nacer y porque seguirán haciéndolo durante toda mi vida. A cada uno de vosotros, seres especiales y únicos, hoy digo *GRACIAS*. A mi madre por poner todas sus fuerzas en la familia. A mi padre por ser un ejemplo de lealtad, responsabilidad y dedición en la vida privada y profesional. A mi hermana Maria Elena, porque aunque seamos dos personas tenemos un corazón único. A mí cuñado Pierluigi por participar a mis miedos, alegrías, luchas y éxitos con amor fraternal. Al pequeño Francesco por ser una semilla de alegría y esperanza para toda la familia.

Gracias a la Fraternità Francescana di Betania por ser mi indispensable sustento espiritual. Gracias a padre Pierluigi, padre Igino, padre Matteo, padre Alberto, padre Francesco e padre Jesus por ser la hermosa expresión de todas las atenciones, los mimos y el amor de Dios hacia mí.

Agradezco mucho la Prof. Egle De Stefano por haber vivido juntas estos 4 años de trabajo y dificultades con paciencia y confianza, compartiendo conmigo el amor para nuestro trabajo y las cosas pequeñas. Gracias a la Prof. Maria Trinidad Herrero, mi tutora en España, por haberme acogido durante dos años en su laboratorio, por poner a mi disposición sus conocimientos y por apoyarme siempre afectuosamente.

Gracias a todos “mis hijitos”, Matteo, Tania, Angela, Ivan, Eleonora e Ilaria por haber llenado mi corazón con sus palabras, gestos y abrazos, porque han estado la mejor recompensa para todos los interminables días pasados en el laboratorio. Gracias a la doctora Loredana Lombardi por su constante presencia y disponibilidad encomiables. Gracias a la prof. Paola Paggi por nos haber siempre animado a hacer bien nuestro trabajo. Gracias a todas las personas especiales que he encontrado en el laboratorio NECEX en Murcia. Gracias al doctor Francisco Ros Bernal por los paseos, el cariño y la grande simpatía, a la doctora Cristina Nombela Otero por su sincera amistad, a María Ángeles Carrillo por haberme enseñado a nadar, por no haberme negado nunca una sonrisa y su apoyo y por rezar por mí. Gracias de todo corazón a Aurora Gómez por haberme acogido en su familia como una hermana, a la doctora Marcela Bermúdez porque encontrar un alma tan bonita como la suya es un don de Dios. Gracias a José Enrique Yuste por su humor, alegría y fuerza y a Carmen María Ros por haberme siempre ayudado con todos los papeleos. En final, sinceramente agradezco al doctor Carlos Barcia, mi padrino, mentor y amigo, que siempre tendrá un sitio especial en mi corazón.